2009

The Removal and Recovery of Oxo-Anions from Aqueous Systems using Nano-Porous Silica Polyamine Composites

Varadharajan Kailasam
The University of Montana

THE REMOVAL AND RECOVERY OF OXO-ANIONS FROM AQUEOUS SYSTEMS USING NANO-POROUS SILICA POLYAMINE COMPOSITES

By

VARADHARAJAN KAILASAM

B.Sc. Chemistry, Bharathiyar University, Tamilnadu, India, 1996
M.Sc. Applied Chemistry, Bharathiyar University, Tamilnadu, India, 1998
M.S. Environmental Engineering, Montana Tech, Butte, Montana, USA, 2004

Thesis

presented in partial fulfillment of the requirements
for the degree of

Doctor of Philosophy
in Chemistry, Inorganic

The University of Montana
Missoula, MT

Summer 2009

Approved by:
Dr. Perry J. Brown, Associate Provost
Graduate Education

Dr. Edward Rosenberg, Committee Chairperson
Department of Chemistry

Dr. Alexander Ross, Committee Member
Department of Chemistry

Dr. Donald Kiely, Committee Member
Department of Chemistry

Dr. Earle Adams, Committee Member
Department of Chemistry

Dr. Johnnie Moore, Committee Member
Department of Geosciences

Kailasam, Varadharajan, Ph.D., Summer 2009 Chemistry

The Removal and Recovery of Oxo-Anions from Aqueous Systems using Nano-Porous Silica Polyamine Composites

Chairperson: Dr. Edward Rosenberg, Department of Chemistry

Abstract

Environmental contamination due to anthropogenic wastewater discharges containing high concentrations of toxic metals is omnipresent in the environment. Heavy metal ions from manufacturing sources can compromise the integrity of various ecological cycles as well as negatively impacting the health of humans through drinking water and the food chain. Increased levels of well known poisonous metals such as arsenic, selenium, lead and mercury are frequently detected in aqueous wastes. Arsenic and selenium are highly toxic elements to human health and the environment. The Maximum Contaminant Level (MCL) for both these toxic metals continue to become more and more stringent. Although there are several metal remediation technologies available commercially, most of them are not feasible and/or are very expensive. The ferrihydrite process (precipitation with iron (III) oxyhydroxides) is by far the most economical and effective of these technologies and has been widely employed on a large scale. However, it has the significant disadvantage of creating a large amount of sludge for ultimate disposal and leaching of colloidal iron oxides into aquifers. The other methods suffer from a lack of specificity, low selectivity over sulfate (ion exchange), low mass-to-volume concentrations (bio-reduction), and/or high cost (membrane technologies).

This led us to the development of silica polyamine composites (SPCs) functionalized with metal selective ligands for the removal of heavy metals from wastewater streams. High capacities were obtained for arsenic, selenium, molybdenum, and tungsten oxoanions by immobilizing zirconium on the phosphonic acid modified SPC (BPAP). The oxo-anions of these metals bind to the net positive charge on the zirconium, thereby removing them from the wastewater stream and reducing the metal concentrations below their respective MCLs. These silica polyamine composites can also be acid stripped and regenerated for reuse. This aspect is very useful in commercial applications where the toxic metal ions can be selectively extracted and efficiently recovered from acid mine drainage in the presence of high sulfate concentrations, and in their removal from seawater systems. Alkylated SPCs tested for the removal of bacteria and viruses from drinking water systems have also shown promise. Further characterization of the SPCs are being carried out using surface analytical techniques and the SPC chemistry is being extended for applications on surface oxidized silicon wafers.

ACKNOWLEDGEMENTS

I will always look back at the time I spent at The University of Montana with fond memories. I would like to convey my most sincere thanks to everyone who made my stay and my graduate school years memorable. I have great respect for Professor Edward Rosenberg and would like to gratefully acknowledge him for his invaluable support, mentoring, and encouragement throughout my graduate school years. The Chemistry Department has been more than supportive during my stay here and I would never forget my time spent here as a graduate student. I appreciate the guidance and help of my fellow graduate students who have worked in the Rosenberg group – Paul Miranda, Daniel Nielsen, Mark Hughes, William Gleason, Jesse Allen, Carolyn Hart and Jessica Wood. I would also like to acknowledge the contributions of undergraduate research students, most notably Tegan Shoener, Richard Kraude, Chauncey Means, and Mary Burroughs. I am also thankful for the positive criticism and encouragement of my thesis committee members. My fellow researchers and advisor from Toyo University, Japan and Montana State University, Bozeman have helped me understand the important aspect of collaborating with scientists from fields other than chemistry. I am eternally indebted to my family in India as well as my family in Whitefish, Montana for their unconditional love and support throughout my time at UM. I will always strive to work hard in my career and give it my all to make them proud. Finally, I want to express my deepest love and affection to my wife Molly for her patience and understanding, and for standing by my side throughout my time as a graduate student at UM.

TABLE OF CONTENTS

LIST OF FIGURES

LIST OF TABLES

CHAPTER 1: BACKGROUND

1.1 Introduction

This dissertation deals with the development of improved methods for arsenic remediation using the newly developed Immobilized Metal silica Polyamine Composite (IMPAC) technology. In order to fully appreciate the impact of metals on our environment, this chapter provides a brief summary of metals, their toxicities, sources of heavy metal contamination, and various remediation technologies that are being used commercially.

Metals have played a key role in our society for a long time. The extent of their use can be defined as a criterion of prosperity. Over the last few centuries, the demand for metals has only been increasing. Currently there are 86 known metals. Before the 19th century only 24 of these metals had been discovered and, of these 24 metals, 12 were discovered in the 18th century. Therefore, from the discovery of the first metals – gold and copper until the end of the 17th century, only 12 metals were known. Four of these metals, arsenic, antimony, zinc and bismuth were discovered in the thirteenth and fourteenth centuries, while platinum was discovered in the 16th century. The other seven metals, known as the 'metals of antiquity' were the metals upon which civilization was based. These seven metals were: (1) Gold (ca) 6000BC; (2) Copper,(ca) 4200BC; (3) Silver,(ca) 4000BC; (4) Lead, (ca) 3500BC; (5) Tin, (ca) 1750BC; (6) Iron (smelted), (ca) 1500BC; (7) Mercury, (ca) 750BC. Several other metals were isolated during the 1700's. These were cobalt, nickel, manganese, molybdenum, tungsten, tellurium, beryllium, chromium, uranium, zirconium, and yttrium.[1,2]

Metals in general have superior electric and thermal conductivity, high luster and density, and the ability to be deformed under stress without cleaving. While there are several metals that have low density, hardness, and melting points, these (the alkali and alkaline earth metals) are extremely reactive, and are rarely encountered in their elemental, metallic form. The majority of metals have higher densities than the majority of nonmetals. Nonetheless, there is wide variation in the densities of metals; lithium is the least dense solid element and iridium is the densest metal. Ductility and malleability are mechanical properties used to describe the extent to which materials can be deformed plastically without fracture. The nondirectional nature of metallic bonding is thought to be the primary reason for the malleability of metal. Planes of atoms in a metal are able to slide across one another under stress, accounting for the ability of a metal to deform without shattering.[2,3] Metals readily form useful compounds with many other elements. These properties and many other useful traits make metals useful for a wide range of applications. A wide range of industries which include aerospace, biomedical applications, computers, communications, construction, decoration, electronics, energy and utilities, food and agriculture, household appliances, transportation, etc. use metals.[4,5]

As the population continues to grow, so does the demand for metals. As a result of the great significance of metals to modern society, a large amount of resources have been and continue to be, invested in the extraction of metals from the earth's crust.[3,5] The depletion of metals from earth's limited supply has been a growing concern for a long time. It is estimated that ~25% of the earth's copper is now lost as waste – aqueous and soil.[6] Mining has played an important role in the extraction of metals and non metals from the earth's crust. Mining can have significant environmental impacts involving visual intrusions, dust, noise,

blasting, traffic, and hydrology. The processes of mineral extraction, processing, smelting and refining will never approach to becoming environmentally neutral, but the areas of impact can be mitigated, sometimes to a major degree, by long-term monitoring from the initiation of a project to the phases of a restored or remediated mine and/or refinery.[7]

Pollution of the biosphere by the toxic metals is a global threat that has accelerated dramatically since the beginning of the industrial revolution. The primary source of this pollution includes the industrial operations such as mining, smelting, metal forging, combustion of fossil fuels and contamination by sewage sludge agronomic practices.[8] Environmental contamination due to anthropogenic wastewater discharges containing high concentrations of toxic metals is omnipresent in the environment. Some of the sources of heavy metal contamination include industries such as mining, pigment, paint coatings, tanneries, electronics, metal plating, power plants (thermal and nuclear), municipal landfills and more. Stringent regulations on wastewater discharges have stimulated increased activity in the removal and recovery of these metals from various wastewater systems, thereby remediating the contaminated sites.[9] Heavy metal ions from manufacturing sources can compromise the integrity of various ecological cycles as well as negatively impacting the health of humans through drinking water and the food chain. Increased levels of well known poisonous metals such as arsenic, selenium, lead and mercury are frequently detected in aqueous wastes.[9] Other hazardous heavy metal ions including cadmium, barium, copper, nickel, and chromium are also found at alarming concentrations.[10-12] Heavy metals can cause acute and chronic illnesses in humans and other animals.[13] Eradication of these metal ions from waste media is a necessity. Concurrently, enormous amount of research is being devoted to meeting the challenge posed by heavy metal pollution. The next sections discuss

the details of the sources of heavy metal pollution, metal toxicities, currently available technologies for metal recovery, and our proposed IMPAC technology.

1.2 Motivations for the Research

1.2.1 Mine and Mineral Processing

Mineral processing, also known as mineral dressing, is the practice of beneficiating valuable minerals from their ores. Industrial mineral treatment processes usually combine a number of unit operations in order to liberate and separate minerals by exploiting the differences in physical properties of the different minerals that make up an ore. Many active mining projects implement a leaching process in which metals are extracted from ores using various acids. Consequently, the majority of aqueous mine process solutions contain high concentrations of metal ions at low pH (usually < 3).[14,15] For example leach solutions from Laterite ores and oil shales near Julia Creek, Australia contain a significant amount of several main group metal ions and transition metal ions.[16] Abundances and mineralogical residences have been determined for a comprehensive range of trace elements in Julia Creek oil shale. Many trace elements are well above normal abundances in shales. Of these elements, vanadium and molybdenum are potentially useful by-products, whereas arsenic, selenium, molybdenum, cadmium, thallium, and uranium are of possible environmental or occupational health concern.[17,18] It is the abnormally large concentrations of nickel and molybdenum that are targeted for extraction. Recently, there has been extraordinary increase in demand for technologies directed towards the extraction of nickel and cobalt from various types of ores. Laterite ores found in Australia contain 1% to 2% nickel by weight. In fact approximately 70% of the world's nickel reserves are found in laterite ores and only 30% of the world's

nickel production comes from mining these ores.[19,20] Hence it is evident that there is an absence of efficient and viable technologies for the processing of nickel from laterite leach solutions.

In general, contemporary metallurgical processes such as hydrometallurgy and pyrometallurgy are not environmentally benign and are energy intensive. Pyrometallurgical processing consists of a thermal treatment of solid ores to produce physical and chemical transformations that allow the recovery of valuable metals. On the other hand hydrometallurgy is the use of aqueous chemistry for the recovery of metals from ores and leaching is an excellent example of a hydrometallurgical technique. Two existing methods for the processing of ores include the Nicaro process, in which the nickel, cobalt, molybdenum, and vanadium oxides are reduced to a metallic form by roasting and leaching the metals in an ammonia solution. The second process is a Sherritt process in which the oxides are subjected to a high pressure acid leach (HPAL) followed by a selective sulfide precipitation.[21,22] Molybdenum is selectively extracted from an aqueous solution containing various other metal values, e.g. copper, arsenic, iron, bismuth, antimony, tin, and lead in addition to molybdenum. The molybdenum–bearing solution is adjusted to a pH of about 2.0 or less, then intimately contacted with an organic extracting solution containing an alpha–hydroxy oxime (**Figure 1.1**). The loaded organic phase, containing extracted molybdenum values, is separated from the aqueous raffinate, and the molybdenum values contained in the organic phase are stripped therefrom using an aqueous stripping solution containing ammonium hydroxide. The efficiency with which the molybdenum is stripped from the loaded organic solution is poor unless

nonylphenol is present in the organic solution as it is being stripped. Nonylphenol (**Figure 1.1**) is an organic compound of the wider family of alkylphenols which are used as industrial surfactants in manufacture of wool and metal, as emulsifiers for emulsion polymerization and in some pesticides and laboratory detergents. The nonylphenol can be added to the system anytime prior to the ammonium hydroxide stripping step, e.g. it can be added to the organic solution before the extraction step, or it can be added to the aqueous-organic mixture during the extraction step (in which case it reports to the organic phase), or it can be added to the organic solution just prior to the stripping step.[23,24]

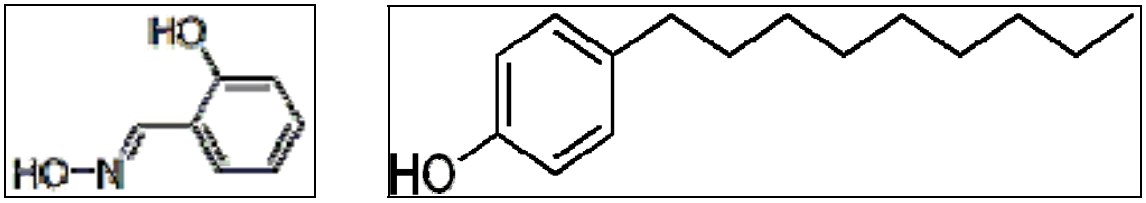

Figure 1.1: Left – structure of α–hydroxy oxime (salicylaldoxime). Right – structure of nonylphenol.

To separate the metals of importance from impurities, an ammonia leach from hydroxide neutralization after iron precipitation can be used to yield a product solution that is high in nickel, molybdenum, cobalt and vanadium. A direct solvent extraction–electrowinning (SX–EW) process has also been employed after iron neutralization, as well as a selective sulfide precipitation technique.[25] Unfortunately, precipitation methods, re-leaching, and solid–liquid separation techniques are cost and labor intensive. Extensive research is also underway to selectively extract these metals using cross-linked polystyrene resins and other solid phase adsorbents (vide infra).[26]

1.2.2 Industrial Waste Streams

Most industries produce some wet waste although recent trends in the developed world have been to minimize such production or recycle such waste within the production process. However, many industries remain dependent on processes that produce wastewaters. Industrial wastewater treatment covers the mechanisms and processes used to treat waters that have been contaminated in some way by anthropogenic industrial or commercial activities prior to its release into the environment or its re-use. These waste streams if not treated properly adversely affect the environment surrounding it.[27] Since the onset of the industrial revolution (18^{th} century onwards), inland waters have experienced elevated levels of pollutants (metals and non-metals) from manufacturing effluents. In particular, increased concentrations of metal ions are commonly found in waters emanating from tanneries, steel pickling plants, metal plating factories, pigment industries, municipal landfills, wastewater treatment facilities, nuclear weapons production facilities, nuclear power generators as well as natural resource mining projects.[28-31]

There are approximately 70 trace elements that are necessary for human life. However, elements like mercury, lead, cadmium, arsenic, and chromium have no natural function in the human body and are highly toxic.[32] Toxic heavy metals compete with nutrient elements for binding sites on transport and storage proteins, metalloenzymes and receptors. For example, it is known that the Hg^{2+} ion forms a strong bond with selenium. Through forming this bond Hg^{2+} removes selenium from its critical role as a constituent

of the tetrameric glycoprotein, glutathione peroxidase, which is a vital protection against oxidative damage.[33] Selenium is also toxic at levels higher than 400 micrograms per day.[34] The prevention of toxic metal ions entering domestic waters is a necessity.

1.2.3 Nuclear Waste Processing

Nuclear or radioactive wastes are waste types containing radioactive chemical elements that do not have a practical purpose. They are usually the products of nuclear processes, such as nuclear fission. However, industries not directly connected to the nuclear industry may produce large quantities of radioactive waste. The majority of radioactive waste is "low-level waste", meaning it contains low levels of radioactivity per mass or volume. This type of waste often consists of used protective clothing, which is only slightly contaminated but still dangerous in case of radioactive contamination of a human body through ingestion, inhalation, absorption, or injection.[35] Allowing radioactive metal ions with long lifes to interact with natural waters is disastrous to the environment. Chronic exposure to drinking water containing uranium can have toxic consequences for the human liver and exposure to other radionuclides in excess of the maximum contaminant level (MCL) leads to cancer.[36] Long-lived radionuclides are a consequence of nuclear power generation and weapons production.[37] The issue of disposal methods for nuclear waste is one of the most pressing current problems the international nuclear industry faces when trying to establish a long term energy production plan, yet there is hope that it can be safely solved. A report giving the Nuclear Industry's perspective on this problem is presented in a document from the IAEA (The International Atomic Energy Agency) published in October 2007. It summarizes

the current state of scientific knowledge on whether waste could find its way from a deep burial facility back to soil and drinking water and threaten the health of human beings and other forms of life. In the United States, the Department of Energy (DOE) has made progress in addressing the waste problems of the industry, and successful remediation of some contaminated sites, yet, there exist major uncertainties and sometimes complications and setbacks in handling the issue properly, cost effectively, and in the projected time frame.[38] In other countries with a lower ability or will to maintain environmental integrity the issue would be even more problematic.

In the United States alone, the Department of Energy stated that there are "millions of gallons of radioactive waste" as well as "thousands of tons of spent nuclear fuel and material" and also "huge quantities of contaminated soil and water." Despite copious quantities of waste, the DOE has stated a goal of cleaning all presently contaminated sites successfully by 2025. The Fernald, Ohio site for example had "31 million pounds of uranium product", "2.5 billion pounds of waste", "2.75 million cubic yards of contaminated soil and debris", and a "223 acre portion of the underlying Greater Miami Aquifer had uranium levels above drinking standards." The United States has at least 108 sites designated as areas that are contaminated and unusable, sometimes many thousands of acres. DOE wishes to clean or mitigate many or all by 2025, however the task can be difficult and it acknowledges that some will never be completely remediated. In just one of these 108 larger designations, Oak Ridge National Laboratory, there were for example at least "167 known contaminant release sites" in one of the three subdivisions of the 37,000-acre (150 km^2) site.[38,39] This is an area of intense and active

research that may serve to ameliorate nuclear waste disposal and may lead to comprehensive advances in the recovery of f-element ions from aqueous nuclear wastes.[40-44]

1.2.4 Acid Mine Drainage

Acid mine drainage (AMD), or acid rock drainage (ARD), refers to the outflow of acidic water from (usually) abandoned metal mines or coal mines. However, other areas where the earth has been disturbed (e.g. construction sites, subdivisions, transportation corridors, etc.) may also contribute acid rock drainage to the environment. In many localities the liquid that drains from coal stocks, coal handling facilities, coal washeries, and even coal waste tips can be highly acidic, and in such cases it is treated as acid rock drainage. Acid mine drainage occurs naturally within some environments as part of the rock weathering process but is exacerbated by large-scale earth disturbances characteristic of mining and other large construction activities, usually within rocks containing an abundance of sulfide minerals. Metal mines may generate highly acidic discharges where the ore is a sulfide or is associated with pyrites. In these cases the predominant metal ion may not be iron but rather zinc, copper, or nickel. The most commonly-mined ore of copper, chalcopyrite, is itself a copper iron sulfide mineral ($CuFeS_2$) and occurs with a range of other sulfides. Thus, copper mines are often major culprits of ARD.[45] The past fifty years of coal and metal mining have left the surface of the land scarred, and has polluted 13,000 miles of streams.[46] Many laws and regulations have been passed to help treat and control the problem of acid drainage. The EPA has helped establish new U.S. effluent limits including reduced drainage acidity in which the

pH must fall between 6 and 9, and the average iron content must not exceed 3 mg/L.[47] Mines in operation since 1978 must chemically treat their effluent water, at an estimated cost of $1 million per day.[47] Processes preventing acid discharge include use of filtration equipment and drainage ponds. Chemical and biological processes are the most common methods to treat acid drainage.[47] Acid mine drainage is polluted water that normally contains high levels of iron, aluminum, and acid. Drainage acidity arises from oxidation of pyrite, the crystalline form of iron sulfide. The contaminated water is often reddish-brown in color, indicating high levels of oxidized iron. Mining disturbs pyrite and, as a result, pyrite weathers and reacts with oxygen and water in the environment making the waters highly acidic.[46] However, in many cases when the mine is non-operational, a build-up of water below the water table will occur. The following equations illustrate some of the major contributors to AMD:[45]

Pyrite

$$2FeS_{2\,(s)} + 7O_{2\,(g)} + 2H_2O_{\,(l)} \longrightarrow 2Fe^{2+}{}_{(aq)} + 4SO_4{}^{2-}{}_{(aq)} + 4H^{+}{}_{(aq)} \quad (1.1)$$

$$4Fe^{2+}{}_{(aq)} + O_{2\,(g)} + 4H^{+}{}_{(aq)} \longrightarrow 4Fe^{3+}{}_{(aq)} + 2H_2O_{\,(l)} \quad (1.2)$$

$$FeS_{2\,(s)} + 14Fe^{3+}{}_{(aq)} + 8H_2O_{\,(l)} \longrightarrow 15Fe^{2+}{}_{(aq)} + 2SO_4{}^{2-}{}_{(aq)} + 16H^{+}{}_{(aq)} \quad (1.3)$$

Arsenopyrite

$$FeAsS_{\,(s)} + 5SO_{2\,(g)} + 3H_2O_{\,(l)} \longrightarrow 2As(OH)_{3\,(s)} + 2SO_4{}^{2-}{}_{(aq)} + Fe^{2+}{}_{(aq)} \quad (1.4)$$

Chalcocite

$$Cu_2S_{\,(s)} + 2.5O_{2\,(g)} + 2H^{+}{}_{(aq)} \longrightarrow 2Cu^{2+}{}_{(aq)} + SO_4{}^{2-}{}_{(aq)} + H_2O_{\,(l)} \quad (1.5)$$

Iron Oxidation

$$2Fe^{2+}_{(aq)} + 0.5O_{2\,(g)} + 5H_2O_{(l)} \longrightarrow 2Fe(OH)_{3\,(s)} + 4H^{+}_{(aq)} \quad (1.6)$$

The production and subsequent oxidation of ferrous to ferric iron (Fe^{2+} to Fe^{3+} – Eqn. 1.6) produces a significant amount of H^+ which decreases the pH. Although the reaction is exothermic (ΔH = -349 kcal/mole), the oxidation process is relatively slow.[45b] As a result, when water temperatures have been reported to reach 50°C, oxidation is faster and the solution pH have been reported to decrease below pH 0.[48] Very low pH values are often an outcome of the evaporation of water leading to the concentration of H^+. AMD is a major problem in the Western United States. Although there are many AMD sites around the world, the Berkeley Pit copper mine in Butte, Montana, USA is one of the largest and most contaminated superfund sites.[45] The pit was first mined in 1955 and since then one billion tons of earth has been removed creating a huge trench. It is approximately 900 feet deep, about one mile wide and contains roughly 37 billion gallons of water contaminated with heavy metals and has a pH of approximately 2.5. Due to the movement of groundwater, the pit fills with water at a rate of 2.55 million gallons/day.[49] In addition to a high copper and sulfate content, the Berkeley Pit water contains manganese, iron, aluminum, zinc, cadmium, magnesium, calcium and arsenic at levels that are toxic to humans.[9] The copper, iron and zinc concentrations have elevated in the pit to the point that the water has been considered as a potential commercial source for the metal. Due to the concentrations of toxic metals like arsenic, and cadmium, the pit water has become a major concern and must be treated before the toxic metals enter the drinking water supply. Precipitation and subsequent leaching can permit metals

access to surface and subsurface waters. The cleanup of these highly polluted waters is of prime importance to the survival of the surrounding aquifer and local ecosystems. Several methods of cleanup have been used to tackle the polluted water resulting from AMD.[50-53] However, none of these techniques can separate those metals with economic value from toxic or less valuable metals. Furthermore, issues such as the expense of the disposal of resulting precipitates, as well as the construction and maintenance of large areas of wetlands, are some of the significant disadvantages.[54]

1.3 Metal Toxicities

There are 35 metals that concern us because of occupational or residential exposure; 23 of these are the heavy elements or "heavy metals": antimony, arsenic, bismuth, cadmium, cerium, chromium, cobalt, copper, gallium, gold, iron, lead, manganese, mercury, nickel, platinum, silver, tellurium, thallium, tin, uranium, vanadium, and zinc. Interestingly, small amounts of these elements are common in our environment and diet and are actually necessary for good health, but large amounts of any of them may cause acute or chronic toxicity (poisoning). Heavy metal toxicity can result in damaged or reduced mental and central nervous function, lower energy levels, and damage to blood composition, lungs, kidneys, liver, and other vital organs. Long-term exposure may result in slowly progressing physical, muscular, and neurological degenerative processes that mimic Alzheimer's disease, Parkinson's disease, muscular dystrophy, and multiple sclerosis. Allergies are not uncommon and repeated long-term contact with some metals or their compounds may even cause cancer.[54,55] For some heavy metals, toxic levels can be just above the background concentrations naturally found in nature. Therefore, it is important for us to inform ourselves about the heavy metals and to take protective measures against excessive exposure. The following sections discuss in detail the toxicities of metals that have extensively researched.

1.3.1 Arsenic

A nonessential toxic element, arsenic is a metalloid that occurs naturally as an element and ranks 20th in natural abundance in the earth's crust (NRC, 1977) and is

widely distributed in the environment. Its association with some weatherable mineral deposits (e.g., sulphide minerals) has contributed to its release in large amounts into the environment.[55] Arsenic exists mainly in three valence states, -2, +3, +5. Trivalent arsenic (As^{3+}) and pentavalent arsenic (As^{5+}) are widely present in natural waters and are soluble over a wide range of pH and Eh conditions.[56,57] Arsenic metal (As^0) rarely occurs in nature. In oxidizing environmental conditions, As^{5+} species are more stable and predominant, whereas in reducing environmental conditions, As^{3+} species are predominant. Under anaerobic conditions, arsenite can be reduced to arsine gas by microorganisms in soil. Arsenic species may also be methylated as monomethylarsonic acid (MMAA), dimethylarsinic acid (DMAA), and trimethylarsine oxide (TMAO) by microorganisms, humans and animals. The trivalent compounds are generally more toxic than the pentavalent compounds. The most toxic of all the arsenic species is the arsine gas (AsH_3), although it occurs only at very low pE values. Arsenic is used in hardening of alloys and in production of semiconductors, pigments, glass manufacturing, pesticides, rodenticides and fungicides. It was also used as an ingredient in drugs for the treatment of some diseases (e.g., sleeping sickness, chromic myeloid leukemia).[58-60] Because of its usefulness and exploitation, arsenic contamination is now widespread in the environment.

Arsenic toxicity could affect a wide variety of organisms including humans. Chronic arsenic effects in humans have been well documented and reviewed.[58,61] Organs most affected are those involved with arsenic in absorption, accumulation and/or excretion. These organs are the gastro-intestinal tract, circulatory system, liver, kidney, skin, tissues very sensitive to arsenic and those tissues secondarily affected such as the

human heart. Signs of arsenic toxicity include dermal lesions, peripheral neuropathy, skin cancer and peripheral vascular disease. These signs have been mostly observed in populations whose drinking water contains arsenic.[62] Among these symptoms, dermal lesions are more prominent and are also known to occur within a period of about 5 years. The skin is known to localize and store arsenic because of its high keratin content, which contains several sulfhydryl groups to which As^{3+} may bind and may be the reason for its sensitivity to the arsenic toxic effect.[63] Skin cancers, including in situ cell carcinoma (Bowen's disease), invasive cell carcinoma and multiple basal cell carcinoma, are all known to be associated with chronic arsenic exposure. Other effects of arsenic exposure are depression, anhydremia (loss of fluid from blood into tissue and the gastrointestinal tract), liver damage characterized by jaundice, sensory disturbance, anorexia and loss of weight.[63] Although the effects of arsenic, as recounted above, result in several kinds of diseases, it certainly may also adversely impact the immune system. Arsenic poisoning from consuming moderate amounts of the toxic element is a slow, debilitating process that ultimately can result in death.

Aqueous arsenic in ground and surface waters exist primarily as oxyanions with formal oxidation states of III and V. Depending on the environment (oxic, sulfidic, or methanic) in the aqueous system, arsenic species differ as well. Either arsenate or arsenite can be the dominant form in aqueous systems. Arsenate ($H_nAsO_4^{n-3}$) generally is the dominant form in oxic waters. In contrast arsenite ($H_nAsO_3^{n-3}$) dominates in sulfidic and methanic waters including deeply circulating geothermal waters. In strongly sulfidic environments that are near saturation with respect to orpiment (As_2S_3), arsenic sulfide

complexes may form with a generic formula $H_nAs_3S_6^{n-3}$.[64] **Figure 1.2** shows the existence of different arsenic species at a pH range 0-14 with respect to pE and Eh.

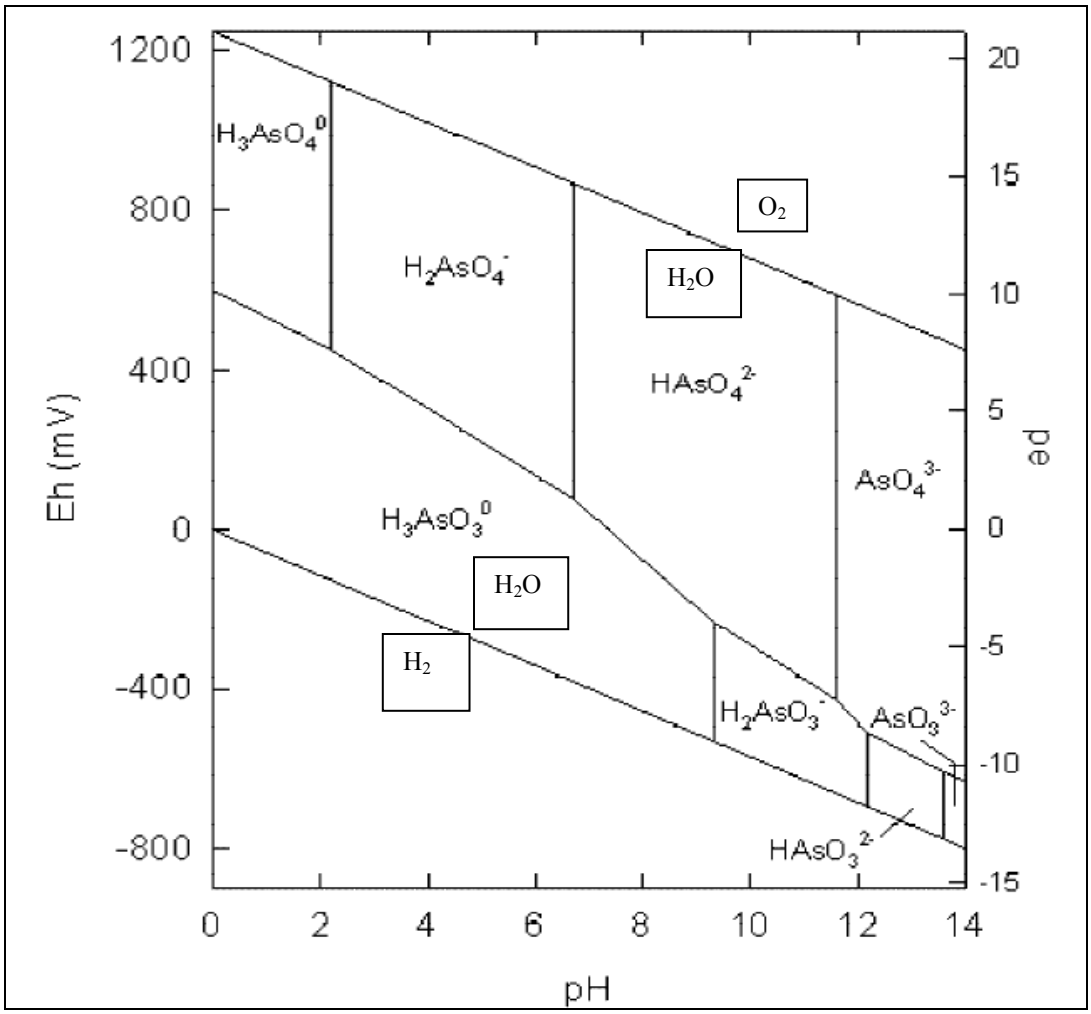

Figure 1.2: Eh–pH–pE diagram of arsenic species in the system As–O_2–H_2O at 25ºC and 1 bar total pressure.

Although, this research is more inclined toward arsenic removal at neutral pH (since ground and surface waters have a circum-neutral pH), we would like to develop arsenic removal systems that have broader operating pH range.

1.3.2 Selenium

Selenium is a naturally occurring trace element that can be released in the waste materials from certain mining, agricultural, petrochemical, and industrial manufacturing operations. Selenium exists in three states (0, -2, +4, +6). Selenium and sulfur are very similar elements among the group. The most important general distinction between the two is the increased difficulty in oxidation for selenium. Thus elemental selenium occupies a much larger part of the Eh-pH diagram (**Figure 1.3**). The Se(VI) states are particularly difficult to attain. Note also that there is a huge overlap zone between the element and the neighboring species on either side of the equilibrium. Once in the aquatic environment, it can rapidly attain levels that are toxic to fish and wildlife because of bioaccumulation in food chains and resultant dietary exposure (**Figure 1.4**). This rapid bioaccumulation causes the response curve for selenium poisoning to be very steep. For example, a transition from no effect to complete reproductive failure in fish can occur within a range of only a few µg/L of waterborne selenium.

Selenium pollution is a worldwide phenomenon and is associated with a broad spectrum of human activities, ranging from the most basic agricultural practices to the most high-tech industrial processes. Consequently, selenium contamination of aquatic habitats can take place in urban, suburban, and rural settings alike – from mountains to plains, from deserts to rainforests, and from the Arctic to the tropics. For many years, selenium has been a largely unrecognized pollutant, particularly in developing nations, and has been overshadowed by issues involving contaminants such as industrial chemicals, heavy metals, pesticides, and air pollutants – just to name a few. However,

during the past decade, aquatic pollution surveillance and monitoring programs have expanded markedly and as a result, selenium has emerged as an important environmental contaminant, and has gained the attention of natural resource managers and water quality regulators around the world.[63] Selenium is required in trace levels by our human body as a micronutrient. But, if the selenium levels in humans exceed trace quantities, it affects the respiratory system, kidneys, and livers. In some studies, loss of appetite has also been reported.[65]

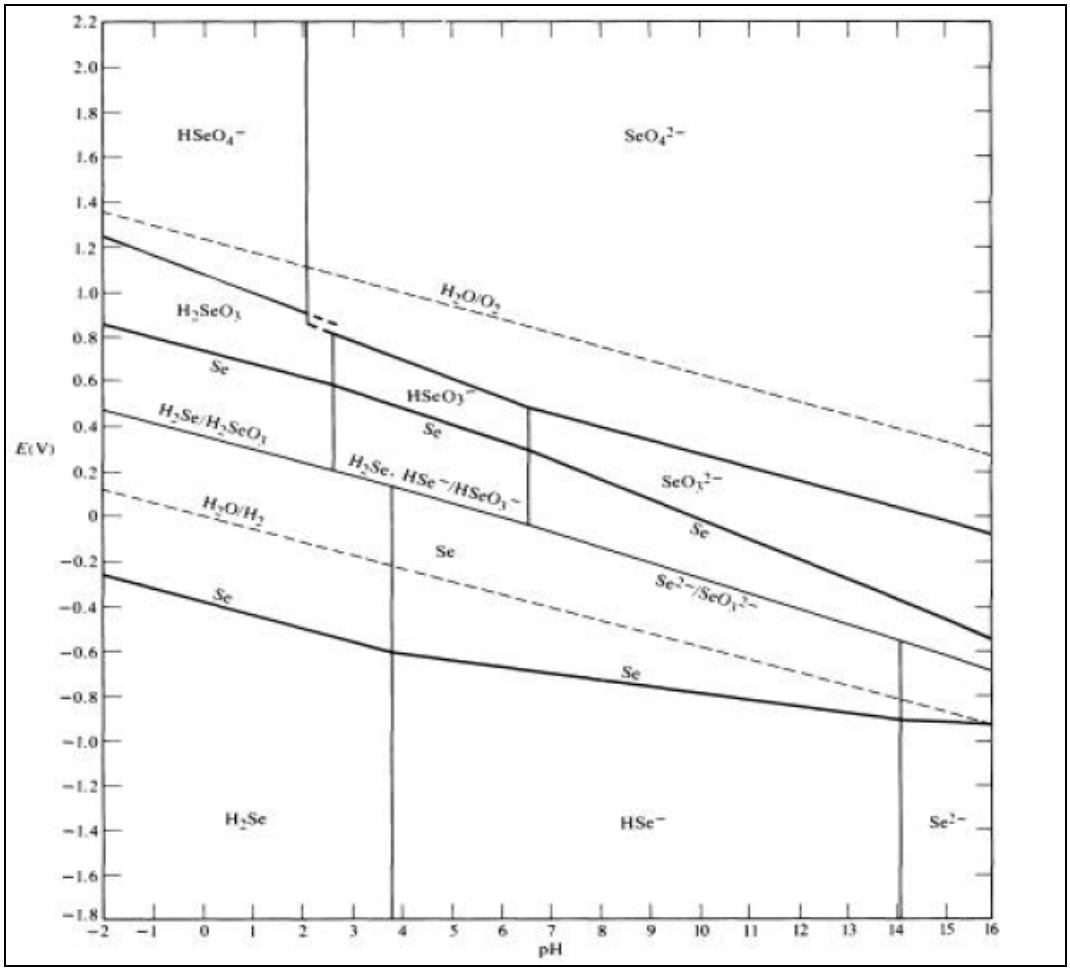

Figure 1.3: Eh-pH diagram of selenium species in the system Se–O_2–H_2O at 25ºC and 1 bar total pressure.

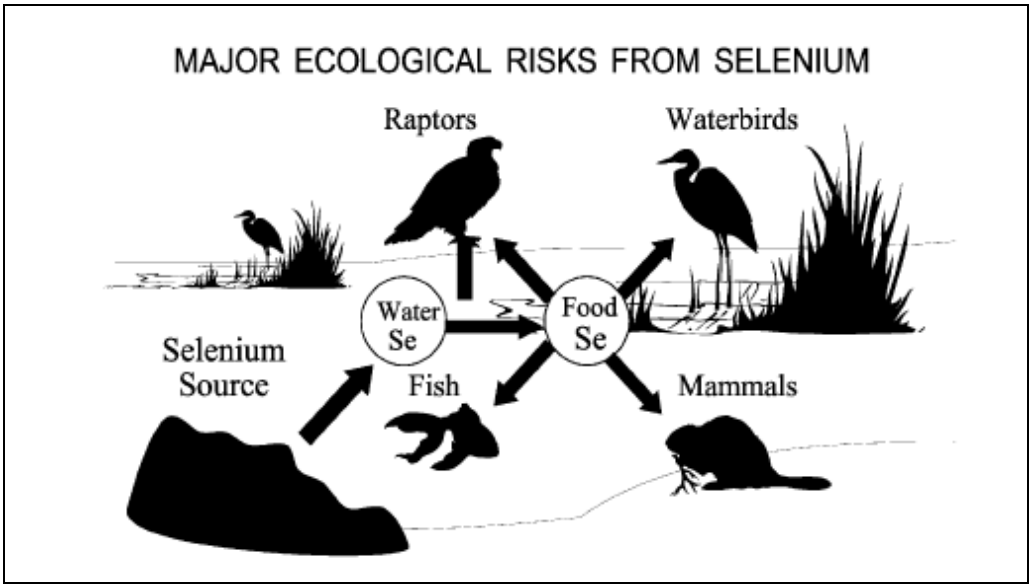

Figure 1.4: Pathways for selenium movement and bioaccumulation in food chains.

1.3.3 Molybdenum

Molybdenum is an essential trace element that is ubiquitous in the environment and vital in plant and animal biochemistry. In human nutrition, molybdenum is assimilated primarily from vegetables. It is closely associated with copper and iron metabolism and enzymatic redox processes involving an equilibrium between the Mo^{6+}, Mo^{5+}, and Mo^{4+} forms, (in the oxidation of aldehydes, sulfites, and nitrates, and of molecular nitrogen).[66] In plants, the so called MoFe protein, a component of nitrogenase, is essential for nitrogen fixation.[67] Toxic levels of molybdenum are rarely attained, as the metal is rapidly eliminated renally from mammalian organisms. In humans, gout, characterized by high levels of uric acid excretion, is more prevalent in regions with high molybdenum concentrations in agricultural soil and plants.[68,69] High levels of exposure to molybdenum as the mineral dust occur in the foundry industry and in molybdenum ore mining. Frequent occurrence of occupational skin diseases (such as dermatitis and

eczema) have been noted in molybdenum production workers where high levels of airborne metal dust are present. Studies in rats with systemic administration of ammonium molybdate show accumulation in skin, with molybdenum mainly bound to collagen. Molybdenum apparently alters the mechanical and chemical properties of collagen, with an inhibitory action on crosslinking in particular.[70-72]

1.3.4 Vanadium

Vanadium occurs in biological systems primarily in the tetravalent and pentavalent forms. In body fluids at pH 4-8 the predominant forms of free vanadium are orthovanadates, HVO_4^{2-} and $H_2VO_4^-$, where its oxidation state is +5. Once inside a cell it is reduced to the +4 state or vanadyl, i.e., VO^{2+}. Both oxidation states have similar biochemical and physiological function. Vanadate competes with phosphate for active sites in phosphate transport proteins, inhibiting the action of phosphates, and also has a pronounced inhibitory action on Na^+/K^+ ATPase activity. As vanadyl, the metal competes with other metal ions for binding sites on metalloproteins.[73] Vanadium is an essential nutrient for higher animals, including humans; it is present in mammalian tissues at concentrations below 1mM.[74] A homeostatic mechanism maintains normal levels in the mammalian organism, and excess is rapidly excreted in the urine.[75] Vanadium deficiency induced in animals suggest that the metal has a function in thyroid hormone metabolism and can mimic growth factors such as epidermal and fibroblast growth factors.[74]

Significant exposure to vanadium occurs only in certain industrial operations: mining, petroleum refining, steel and utilities industries, as fossil fuels; in addition,

certain ores contain this metal. Particularly in times of energy crises when still bottoms of petroleum refining operations are increasingly used in oil-fired, electricity generating plants for their Btu value, accumulated vanadium residues are volatilized as oxides or as carbonyl complexes. Toxicity of vanadium is primarily associated with inhalation of vanadium pentoxide. Chronic exposure gives rise to symptoms of irritation, sometimes delayed, of the upper and lower respiratory tract, and inflammatory changes characterized by cough, wheezing, mucus production, chest tightness, bronchopneumonia, rhinitis, and sore throat; these symptoms collectively described as "boilermaker's bronchitis", can be disabling.[76-78] At the turn of the century, vanadium therapy was widespread in the treatment of tuberculosis, chlorosis, and diabetes. Evidence gathered from that medical use shows that, taken orally, it produces no signs of toxicity, due to poor absorption from the intestine (about 1%) and its relatively rapid excretion (about 60% in the urine within 24 hrs).[73-75] Clinical data indicate that a chronic oral dose of 24-80 mg/day vanadium is well tolerated by most humans.[79]

1.4 Metal Removal & Recovery

1.4.1 Overview

Over the last few decades, extensive research has been carried out in developing techniques and methods for the removal and recovery of heavy metals (toxic and non-toxic) from aqueous systems. The areas of research that have been promising include solvent extraction,[80] floatation techniques, sorption onto solid surfaces, membrane filtration,[81] ion exchange, bio-sorption, phyto-remediation,[82] chemical precipitations, centrifugation, bio-magnetic separations, wet-land construction, and solid-liquid separations. According to the literature and recent developments in metal recovery, some important criteria are kept in mind when designing any new metal removal and recovery system(s). The general criteria are given below:

- High capacity for the target metal ions
- Long usable lifetime & reduction of metal ions to extremely low levels
- Greater mechanical and chemical integrity
- Favorable mass transfer kinetics
- Broad operational pH range
- Selectivity of target metal ions over other metal ions
- Economically viable
- Feasible operation

Although several technologies for the removal of metal ions exist from aqueous systems, the most common methods are solvent extraction (SX), membrane filtration

(MF), and ion exchange (IX).[80,83] SX was initially developed for the purification of uranium for constructing nuclear devices in the 1950's and 1960's.[84] SX is still one of the most frequently used technologies for commercial metal ion separations. SX is now used for many metals including copper, nickel, zinc, cobalt, gallium, molybdenum, tungsten, and vanadium.[85-87] Other recovery systems have been developed that give a better edge over SX for heavy metal recovery. In the case of oxo-anion removal and recovery, coagulation is the most common arsenic and selenium removal technology. Cementation and co-precipitation of the anion species has also been proven to be the most efficient way for arsenic removal. Zero-valent iron particles and/or iron oxyhydroxides (ferrihydrite) are the most widely used media for oxo-anion removal, especially arsenic and selenium.[88] Co-precipitation with ferric chloride works best at pH below 8. Alumina has a narrower effective range (pH 6-8) and activated alumina which works similar to ion exchange resins works best in acidic waters (pH 5.5-6). Ion exchange resins can only remove arsenate effectively. Membrane methods are more expensive than other arsenic removal options and are more appropriate in municipal settings, where very low levels of arsenic are required. The following sections provide a summary of some commercially active techniques. Advantages and disadvantages have been identified.[89]

1.4.2 Solvent Extraction (SX)

Also known as liquid-liquid extraction (LLE), solvent extraction and partitioning, is a method to separate compounds based on their relative solubilities in two different immiscible liquids, usually water and an organic solvent. It is an extraction of a

substance from one liquid phase into another liquid phase. Liquid-liquid extraction is a basic technique in chemical laboratories, where it is performed using a separatory funnel. This type of process is commonly performed after a chemical reaction as part of the work-up. In other words, this is the separation of a substance from a mixture by preferentially dissolving that substance in a suitable solvent. By this process a soluble compound is usually separated from an insoluble compound. Solvent extraction is used in nuclear reprocessing, ore processing, the production of fine organic compounds, the processing of perfumes, and various other industries. A complete solvent extraction process for extracting metals typically comprises of the following four steps:

1. *Extraction* – Transfer of the metal ion from aqueous phase into the organic phase by chemical reaction with an extractant (a ligand selective for the target metal ion) during mixing of solvents.
2. *Scrubbing* – Removal of co-extracted materials for the purpose of increased purity.
3. *Stripping* – Transfer of the metal ion back into a pure aqueous phase for further processing.
4. *Make-up* – Purification by treatment with a third aqueous phase, replenishing lost solvent or extractant, and removal of crud build up.

In solvent extraction, a distribution ratio is often quoted as a measure of how well a species is extracted. The distribution ratio (D) is equal to the concentration of a solute in the organic phase divided by its concentration in the aqueous phase. Depending on the system, the distribution ratio can be a function of temperature, the concentration of chemical species in the system, and a large number of other parameters. Sometimes the

distribution ratio is referred to as the partition coefficient, which is often expressed as the logarithm.

$$D = C_{org} / C_{aq} \quad (1.7)$$

A common extractant that has been widely used for solvent extraction is di(2-ethylhexyl) phosphoric acid (D2EHPA). D2EHPA (**Figure 1.5**) has been used to remove various transition metals from acidic and mine waste solutions. The phosphoric acid portion of the molecule engages in coordination and the hydrocarbon portion ensures solubility in an organic solvent. An example of using D2EHPA is extraction of zinc ion from aqueous solutions at acidic pH. The zinc ion replaces the proton from two D2EHPA molecules at a high pH (around pH 4-5 Zinc is selective). To strip the Zinc from the D2EHPA, sulfuric acid is used, at a strength of about 170g/L.[83a]

$$Zn^{2+}_{(aq)} + 2(D2EHPA)H_{(org)} \longrightarrow 2H^{+}_{(aq)} + Zn^{2+}(D2EHPA)_{2\,(org)} \quad (1.8)$$

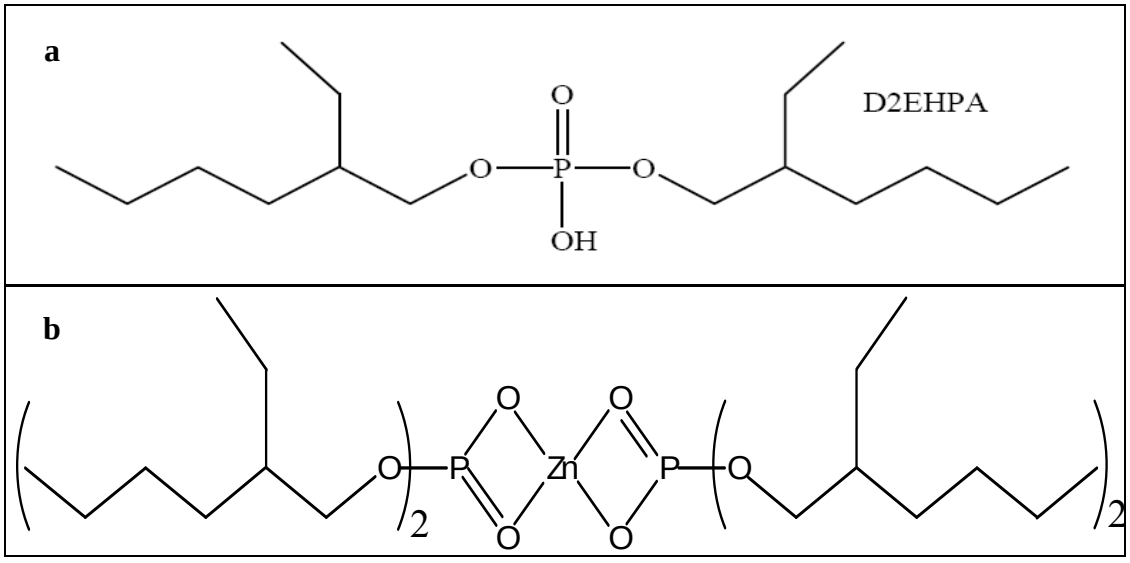

Figure 1.5: (a) Di (2-ethylhexyl) phosphoric acid for solvent extraction (SX); **(b)** Structure of $Zn^{2+}(D2EHPA)_2$.

As a result of this process, Zn^{2+} is transferred from an aqueous phase into an organic phase.[83] To complete the process and maintain charge balance, two equivalents of H^+ transfers from the organic based extractant to the aqueous phase. If the constant for this chemical reaction is greater than one, the extraction of zinc from aqueous phase to the organic phase is favorable. Therefore in SX one typically utilizes the extractant with the highest equilibrium constant for the purpose of increasing efficiency.

SX has many established advantages over the previously prevalent methods such as reduced overall process time, improved primary yields, flexibility and versatility, increased process control, simplicity and detailed understanding of concept. As a result of tailored extractants SX can have a high degree of metal ion selectivity. However, there are also many disadvantages of SX that have led to a growing interest in other technologies. These disadvantages include a finite solubility of extractants and modifiers in the aqueous layer, evaporation of volatile, flammable and often toxic organics, build-up of solid crud at the solid liquid interface, the difficulty of recovering the extracted ion from the organic solvent and the inability of solvent extraction to practically reduce metal ion content in the aqueous phase to negligible levels.[83c]

1.4.3 Ferrihydrite Process

Arsenic removal with metal salts have been shown since at least 1934.[90] The most commonly used salts are aluminum salts such as alum, and ferric salts such as ferric chloride or ferric sulfate. Ferrous sulfate has also been used, but is far less effective.[91,92] Excellent arsenic removal procedures have been reported in laboratories with over 99 % removal under optimal conditions, and residual arsenic concentrations of less than

10μg/L.[93] Full-scale plants typically report a somewhat lower efficiency, from 50 % to over 90 % removal. Among a suite of arsenic and selenium water treatment techniques proposed in the literature, techniques involving the precipitation of iron and immobilization of arsenic and selenium by sorption onto the iron (III) precipitates have received much attention.[88] Ferrihydrite or iron oxyhydroxide process for the removal of arsenic and selenium is the most prevalent system today.[88,89] Introduction of zero-valent iron (ZVI) filings in home filters to treat water is showing great promise.

During coagulation and filtration, arsenic is removed through three main mechanisms mentioned below:[94]

- precipitation: the formation of the insoluble compounds $Al(AsO_4)$ or $Fe(AsO_4)$
- coprecipitation: the incorporation of soluble arsenic species into a metal hydroxide phase
- adsorption: the electrostatic binding of soluble arsenic to the external surfaces of the insoluble metal hydroxide

All three of these mechanisms can independently contribute towards contaminant removal. In the case of arsenic removal, direct precipitation has not been shown to play an important role. However, coprecipitation and adsorption are both active arsenic removal mechanisms. Numerous studies have shown that filtration is an important step to ensure efficient arsenic removal. After coprecipitation and simple sedimentation, hydrous aluminum oxide (HAO) and hydrous ferric oxide (HFO), along with their sorbed arsenic load, can remain suspended in colloidal form. Various researchers have shown that precipitation-coprecipitation and sedimentation without filtration achieved arsenate

removal efficiencies of 40 %; after filtration through a 1.0 micron filter, efficiency was improved to over 96 %. Only marginal improvements were observed by reducing the filter size to 0.1 micron.[92] In field applications, some plants improve arsenic removal with a two-stage filtration system.[95]

The removal of arsenic by ZVI has received increased attention because studies have shown that ZVI has a high arsenic removal capacity. Yet, because arsenic removal mechanisms apparently involve adsorption and possibly coprecipitation, the performance of ZVI is ultimately limited by its initial removal capacity and any additional capacity that may come about after the iron metal corrodes in water. Almost all the studies were conducted at relatively low arsenic concentrations ($\leq$ 1mg/L).[96] Various investigations on the removal of arsenite with ZVI suggests that iron can be used as an effective remedial reagent for in situ remediation of groundwater contaminated with arsenic. However, the abundance of arsenate observed in the solid phase suggests that an unusual surface oxidation process was involved in reducing conditions.[96,97]

1.4.4 Membrane Filtration

Membrane filtration (polymer filtration) is another example of using water soluble chelating complexing agents to selectively extract metals from aqueous solutions.[98] The key to membrane filtration is a semi-permeable membrane that is selective to a particular target metal(s).[99] Membrane filtration has the advantage of removing many contaminants from aqueous systems, including bacteria, salts, and various heavy metals. Certain elements of an aqueous solution will pass through the membrane (permeate), leaving a portion behind (retentate). The factors that determine the composition of permeate and

retentate include solution composition, pH, temperature, membrane material, pore size and more. The size of the dissolved species plays the most important role for membrane separation techniques.

Membranes can be classified into two classes: low-pressure membranes (microfiltration and ultrafiltration); and high-pressure membranes (nanofiltration and reverse osmosis). Low-pressure membranes have larger nominal pore sizes, and are typically operated at pressures of 10-30psi. The tighter high-pressure membranes are typically operated at pressures from 75 to 250psi, or even higher.[100] From figure 1.6 below, it is clear that reverse osmosis (RO) and nanofiltration (NF) membranes have pore sizes appropriate for removal of dissolved arsenic, which is in the 'metal ion' size range. Both RO and NF membranes are most often operated in lateral configurations, in which only a small amount of the raw water (10-15%) passes through the membrane as permeate. In household systems, where only a small amount of treated water is required for cooking and drinking, low recovery rate may be acceptable. Municipal systems achieve higher recovery rates (80 to over 90%) by using multiple membrane units in series.[100]

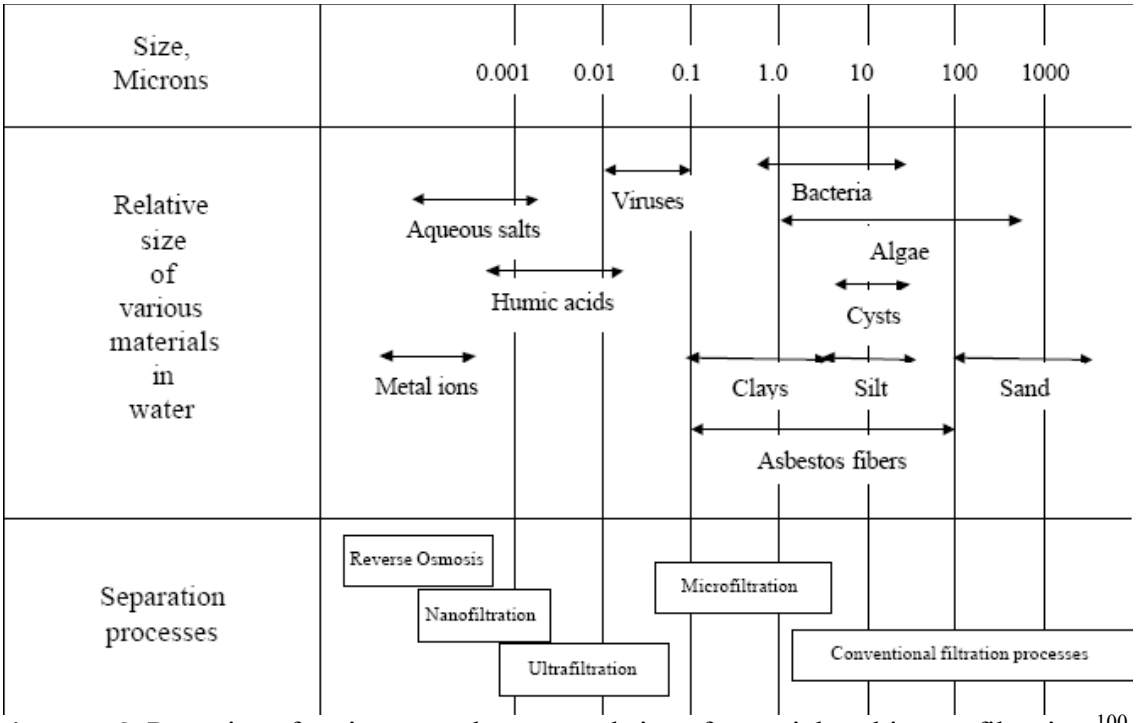

Figure 1.6: Pore size of various membranes, and size of materials subject to filtration.[100]

In recent years, a new generation of RO and NF membranes have been developed that are less expensive and operate at lower pressures, yet allow improved flux and are capable of efficient rejection of both arsenate and arsenite.[101] Researchers have showed that some of the new membranes, operated at pressures ranging from 40-400psi, were able to reject from 96-99% of both arsenate and arsenite in spiked natural waters. This rejection of arsenite is attributed to the relatively large molecular weight of both arsenate and arsenic, rather than charge repulsion.[101] At these high arsenic rejection rates, membrane filtration can result in extremely low arsenic levels in treated water. Arsenic removal was found to be independent of pH and the presence of co-occurring solutes at lower temperatures. Interestingly, the NF membranes performed comparably to the RO membranes, even with lower operating pressures (40-120psi vs. 200-400psi).[101]

Membrane filtration requires a relatively high-quality influent water. Membranes can be fouled by colloidal matter in the raw water, particularly organic matter. High levels of iron and manganese in the influent water can also lead to scaling and membrane fouling. To prevent fouling, reverse osmosis filters are almost always preceded by a filtration step.

In an ideal separation, the target species would be located in high yield in the retentate and the non-target species will be found in high yield in the permeate. If the target and the non-target components do not differ substantially in size, then there will be a low degree of separation of target from the other species. In order to improve the separation, the target species can be bound to a macromolecule so that it now differs substantially in size and molecular weight from the non-target species. Thus, polymers are used to form an ionic interaction or a coordination complex with a target metal ion. The polymer must be water soluble and must have an affinity for the target metal ion in the appropriate aqueous solution. The polymer agent must also have a high molecular weight, chemical and mechanical stability, low cost, low toxicity and it must be possible to strip and reuse the macromolecule for continued use.[102] There are several disadvantages associated with polymer filtration such as polymer sorption into the pores of the membrane which negatively impacts permeate flux. In addition, the sensitivity of macromolecules to colloidal particles can lead to the polymer acting as a flocculent.[102]

Membrane filtration has the advantage of lowering the concentrations of many other components in addition to arsenic. Even ultrafiltration (UF) membranes are able to remove over 99.9% of bacteria, Giardia and viruses. Also, the membrane itself does not accumulate arsenic, so disposal of used membranes would be simple. Operation and

maintenance requirements are minimal: no chemicals need be added, and maintenance would consist of ensuring a reasonably constant pressure, and periodically wiping the membrane clean. The main disadvantages are low water recovery rates (typically only 10-20% of the raw water passes through the membrane), the need to operate at high pressures, relatively high capital and operating costs, and the risk of membrane fouling. Also, particularly with RO, the treated water has very low levels of dissolved solids, and can be very corrosive, and deficient in minerals which can be important micronutrients for humans.[98,101]

1.4.5 Ion Exchange

An ion exchange material permits the exchange of ions on and off a polymeric material (organic ion exchanger) or a crystalline material (inorganic ion exchanger). Synthetic ion exchange resins are widely used in water treatment to remove many undesirable dissolved solids, most commonly hardness, from water. These resins are based on a cross-linked polymer skeleton, called the 'matrix'. At no point during the association or dissociation of ions does the matrix dissolve. This heterogeneous nature of ion exchange materials has been exploited to yield flexible and versatile metal removal processes with many advantages.

Ion exchange resembles sorption. In both ion exchange and sorption a solid extracts a dissolved species. The difference between ion exchange and sorption is the stoichiometric nature of ion exchange. Sorption removes species from solution but does not replace that species by donating to the solution. In contrast, ion exchange must satisfy balance of charge by the stoichiometric transfer of a species back into solution.

Typically IX materials possess a functional group immobilized on a solid support. The solid support or matrix may be organic or inorganic in nature. The most commonly used IX materials are organic IX materials. Organic IX matrixes are comprised of a three dimensional cross-linked polymeric structure onto which functional groups can be attached. The most common matrix that has been used is composed of polystyrene cross-linked with divinylbenzene (**Figure 1.7**). Charged functional groups are attached to the matrix through covalent bonding, and fall into four groups:[89]

- Strongly acidic [e.g. sulfonate, $-SO_3^-$]
- Weakly acidic [e.g. carboxylate, $-COO^-$]
- Strongly basic [e.g. quaternary amine, $-N^+(CH_3)_3$]
- Weakly basic [e.g. tertiary amine, $-N(CH_3)_2$)]

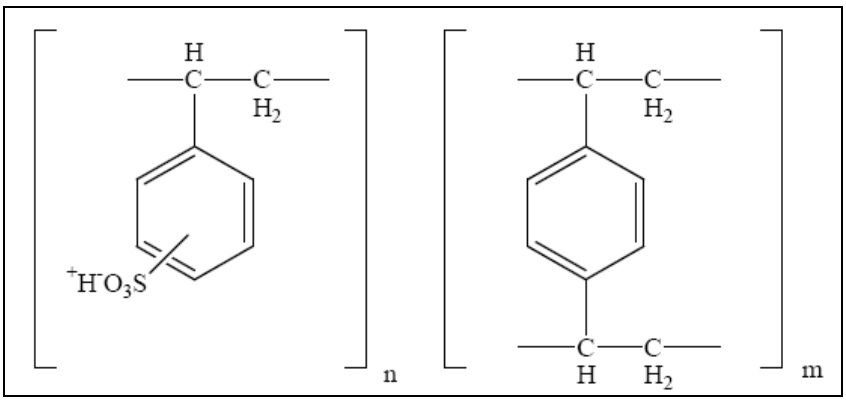

Figure 1.7: A typical example of ion exchange resin is sulfonated polystyrene cross-linked with divinylbenzene.

The acidic resins are negatively charged, and can be loaded with cations (e.g. Na^+), which are easily displaced by other cations during water treatment. This type of cation exchange is most commonly applied to soften hard waters. Conversely, strongly basic resins can be pretreated with anions, such as Cl^-, and used to remove a wide range

of negatively charged species. Literature suggests the following relative affinities of some common anions for a type 1 strong-base anion resins:[89]

$$CrO_4^{2-} >> SeO_4^{2-} >> SO_4^{2-} >> HSO_4^- > NO_3^- > Br^- > HAsO_4^{2-} > SeO_3^{2-} > HSO_3^{3-} > NO^{2-} > Cl^-$$

Different resins will have differing selectivity sequences, and resins have been developed specifically to optimize removal of sulfate, nitrate, and organic matter. Various strong-base anion exchange resins are commercially available which can effectively remove arsenate from solution, producing effluent with less than 1μg/L arsenic. Arsenite, being uncharged, is not usually removed under the same conditions. Analysts have taken advantage of this specificity to develop procedures for analytical differentiation of arsenite and arsenate.[103,104a] Therefore, unless arsenic is present exclusively as arsenate, an oxidation step will be a necessary precursor to arsenic removal.

Conventional sulfate-selective resins are particularly suited for arsenate removal. Nitrate-selective resins also remove arsenic, but arsenic breakthrough occurs earlier. Most commonly, resins are pretreated with hydrochloric acid, to establish chloride ions at the surface, which are easily displaced by arsenic, though the resin can be primed with other anions such as bromide and/or acetate.[104] Packed beds are commonly designed to have an Empty Bed Contact Time (EBCT) of 1.5 to 3 minutes. Arsenate removal is relatively independent of pH and influent concentration. But on the other hand, competing ions, especially sulfate have a strong effect. In low-sulfate waters, ion exchange resins can easily remove over 95% of arsenate, and treat from several hundreds to over a thousand bed volumes before arsenic breakthrough occurs. Accordingly, the

USEPA recommends that ion exchange resins not be used in waters with >120mg/L sulfate or >500mg/L TDS, and will be most effective in waters with even lower sulfate levels (<25mg/L). Ion exchange capacity, analogous to the adsorption capacity is a measure of the number of exchange sites, and is usually measured in milliequivalents (meq) per mL (wet volume, including pore spaces). The operating capacity measures actual performance of resins under environmental conditions, and is always less than the advertised exchange capacity, due to incomplete regeneration and contaminant leakage. Table 1.1 gives a brief summary of various arsenic removal technologies that are commercially available as of date.

Table 1.1: Summary of technologies used for arsenic removal.

Technology	Removal Efficiency		Experience and issues
	As (III)	As (V)	
Coagulation with iron salts	++	+++	Well proven at central level, piloted at community and household levels. Phosphate and silicate may reduce arsenic removal rates. Generates arsenic-rich sludge. Relatively inexpensive.
Coagulation with alum	--	+++	Well proven at central level, piloted at community and household levels. Phosphate and silicate may reduce arsenic removal rates. Optimal over a relatively narrow pH range. Generates arsenic-rich sludge. Relatively inexpensive.
Lime softening	+	+++	Proven effective in laboratories and at pilot scale. Efficiency of this chemical process should be largely independent of scale. Chiefly seen in central systems in conjunction with water softening. Disadvantages include extreme pH and large waste volume generated. More expensive than coagulation methods.
Ion exchange resins	--	+++	Pilot scale in central and household systems, mostly in industrialized countries. Interference from sulfate and TDS. High adsorption capacity

			but poor long-term performance of regenerated media. Waters rich in iron & manganese require pre-treatment to prevent media clogging. Moderately expensive.
Activated alumina	+ / ++	+++	Pilot scale in central and household systems, mostly in industrialized countries. Arsenite removal is poorly understood, but capacity is much less than for arsenate. Regeneration requires strong acid and base and produces arsenic-rich waste. Waters rich in iron & manganese require pre-treatment to prevent media clogging. Moderately expensive.
Membrane methods	-- / +++	+++	Shown effective in laboratory studies in industrialized countries. Further research needed for arsenite removal and efficiency at high recovery rates (low pressure membranes). Pretreatment usually required. Relatively expensive, especially if operated at high pressures.
Fe-Mn Oxidation	?	+ / ++ / +++	Small-scale application in central systems, limited studies in community and household levels. More research needed on which hydro-chemical conditions are conducive for good arsenic removal. Inexpensive.
Porous media adsorbents (iron oxide coated sand, greensand, etc.)	+ / ++	++ / +++	Shown effective in laboratory studies in industrialized countries. Need to be evaluated under different environmental conditions and in field settings. Simple media are inexpensive, advanced media can be relatively expensive.
In-situ immobilization	++	+++	Very limited experience. Long-term sustainability and other effects of chemical injection not well documented. Major advantage is no arsenic-rich wastes generated at the surface. Major disadvantage is the possibility of aquifer clogging. Relatively inexpensive.

Key: +++ Consistently >90% removal
++ Generally 60-90% removal
+ Generally 30-60% removal
-- <30% removal
? Insufficient information

1.4.6 Silica based Adsorbents

An alternative to solvent extraction, membrane filtration, ion exchange resins, and precipitation/co-precipitation are amorphous silica gel polyamine composites (SPCs), as developed and patented by the Rosenberg group at the University of Montana (UM) in cooperation with Purity Systems Inc. (PSI), Missoula, MT, USA.[105] Among the commercialized metal sequestration technologies used today, silica polyamine composites (SPC) are relatively new and have been used very recently in the successful recovery and removal of transition metals, precious metals and mercury from diverse waste streams and mining leaches.[106] SPC materials have exhibited promising extraction capacities for heavy metal ions from aqueous systems. SPCs possess all the advantages that the other mentioned techniques have and direct comparisons with commercially available technologies have demonstrated several advantages over organic ion exchange resins. These advantages include improved mechanical and chemical stability, absence of shrink/swell characteristics, higher operational temperatures, and improved mass transfer kinetics.[107] SPCs are composed of a polyamine attached through a functionalized silane layer to an amorphous silica gel matrix. The polyamine can be further functionalized with metal selective ligands to yield a novel organic/inorganic hybrid chelating material. It is through this strategy that an ion exchange material has been prepared that has both the advantages of organic based ion exchange materials as well as those of inorganic based ion exchange material as shown in **Figure 1.8**.[108] A detailed discussion of SPCs is described in chapter 3.

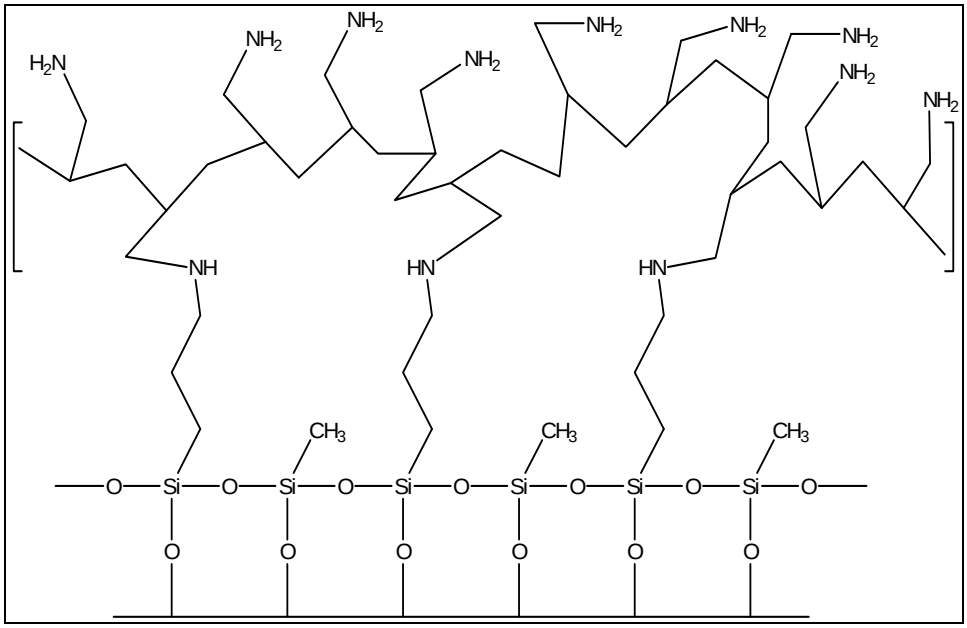

Figure 1.8: Schematic representation of the surface structures of **BP1M** composite (made with a 1:1 mixture of methyl trichlorosilane and chloropropyl trichlorosilane).

1.5 Overall Research Goals

The overall goal of this proposed research is to develop a line of Immobilized Metal silica Polyamine Composites (IMPACs) that can remediate and recover the target metal anions selectively over other competing anions over a wide range of pH and varying concentrations. We have observed that highly charged cations when immobilized on the silica composites, WP2, BPED, and BPAP remove oxo-anions of arsenic and selenium. This represents a new direction for the toxic metal removal/recovery technology. This effort seeks to permanently immobilize metal-cations on the silica polyamine composite resulting in an affinity for the toxic anions arsenate, arsenite, selenate and selenite selectively over the common co-contaminants – sulfate and chloride. We therefore, decided to take the immobilized metal (cation) approach to anion

capture which relies on the fact that highly charged metals (+3 or +4) can be immobilized on a variety of our SPC composites that have a net positive charge. In order to accomplish the above mentioned goal, the following key objectives will be achieved:

- To make a detailed comparison of the performance characteristics of the newly developed Zr^{4+}-BPAP and Fe^{3+}-BPAP with Zr^{4+}-WP2, including anion selectivity, breakthrough and regeneration testing with real mining solutions.
- To develop other IMPAC systems by varying the immobilized metal (Al^{3+}, Ce^{3+}, Ce^{4+}, Th^{4+}) and comparing their anion capacities and selectivity.
- To characterize and compare the newly developed Zr^{4+}-BPED and Fe^{3+}-BPED systems at various pH, anion removal capacity and regeneration.
- To characterize the Co^{3+}-WP1 system with regard to anion selectivity, operational range, capacity and regeneration.
- To evaluate the usable lifetimes of the above mentioned IMPACs.
- To characterize and optimize the performance of a non-IMPAC system, BPQA (a quaternary amine functional group analogous to a polystyrene system available commercially).
- To test the arsenic and selenium selectivity of all the above composites in a low level metal solution with very high levels of sulfate as an interfering ion.
- To evaluate their overall performance and economic viability for the best composite-anion pair(s).
- To characterize and better understand the surface of SPC and IMPAC materials using SEM/EDX, AFM, and XPS.

In order to address these research objectives, we will try to answer the following questions:

1. What are the relative importance of the three factors that govern anion selectivity and operational pH: a) the metal; b) the functional group on the composite; c) the net charge on the composite?
2. What is the degree of leaching of the immobilized metal due to the nature of the functional group it is bound to?
3. What is the best arsenite removal system that can be developed using IMPACs?

Achieving the above objectives will verify the feasibility of using the IMPACs for oxo-anion remediation. This work will possibly lay the foundation for the development of a commercial line of IMPACs.

CHAPTER 2: EXPERIMENTAL

2.1 Materials

Silica gel (267Å pore diameter, 2.82mL/g pore volume, 84.7% porosity, 422m^2/g surface area) was obtained from INEOS enterprises Ltd., UK (previously Crossfield UK) and Qingdao Meigao Ltd., China and were sieved to 150–250 microns. All chemicals were reagent grade and were purchased from Sigma-Aldrich Co. Stock solutions of Zr(IV), Fe(III), Th(IV), Ce(III), Ce(IV), Al(III), As(III), As(V), Se(IV), Se(VI), Mo(VI), V(V), and W(VI) were prepared using zirconyl chloride ($ZrOCl_2 \cdot 8H_2O$), ferric sulfate ($Fe_2(SO_4)_3 \cdot 4H_2O$), thorium nitrate ($Th(NO_3)_4 \cdot xH_2O$), cerium(III) chloride ($CeCl_3 \cdot 7H_2O$), cerium(IV) sulfate ($Ce(SO_4)_2$), aluminum sulfate ($Al_2(SO_4)_3 \cdot xH_2O$), sodium meta-arsenite ($NaAsO_2$), sodium hydrogen arsenate ($Na_2HAsO_4 \cdot 7H_2O$), sodium selenite (Na_2SeO_3), and sodium selenate (Na_2SeO_4), sodium orthovanadate (Na_3VO_4), sodium tungstate ($Na_2WO_4 \cdot 2H_2O$), sodium molybdate ($Na_2MoO_4 \cdot 2H_2O$) respectively. Metal solutions were prepared by dissolving the appropriate quantity of the salt in deionized (DI) water. Solution pH was adjusted from the intrinsic pH, where necessary, using hydrochloric acid and sodium hydroxide. Stripping and recovery of metals were achieved with 2M–H_2SO_4 and/or brine. Metal standards for AA and ICP analysis were obtained from Fisher Scientific Co. Chloropropyl trichlorosilane (CPTCS), and methyl trichlorosilane (MTCS) were used as received from Aldrich Chemicals Co. Poly(ethyleneimine) (PEI, 1200 MW and 25000 MW) were obtained from Aldrich

Chemicals Co. Poly(allylamine) (PAA, 15000 MW) was obtained from Summit Chemicals Inc., NJ, USA. Both the polymers were used in their free base form. The syntheses of all SPCs were repeated several times to ensure reproducibility. Silicon wafers for modification with the SPC chemistry were obtained from University Wafer Inc. (USA). The wafers had a native thermal oxide coating on it; the oxide thickness as per the manufacturer was 1-2nm.

2.2 Instrumentation

Elevated temperature pH measurements were recorded using a Thermo Orion 250A plus pH meter with a Thermo Orion Triode electrode. Ambient pH measurements were done using a VWR sympHony SB20 meter with a Posi-pH1o electrode. Reactions were stirred using an overhead TALBOYS laboratory stirrer (Model 134-1) made by Troemner, LLC. Reaction flasks were heated using a GLAS-COL heating mantle controlled via a STACO Inc. variable autotransformer. Batch capacity experiments were conducted in a Precision Scientific 360° shaker bath (Precision Scientific, Inc., Chicago, IL). Dynamic experiments were conducted with a 5cc column fashioned from a disposable syringe fitted with frits at both ends. Columns were packed dry and the challenge solution was fed by a variable-flow FMI Lab Pump model QG150 (Fluid Metering Inc., Syosset, N.Y.). Metal ion concentrations were determined via a Flame Atomic Absorption (FAA) method using a S2 FAA Spectrometer from SOLAAR, UK and via an Inductively Coupled Plasma/Atomic Emission Spectroscopy (ICP/AES) (Thermo Electron Corp.). The samples that were above the calibration range of the FAA

were diluted using a solution mixture of 2%/2% – HNO_3/KCl. A nitrous oxide/acetylene flame was used to analyze arsenic and selenium. Samples for the ICP/AES analysis were prepared by filtering to get rid of suspended particles and diluting them (where necessary) with a 5%/5% – HCl/HNO_3. The dilutions for FAA and ICP/AES were done in triplicate and standards were analysed after every 10 samples. Elemental analyses (carbon, hydrogen, nitrogen, phosphorus, chlorine, sulfur) were conducted by Schwarzkopf Micro-analytical Laboratory, Woodside, NY, USA. The error in elemental analysis was reported as no more than 0.3% absolute for the elements mentioned above.

2.3 Spectroscopic Characterization

Infrared characterization of modified composites was carried out with a Thermo-nicolet Nexus 670 FT-IR spectrophotometer as KBr pellets. Solid state ^{13}C and ^{31}P CPMAS spectra were obtained on Varian NMR Systems 500MHz spectrometer at 125 and 203MHz respectively and spinning speeds of 5–10KHz. ^{13}C and ^{31}P chemical shifts are reported relative to external tetramethyl silane and external phosphoric acid respectively. The ^{31}P–^{1}H 2D correlation experiment was run using the Lee-Goldberg pulse sequence at a spin rate of 10KHz and resonance frequencies of 206 and 500MHz for phosphorus and proton respectively. Scanning Electron Microscopy/Energy Dispersive X-ray spectroscopy (SEM/EDX) data were obtained on a Hitachi S–4700 Type II. In this technique an electron beam is scanned across a sample's surface and when the electrons strike the sample, X-rays are emitted and detected. The emitted X-ray has an energy characteristic of the parent element. The samples were prepared by

spreading a thin layer of the sample particles on an adhesive carbon tape which was stuck to a metal disc and loaded into the analysis chamber. Initially the samples were observed under a low magnification scan. Specific sites on different silica particles of the same sample were chosen at random and analyzed for their elemental compositions. Reported EDX data are average values of element content obtained by examination of different silica composite particles. Atomic Force Microscopy (AFM) data were obtained on two different AFM instruments: MFP-3D™ Stand Alone AFM (Asylum Research, USA) and MultiMode-V Scanning Probe Microscope (Veeco Instruments, USA). The samples that were analyzed on the MFP-3D AFM were the SPC materials. Whereas the samples that were analyzed on the MultiMode-V were SPC materials and silicon wafers modified with our parented SPC chemistry.

2.4 Hydrated Silica Gel Preparation

Raw silica gels were sieved to ensure particle diameters were in the desired range (150–250μm). 100g of sieved silica gel was added to 400mL of 1.0M–HCl in a 1L three neck round bottom flask. The flask was equipped with an overhead stirrer and a condenser. The contents in the flask were degassed using vacuum (~30mm Hg) while stirring for 15 minutes. After degassing, the mixture in the flask was refluxed at 98°C overnight. The flask was allowed to cool to room temperature and the HCl was filtered off. The silica gel was washed successively with three 400mL water washes and two 400mL methanol washes. After the last methanol wash, the resulting acid washed gel was dried at 120°C in a ventilated oven to a constant mass. A monolayer of water was

introduced on the silica gel's surface by passing air through a side arm flask containing DI water. The humid air (~70% humidity), was then allowed to permeate through the dried silica gel in a 2000mL cylindrical column for 72 hours. The percent mass gain (M) is used to quantify the increase in mass due to the water monolayer. M is calculated using the equation 3.1.

$$M\ \% = \{(M_f – M_i)/M_i\} * 100\ \% \qquad (3.1)$$

M_f is the mass of the modified silica gel, and M_i is the mass of the silica gel prior to modification. Value for water content in an adequately hydrated silica gel was ~7 %.

2.5 Synthesis of CPTCS only Functionalized Silica Gel (CP–Gel)

For the preparation of CPTCS only functionalized silica gel, a 50g quantity of hydrated silica gel was placed in a 500mL three neck round bottom flask equipped with an overhead stirrer. 150mL of hexanes was added to the reaction flask and the resulting mixture was stirred under a constant flow of dry nitrogen. The contents in the flask were degassed using vacuum (~30mm Hg) while stirring for 15 minutes. 150mmol (3mmol/g of hydrated silica gel) of CPTCS was dissolved in 50mL of dry hexanes and added to the reaction flask fitted with a condenser. As the reaction proceeded, HCl gas was evolved and was forced out of the flask through the condenser by the gentle dry nitrogen flow. After 24 hours the reaction was stopped by filtering off the unreacted and excess CPTCS and hexanes. The product was washed three times with 200mL of dry hexanes, and two times with 200mL of methanol. After the final methanol wash, the product was filtered

and dried at 80°C to a constant mass. The mass gain for the modification of hydrated silica gel with CPTCS only was M ~ 20 %.

2.6 Synthesis of MTCS:CPTCS Functionalized Silica Gel (CPM–Gel)

MTCS: CPTCS functionalized silica composites were prepared using three molar ratios of MTCS: CPTCS. In the case of CPTCS only functionalized silica gel, a total of 3mmoles of silanes per gram of silica gel was employed. The silane solution of the requisite molar ratio was prepared in 50mL of hexanes. After this point, the procedure described for CPTCS only silica gel (Section 3.5) was followed. The percent weight gains for the hydrated silica gel functionalized with varying molar ratios of MTCS and CPTCS were in the range M = 9% to M = 15%. Elemental analysis for different ratios of MTCS: CPTCS are shown below.

Table 2.1: Elemental analysis data for MTCS: CPTCS modified silica gel.

Sample	C %	Cl %
0:1	6.26	5.78
7.5:1	3.94	0.73
10:1	3.28	1.4
12.5:1	3.40	1.05

2.7 Synthesis of Silica Polyamine Composite BP1

In a 100mL three neck round bottom flask equipped with a condenser and overhead stirrer, 10g of CP–gel or CPM–gel was added. 25mL of poly(allylamine), 17mL DI water, 10mL methanol were added to the reaction flask. The contents were stirred and degassed under vacuum (30mm Hg) for 15 minutes and then heated to 65°C for 48 hours. The reaction mixture was then cooled, allowed to settle and then the polymer was carefully decanted. The resulting composite was washed five times with 50mL portions of DI water, one 50mL portion of a 1M–NaOH solution, three 50mL portions of DI water, and two 50mL methanol portions. The resulting composite was dried to a constant mass at 70°C. Samples were sent for elemental analysis of carbon, hydrogen, nitrogen, and chlorine). The poly(allylamine) used was a 15,000MW in an aqueous solution containing a mass fraction of 10% polymer. The mass gain for the polymer functionalized silica composite was in the range M = 7 % to M = 14 %. Elemental analysis data is shown below.

Table 2.2: Elemental analysis data for BP1 with differing ratios of MTCS: CPTCS.

Sample	C %	N %
0:1	11.3	2.25
7.5:1	9.16	2.29
10:1	9.9	2.43
12.5:1	9.5	2.55

2.8 Synthesis of Silica Polyamine Composite WP1

In a 100mL three neck round bottom flask equipped with a condenser and overhead stirrer, 10g of CP–gel or CPM–gel was added. 36mL of poly(ethyleneimine), 10mL methanol were added to the reaction flask. The contents were stirred and degassed under vacuum (30mm Hg) for 15 minutes and then heated to 65°C for 48 hours. The reaction mixture was then cooled, allowed to settle and then the polymer was carefully decanted. The resulting composite was washed three times with 50mL portions of DI water, one 50mL portion of 1M–H_2SO_4, three 50mL portions of DI water, one 50mL portion of a 1M–NaOH solution, three 50mL portions of DI water, and two 50mL methanol portions. The resulting composite was then dried to a constant mass at 70°C. Samples were sent for elemental analysis of carbon, hydrogen, nitrogen, and chlorine). The poly(ethyleneimine) used was a 25,000MW in an aqueous solution containing a mass fraction of 18% polymer. The mass gain for the polymer functionalized silica composite was in the range M = 12 % to M = 20 %. Elemental analysis data is shown below.

Table 2.3: Elemental analysis data for WP1 with differing ratios of MTCS: CPTCS.

Sample	C %	N %
0:1	13.8	5.92
12.5:1	11.79	5.31

2.9 Synthesis of Modified Silica Polyamine Composite WP2

In a 100mL three neck round bottom flask equipped with a condenser and overhead stirrer, 10g of the composite WP1 or WP1M was added. 20g of sodium chloroacetate was added with 50mL of DI water. The mixture was stirred and degassed for 15 minutes under vacuum (30mm Hg). It was then heated at 65°C for 24 hours. After an hour of starting the reaction 1mL of 8M–NaOH was added drop wise while monitoring the pH. pH of the reaction was maintained around 9. A further 1mL of 8M–NaOH was added in a similar manner after 18 hours. The maximum recorded pH of the reaction was 10. After 24 hours, the flask was cooled and filtered. The composite was washed three times with 50mL portions of DI water, one 50mL portion of 2M–H_2SO_4, three 50mL portions of DI water, and two 50mL methanol portions. Finally the composite was dried to a constant mass at 70°C. The reaction was repeated for reproducibility and the mass gain was calculated to be M = 12 % to M = 18 %.

IR spectra (KBr pellet): 1640cm^{-1} (υ–COOH). CPMAS ^{13}C-NMR: δ174.06 (–CO_2H), δ54.78 (–NH–**C**H_2–, **C**H_2, **C**H from polymer), δ-0.10 (Si–**C**H_3, for WP2M only). Elemental analysis data is shown below.

Table 2.4: Elemental analysis data for WP2 with differing ratios of MTCS: CPTCS.

Sample	C %	N %
0:1	15.14	3.88
12.5:1	15.64	4.24

2.10 Synthesis of Phosphonic Acid Modified Silica Polyamine Composite BPAP[106]

10g of BP1 or BP1M composite was mixed with a reagent solution of 30mL–2M–HCl and 10g of phosphorus acid (H_3PO_3) in a 250mL flask equipped with an overhead stirrer. The flask was heated to 95°C, and 9mL of formaldehyde (CH_2O) solution (37.7%) was gradually added with stirring. The reaction mixture was heated at 95°C for 24 hours. The flask was cooled and the product was filtered. The resulting composite was washed three times with 40mL of water, once with 40mL of 1M–NaOH, three times with 40mL of water, once with 40mL of 1M–H_2SO_4, two more times with 40mL of water, twice with 40mL of methanol and dried to a constant mass at 70°C. A mass gain of 20 % and 22 % was obtained starting with BP1 and BP1M respectively.

Elemental Analysis: BPAP made from BP1: 14.20%C, 3.03%H, 3.36%N, 4.34%P.

BPAP made from BP1M: 12.08%C, 2.99%H, 2.21%N, 5.56%P.

CPMAS ^{31}P-NMR: δ6.7. CPMAS ^{13}C-NMR: δ59.27 (–NH–**C**H_2–PO_3H_2), δ44.90 (**C**H_2, **C**H from polymer), δ28.19 (Si–**C**H_2), δ-5.23 (Si–**C**H_3, for BPAPM only).

2.11 Synthesis of EDTA Modified Silica Polyamine Composite BPED

EDTA anhydride was first prepared for the synthesis of the modified composite BPED. 27g of EDTA was placed in a three neck round bottom flask with 46mL of pyridine under a gentle flow of nitrogen gas. 36mL of acetic anhydride was then added to the reaction flask and then the mixture was stirred and heated at 65°C for 24 hours. The resulting product was then cooled and filtered under a stream of nitrogen. It was then washed with 200mL of acetic anhydride and 200mL of diethyl ether under high

vacuum and nitrogen. After drying the resulting EDTA anhydride was weighed for decrease in weight due to loss of water. The resultant EDTA anhydride was stored under nitrogen and sealed tight for future use.

For the modification of BP1M (7.5 MTCS: 1 CPTCS) with EDTA anhydride, 10g of BP1M was kept in a three neck round bottom flask fitted with a condenser. 20g of EDTA anhydride and 80mL of ethanol/acetic acid mixture (1:1 ratio) was added to the flask. The reaction mixture was stirred and degassed for 15 minutes under vacuum (30mm Hg). After degassing, the mixture was heated at 70°C for 24 hours. After completion of the reaction, the contents of the flask were cooled and filtered. The contents were then washed with one 50mL portion of 4M–NH_4OH, three 50mL portions of DI water, one 50mL portion of 2M–H_2SO_4, three 50mL portions of DI water, and finally two 50mL portions of methanol. The contents were dried to a constant mass at 70°C. A mass gain of 35 % was obtained starting with BP1M.

Elemental Analysis: BPED made from BP1M: 19.97 % C, 3.26 % H, 5.24 % N.

IR spectra (KBr pellet): 1640cm^{-1} (υN–CO), 1750cm^{-1} (υ–COOH).

CPMAS ^{13}C NMR: δ168 (–CH_2**C**OOH, –NH(**C**O)CH_2NH), δ53.15 (–NH**C**H_2COOH) δ31.8 (PAA **C**H_2, PAA **C**H), δ9.3 ($Si(O_2)$(**C**H_2)$_3$NH–), δ-6.4 ($Si(O_2)$**C**H_3).

2.12 Synthesis of Modified Silica Polyamine Composite BPQA

Two different methods were used in the preparation of BPQA. Both the methods are described below:

2.12.1 BPQA Modified Using Methyl Iodide[109]

10g of BP1 was placed in a three neck round bottom flask equipped with an overhead stirrer and a condenser. 60mL of THF (Tetrahydrofuran) was added and the mixture was stirred. Once stirring started, the contents were degassed for 15 minutes under vacuum (30mm Hg). 17mL of methyl iodide (MeI) was added slowly while heating. The flask was then heated and the temperature was maintained at 65°C for 24 hours. The contents were then cooled and filtered and washed twice with 50mL portions of THF, twice with 50mL portions of DI water, once with 50mL of 6M–HCl, twice with 50mL portions of DI water, and twice with 50mL of acetone. The resulting composite was then dried to a constant mass at 70°C. The mass gain observed was approximately 10 %. To get a better quaternary nitrogen site, the effect of solvent was also studied by using dioxane instead of THF.

Elemental analysis: BPQA made from BP1 (THF): 14.27 %C, 3.41 %H, 2.65 %N.

BPQA made from BP1M (Dioxane): 12.81 %C, 3.54 %H, 3.12 %N.

2.12.2 BPQA Modified Using Dimethyl Sulfate

In a 100mL in a three neck round bottom flask equipped with an overhead stirrer and a condenser, 10g of BP1 was placed. A reagent mixture of 10g Na_2CO_3 and 60mL of DI water was added to the flask. The contents of the reaction flask were stirred and degassed under vacuum (30mm Hg). 25mL of $(CH_3)_2SO_4$ was gradually added and the contents were heated at 95°C for 24 hours. The flask was then cooled and filtered. The contents were then washed with three 50mL portions of DI water, two 50mL portions of

brine, twice with 50mL portions of DI water, once with 50mL of 1M–HCl, twice with 50mL portions of DI water and twice with 50mL portions of acetone. The resulting composite was then dried to a constant mass at 70°C. The mass gain observed was approximately 6 % to 11 %.

Table 2.5: Elemental analysis data for BPQA with differing ratios of MTCS: CPTCS.

Sample	C %	H %	N %	Cl %
7.5:1	14.53	3.39	2.62	4.71
10:1	11.71	2.81	2.20	4.30
12.5:1	12.29	2.55	2.24	3.90

2.13 Synthesis of Modified Silica Polyamine Composite BPQO

10g of BP1 was placed in a 100mL in a three neck round bottom flask equipped with an overhead stirrer and a condenser. 30mL of octyl bromide ($C_8H_{17}Br$) was added to the flask with 50mL dioxane. 25mL of triethylamine was added to the reaction flask. The contents of the flask were stirred and degassed under vacuum. The contents were then heated at 90°C for 24 hours. After completion of the reaction, the contents were washed with three 50mL portions of dioxane, two 50mL portions of DI water, once with 50mL of brine, twice with 50mL portions of DI water, once with 50mL of 1M–HCl, twice with 50mL portions of DI water and twice with 50mL portions of acetone. The resulting composite was then dried to a constant mass at 70°C. The mass gain observed was approximately 24 % to 40 %.

Table 2.6: Elemental analysis data for BPQO with differing ratios of MTCS: CPTCS.

Sample	C %	H %	N %	Cl %
0:1	22.74	4.38	2.66	6.23
7.5:1	29.93	5.32	2.35	5.91

2.14 Synthesis of EDTA Modified Silica Polyamine Composite BPQDD

5g of BP1 was placed in a 100mL in a three neck round bottom flask equipped with an overhead stirrer and a condenser. 11mL of octyl bromide ($C_8H_{17}Br$) was added to the flask with 20mL dioxane. 10mL of triethylamine was added to the reaction flask. The contents of the flask were stirred and degassed under vacuum. The contents were then heated at 90°C for 24 hours. After completion of the reaction, the contents were washed with three 50mL portions of dioxane, two 50mL portions of DI water, once with 50mL of brine, twice with 50mL portions of DI water, once with 50mL of 1M–HCl, twice with 50mL portions of DI water and twice with 50mL portions of acetone. The resulting composite was then dried to a constant mass at 70°C. The mass gain observed was approximately 26 %.

2.15 Synthesis of IMPAC Zr^{4+}-WP2

In a 100mL round bottom flask, 10g of the WP2 composite was mixed with a reagent solution containing 60mL of 1N–HCl and 4.36g of $ZrOCl_2 \cdot 8H_2O$. The reaction mixture was degassed under vacuum and stirred at room temperature for 24 hours. The reaction mixture was degassed under vacuum (30mm Hg) and stirred at room temperature

for 24 hours. After 24 hours the product was filtered. The resulting composite was washed once with 50mL of 2N–HCl, two times with 50mL portions of water, and twice with 50mL portions of methanol and dried to a constant mass at 70°C. The zirconium loading on the composite was determined by analyzing the zirconium feed solution and the final zirconium solutions including all the washes performed. The analysis of zirconium was done via an ICP/AES method. The zirconium loading on WP2 was found to be 1.02mmol/g which fits well with a mass gain of 18 %.

Elemental analysis: Zr-WP2M: 12.82 %C, 2.99 %H, 3.44 %N.

CPMAS ^{13}C-NMR: δ166.99 (–CO_2H), δ48.38 (–NH–**C**H_2–, **C**H_2, **C**H from polymer), δ-5.71 (Si–**C**H_3, for WP2M only).

2.16 Synthesis of IMPAC Zr^{4+}-BPAP

In a 100mL round bottom flask, 10g of the BPAP composite was mixed with a reagent solution containing 40mL of 1N–HCl and 4.24g of $ZrOCl_2 \cdot 8H_2O$. The reaction mixture was degassed under vacuum (30mm Hg) and stirred at room temperature for 24 hours. After 24 hours the product was filtered. The resulting composite was washed once with 50mL of 2N–HCl, two times with 50mL portions of DI water, and twice with 50 mL portions of methanol and dried to a constant mass at 70°C. The zirconium loading on the composite was determined by analyzing the zirconium feed solution and the final zirconium solutions including all the washes performed. The analysis of zirconium was done via an ICP/AES method. The zirconium loading on BPAP was found to be 1.12mmol/g which fits well with a mass gain of 17 %. CPMAS ^{31}P-NMR: δ2.4.

Elemental analysis: Zr-BPAPM: 10.1 %C, 2.72 %H, 1.58 %N, 4.80 %P, 3.35 %Cl.

2.17 Synthesis of IMPAC Fe^{3+}-BPAP

In a 100mL round bottom flask, 10g of the BPAP composite was mixed with a reagent solution containing 50mL of DI water and 15g of $Fe_2(SO_4)_3 \cdot 4H_2O$. The reaction mixture was degassed under vacuum (30mm Hg) and stirred at room temperature for 24 hours. After 24 hours the product was filtered. The resulting composite was washed once with 50mL of 2M–HCl, two times with 50mL of DI water, and twice with 50mL of methanol and dried to a constant mass at 70°C. The iron loading was determined by analyzing the iron feed solution and the final iron solutions including all the washes performed. The analysis of iron was done using the flame atomic absorption (FAA) method. The iron loading on BPAP was found to be 0.98 mmol/g which fits well with a mass gain of 20 %.

2.18 Synthesis of IMPAC Th^{4+}-BPAP

In a 100mL round bottom flask, 10g of the BPAP composite was mixed with a reagent solution containing 50mL of DI water and 10g of $Th(NO_3)_4 \cdot x$H2O. The reaction mixture was degassed under vacuum (30mm Hg) and stirred at room temperature for 24 hours. After 24 hours the product was filtered. The resulting composite was washed once with 50mL of 1M–H_2SO_4, two times with 50mL of DI water, and twice with 50mL of acetone and dried to a constant mass at 70°C. The thorium loading was determined by

analyzing the thorium feed solution and the final thorium solutions including all the washes performed. The analysis of thorium was done using the ICP/AES method. The thorium loading on BPAP was found to be 0.60 mmol/g which fits well with a mass gain of 30 %.

2.19 Synthesis of IMPAC Ce-BPAP

2.19.1 Synthesis of IMPAC Ce^{3+}-BPAP

In a 100mL round bottom flask, 10g of the BPAP composite was mixed with a reagent solution containing 60mL of DI water and 2.8g of $CeCl_3 \cdot 7H2O$. The reaction mixture was degassed under vacuum (30mm Hg) and stirred at room temperature for 24 hours. After 24 hours the product was filtered. The resulting composite was washed once with 60mL of 1M–HCl, two times with 60mL of DI water, and twice with 50mL of acetone and dried to a constant mass at 70°C. The cerium loading was determined by analyzing the cerium feed solution and the final cerium solutions including all the washes performed. The analysis of cerium was done using the ICP/AES method. The cerium (III) loading on BPAP was found to be 0.20 mmol/g which fits well with a mass gain of 4 %.

2.19.2 Synthesis of IMPAC Ce^{4+}-BPAP

In a 100mL round bottom flask, 10g of the BPAP composite was mixed with a reagent solution containing 50mL of DI water and 1.7g of $Ce(SO_4)_2$. The reaction mixture was degassed under vacuum (30mm Hg) and stirred at room temperature for 24

hours. After 24 hours the product was filtered. The resulting composite was washed once with 50mL of 1M–H_2SO_4, two times with 50mL of DI water, and twice with 50mL of acetone and dried to a constant mass at 70°C. The cerium loading was determined by analyzing the cerium feed solution and the final cerium solutions including all the washes performed. The analysis of cerium was done using the ICP/AES method. The cerium (IV) loading on BPAP was found to be 0.3 mmol/g which fits well with a mass gain of 5 %.

2.20 Synthesis of IMPAC Al^{3+}-BPAP

10g of the BPAP composite was mixed with a reagent solution containing 50mL of DI water and 2.2g of $Al_2(SO_4)_3 \cdot xH_2O$ in a 100mL three neck round bottom flask. The reaction mixture was degassed under vacuum (30mm Hg) and stirred at room temperature for 24 hours. After 24 hours the product was filtered. The resulting composite was washed once with 50mL of 1M–H_2SO_4, two times with 50mL of DI water, and twice with 50mL of acetone and dried to a constant mass at 70°C. The aluminum loading was determined by analyzing the aluminum feed solution and the final aluminum solutions including all the washes performed. The analysis of aluminum was done using the ICP/AES method. The aluminum (III) loading on BPAP was equivalent to a mass gain of 3 %.

2.21 Synthesis of IMPAC Zr^{4+}-BPED

In a 100mL round bottom flask, 5g of the BPAP composite was mixed with a reagent solution containing 40mL of 1M–HCl and 5.0g of $ZrOCl_2 \cdot 8H_2O$. The reaction mixture was degassed under vacuum (30mm Hg) and stirred at room temperature for 24 hours. After 24 hours the product was filtered. The resulting composite was washed once with 50mL of 2M–HCl, two times with 50mL of DI water, and twice with 50mL of methanol and dried to a constant mass at 70°C. The zirconium loading was determined by analyzing the zirconium feed solution and the final zirconium solutions including all the washes performed. The analysis of zirconium was done using the ICP/AES method. The zirconium (IV) loading on BPAP was found to be 1.06 mmol/g which fits well with a mass gain of 17 %.

2.22 Synthesis of IMPAC Fe^{3+}-BPED

5g of the BPAP composite was mixed with a reagent solution containing 50mL of DI water and 29g of $Fe_2(SO_4)_3 \cdot 4.6H_2O$ in a 100mL three neck round bottom flask. The reaction mixture was degassed under vacuum (30mm Hg) and stirred at room temperature for 24 hours. After 24 hours the product was filtered. The resulting composite was washed once with 50mL of 2M– H_2SO_4, two times with 50mL of DI water, and twice with 50mL of methanol and dried to a constant mass at 70°C. The iron loading was determined by analyzing the iron feed solution and the final iron solutions including all the washes performed. The analysis of iron was done using the FAA method. The iron

(III) loading on BPAP was found to be 1.16 mmol/g which fits well with a mass gain of 9 %.

2.23 pH Profiles

pH profiles were performed on arsenite, arsenate, selenite, selenate, molybdate, tungstate, and vanadate via equilibrium batch tests. The pH of the challenge solutions was adjusted with hydrochloric acid. The target metal concentrations in challenge solutions were typically 1.0g/L to 1.5g/L. Batch equilibrium tests were conducted by adding 0.2g of a specific SPC to 20mL of the metal solution(s) at the selected pH values. To ensure full equilibration, the metal solutions and SPC mixtures were placed in a 360° shaker. After 24 hours the mixtures were removed from the shaker and allowed to settle. Each supernatant was extracted and diluted as necessary with a nitric acid / KCl solution (2% / 2%) for analysis using FAA. In case of ICP analysis the diluent used was 5%. All pH profile experiments were performed in triplicate.

2.24 Concentration Dependent Isotherms

In order to assess the applicability of the Langmuir and Freundlich isotherm models to SPC metal chelation, concentration dependant adsorption isotherms were performed. Isotherms were obtained by batch experiments as described in section 3.15. Metals investigated include As^{5+}, Zr^{4+}; the metal ion concentrations were varied while keeping the pH steady and samples were shaken in a 360° shaker for 24 hours. Langmuir

and Freundlich parameters were obtained from the appropriate linear regressions for the metal ion(s). The details of these models are described in the chapter 4. All concentration dependent isotherms were performed in triplicate.

2.25 Dynamic Adsorption and Elution Studies

Metal ion breakthrough experiments and consequent stripping was carried out by packing a 5mL column with SPC. The composite was packed using frits at both ends and challenge solutions were run from bottom to top through the column using a variable flow pump. The flow rate was held constant at 1mL/min to 2.5mL/min (0.1 to 0.5 column volume/min). Column experiments were also carried out using a 10mL adjustable Omnifit glass column with a top to bottom flow for these columns. Columns were then conditioned for metal ion extraction by passing the following solutions through the column(s): 20mL DI H_2O, 30mL 2M–H_2SO_4, 100mL DI H_2O. For SPC materials such as BP1 and WP1 that require base regeneration a further 30mL of 4M ammonia solution and 100mL DI H_2O were passed through the column. Acid is used to remove impurities from the packed composite and the ammonia is used to deprotonate the polymer amines to facilitate sorption. Columns were then treated with a metal ion contaminated feed solution adjusted to the necessary pH. All columns were then rinsed with 20mL DI water, stripped with 30mL – 50mL of 2M–H2SO4 and rinsed again with 100mL DI water. The rinse water used in all the cases was DI water. Eluent fractions were collected in 5mL or 10mL aliquots beginning with the first 5mL or 10mL of the challenge solution that passes through the column. The fractions were preserved with

one drop of concentrated HNO_3 and analyzed by FAA and/or ICP/AES. All breakthrough experiments were run three times unless otherwise stated. Also, the acid solutions used were adequate for complete recovery of the metal ions off the column unless otherwise stated.

2.26 Longevity Studies

Experiments for testing the longevity and lifeline of the composites ZrBPAP and BPQA were done in a similar fashion as that for dynamic adsorption studies. However, the longevity testing was done in an automatic setup using a 10mL column with an internal diameter of 0.78cm and a flow rate of 1mL/min at pH6. The automatic setup is a four-way solenoid switch where the flow solutions are switched in the order – rinse > feed > rinse > acid strip > rinse (**Figure 2.1**). The cycle was run 1001 times to test for the lifeline of the composite. ZrBPAP was packed tightly using frits at both the ends and the arsenate feed concentration used was 1.0g/L. The acid used for the strip was 2M–H_2SO_4 and deionized water was used for all the rinses. After the 100^{th} and the 1001^{st} cycles, the column was removed from the automatic setup and was tested for capacity by the dynamic breakthrough test described above.

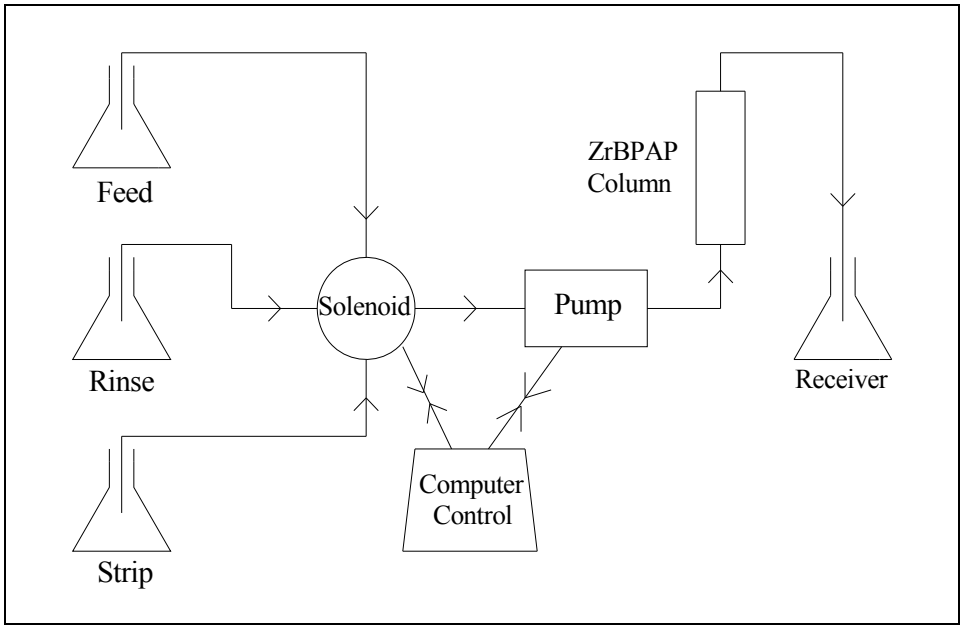

Figure 2.1: Schematic diagram of apparatus used for longevity testing of Zr-BPAP.

2.27 Silicon Wafer Surface Modification

As the sample chamber area for the AFM instrument was 11mm x 11mm, the silicon wafers were cut into 1cm x 1cm squares or smaller using a diamond scribe (Thorlabs Inc.) to ensure that they fit into the sample chamber. Each of the silicon wafer squares was sonicated with 100% ethanol and chloroform for 20 minutes to clean the surface and to form a hydrophilic layer. After sonication the surface of the wafers were dried with a steady flow of nitrogen and air. Once the wafers were clean and dry, they were subjected to the silanization reaction as per the CP gel procedure for SPCs. Although, the silane ratios were maintained constant, the amount and time of the reaction were altered in order for the silicon wafer surface to be silanized. The reaction time was reduced to 2 hours for the silanization step and the washes were done by spraying the

solvent on the wafer surfaces for a few seconds. The wafers were dried as usual using a steady flow of nitrogen. The reaction of the silanized wafer with the polyamine was done much the same way as the silanization reaction step. The reaction time was 2 hours. The prepared wafers were then stored in a nitrogen atmosphere until it was analyzed under the AFM.

2.28 Error Analysis

Every measurement has a degree of uncertainty associated with it. The determination of the degree of uncertainty can be difficult and requires additional effort on the part of the researcher. Nevertheless, evaluation of the uncertainty cannot be neglected because a measurement of totally unknown reliability is worthless. The instrument uncertainties were overcome by calibrating them before operation. The uncertainties in reaction methods, analysis methods were overcome by performing them in triplicate and making sure that concordant values were obtained. Personal judgements and mistakes such as dilution errors, improperly filtered samples for analysis, etc were assigned a maximum standard deviation of 3%. Random errors or random fluctuations in results occur when replicate experimental data are collected. The specific causes were unknown because they have many sources, none large enough to be identified or detected. However, errors in samples analyzed by elemental analysis were 0.3% (provided by Schwarzkopf Microanalytical Laboratories, Inc., and Galbraith Laboratories, Inc.). The relative standard deviation between the triplicate for the samples analyzed by the FAA Spectrometer and the ICPAES were used as errors, respectively. In most cases the errors

were $\leq$ 3%. Any samples that had an error > 5% were reanalyzed with a fresh calibration of the instrument and method used.

CHAPTER 3: POLYMER SURFACE INTERFACE OF SPCs

3.1 Introduction

Depending on the method of production, silica gel particles can have an irregular of spherical shape. The silica gels used for SPC synthesis include amorphous gels that have particle sizes ranging from 30μm – 1000μm, average pore diameters of 8nm – 30nm, pore volumes of 0.8mL/g – 1.5mL/g and surface areas of $250m^2/g$ – $425m^2/g$. For ion exchange materials, the choice of particle size is a trade off between mass transfer kinetics and back pressure during column operations. Decreased particle size promotes improved mass transfer kinetics which allows increased flow rates during column processes. However, an important consequence of smaller particle sizes is greater pressure drops across the column. Large pressure drops across the column requires more energy for pumping when ion exchange resins are employed commercially. Increased particle size has been shown to reduce the metal ion uptake capacity per unit of material as a result of increase in the interstitial space between particles and decreased surface area. SPC materials prepared from raw amorphous silica gel in the range of 150μm – 250μm diameter were initially found to be a reasonable compromise, but more recently particle size range of 350μm – 650μm are being used commercially. In comparison, polymeric ion exchange resins are typically in the range of 250μm – 800μm in diameter.[110]

Table 3.1: Physical characteristics of silica gels used to date in the synthesis of SPCs in the laboratory.

Silica Gel	Diameter (μm)	Pore Diameter (nm)	Pore Volume (mL/g)	Porosity (%)	Surface Area (m^2/g)
Crosfield (Ineos)	150-250	10	2.82	84.7	422
Qingdao Meigao	150-250	20	2.86	85.3	303
Qingdao Meigao	350-650	15	1.30	>80	320

3.2 Synthesis of SPCs

The initial steps for the preparation of SPCs include sieving the silica gel so that the particle diameter is between 150μm – 250μm and washing with 1M–HCl to remove any contaminants (such as sodium ions). The cleaned silica gel is then dried and rehydrated to obtain a monolayer of water on its surface (6-10% by water weight). Previous studies on the development of HPLC columns have identified that a humidifying step promotes lateral polymerization of a silanizing agent which in turn produces a more fully silanized surface.[111] Thus, for the preparation of SPC materials, the hydration step facilitates lateral polymerization of the silanes. Chloropropyltrichlorosilane (CPTCS) is a tri-functional silane that reacts with readily available silanol sites producing a polymeric Si-O-Si($(CH_2)_3$Cl)-O- layer.[112]

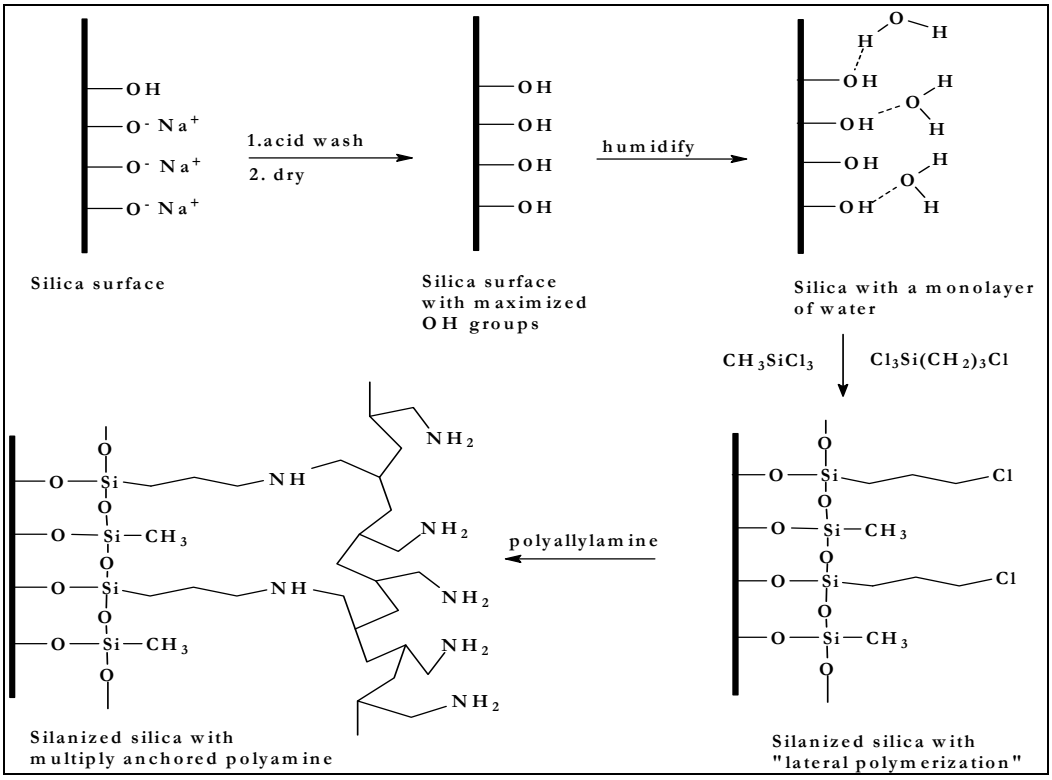

Figure 3.1: The patented synthetic pathway used for the production of SPCs.

For each CPTCS that is reacted with the hydrated silica gel, three equivalents of HCl is released. Once the tri-functional silane is attached to the hydrated silica gel the weight gain for the silanization step is approximately 13%. The ^{29}Si cross polarization/magic angle spinning (CP/MAS) spectrum of amorphous silica gel after treating it with CPTCS is shown in **Figure 3.2**. The assignments shown are based on earlier work done by Wirth *et al.*[111a] All the species expected on the surface of the silanized gel are resolved: 1) the bulk siloxane; 2) the unreacted surface silanols; 3) the geminal silanols ((-O-)Si(OH)$_2$R); 4) the reagent silanols ((-O-)$_2$Si(OH)R); 5) the reagent siloxanes ((-O-)$_3$SiR).[111c]

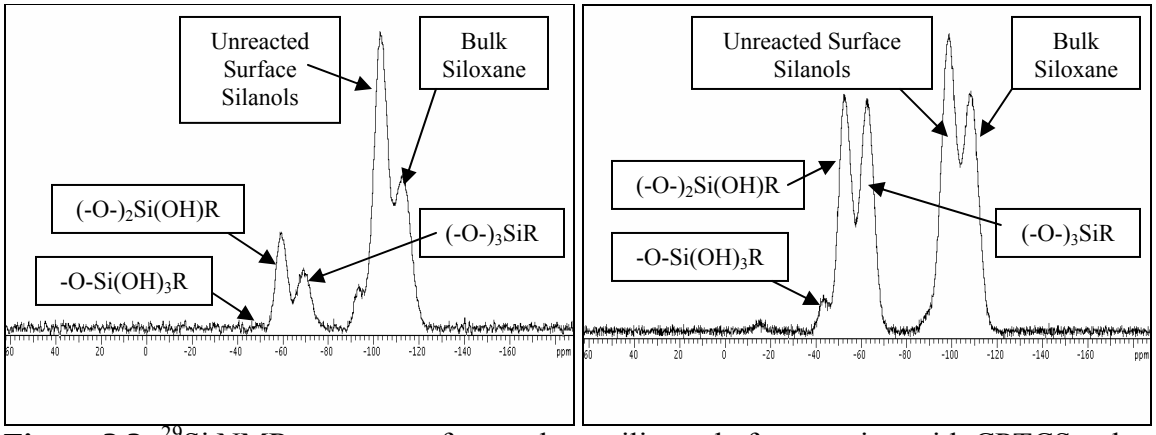

Figure 3.2: ^{29}Si NMR spectrum of amorphous silica gel after reaction with CPTCS only (left)and 7.5:1 MTCS:CPTCS (right).

The non-ideal nature of the silanization process is clearly illustrated by the ^{29}Si NMR spectrum. The presence of unreacted silanols (including geminal) is an indication of the imperfect nature of the silanization on the silica gel surface. Silanes are typically used to impart a degree of hydrophilicity or hydrophobicity on a solid surface.[111a] Regardless of these flaws, silica gels functionalized with chloropropyl moieties (CP Gel), have high silane coverage (45-55% based on the fact that all silica gels have 8-9μmol/m^2). The silane coverage has been found to be approximately 1.5mmol of silanes per gram of functionalized silica gel. The resultant SPCs show excellent stability when compared to other ion exchange materials.[112]

The chloropropyl groups then undergo a nucleophilic attack by the amino groups of a polyamine, as shown in **Figure 3.3**. The polymers that have been used for this project are polyallylamine and polyethyleneimine. The resultant composites that are produced after reacting with the polyamines are named BP-1 and WP-1, respectively. This produces a robust C-N attachment of polyamine to the amorphous silica gel and

releases HCl as a by-product of the reaction. The progress of the reaction can be monitored by pH measurements.

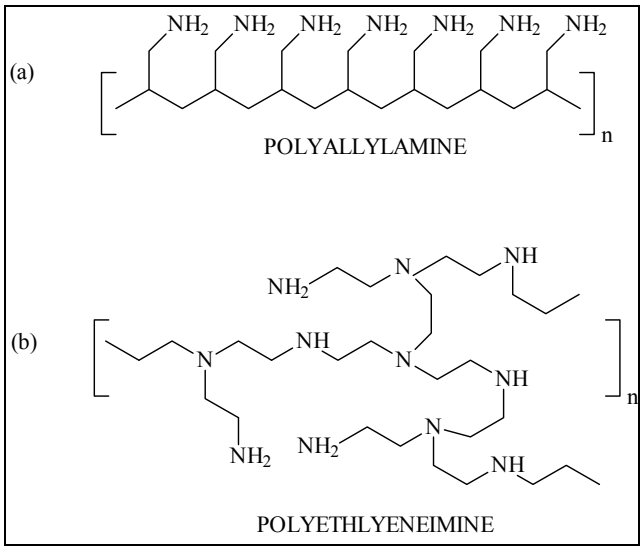

Figure 3.3: The two water soluble polymers that are typically used in the preparation of SPC materials. (a) Polyallylamine (PAA), MW = 15,000; (b) Polyethyleneimine (PEI), MW = 1,200 – 25,000.

The modification of amorphous silica surfaces with functional silane moieties has been researched extensively in the last decade with promising outcomes.[111a] Traditionally, silanes that are used for this purpose are halo-alkyl trichlorosilanes. Different functional silanes have been utilized and each varies in relative reactivity with the silica surface in the order mentioned below:[111b]

$$Si\text{-}NR_2 > Si\text{-}Cl > Si\text{-}NH\text{-}Si > Si\text{-}O(CO)CH_3 > Si\text{-}OCH_3 > Si\text{-}OC_2H_5$$

The advantage of using less reactive silanes ($Si\text{-}OCH_3$ or $Si\text{-}OC_2H_5$) is greater control of the silanization process, as well as creating less toxic and easy to handle byproducts. In general, more reactive silanes have been observed to give better surface silane coverage (mol of silane/m^2 of silica gel). For the production of SPC materials, it is important to

have the highest silane coverage in order to protect the surface from chemical degradation.[83]

The basic structure of a SPC is shown in **Figure 3.1**. A weight gain of approximately 15-20% of the initial silica gel weight is observed, depending on the polymer used, the silica gel used and the reaction conditions applied. The resulting SPC has a higher density compared to the raw silica gel. The surface area that is contained within the pores of the silica gel is greater than 95%. Addition of CPTCS and polymers reduces the surface area and the pore volume of the SPC. Depending on the silica gel type, the polyamine used, and the pendant functional group, the density of SPC ion exchange materials are typically in the range of 0.50g/mL to 0.70g/mL.[113] SPCs are not the first attempt at using polymers in conjunction with a silica gel support. Earlier literature and recent reports suggest similar efforts in the area of chromatography and metal sequestration.[114] There have been attempts at surface and physical sorption and synthetic procedures where the polymers were chemically bound to the surface. Although these attempts had the major drawback of polymer leaching over time and the polymer binding procedures resulted low yields. Reasons include a combination of the absence of the humidifying step, the use of trialkoxysilanes as opposed to trihalosilanes, choice of solvents, and order of steps in the synthetic pathway.[115] The patented pathway used to create SPC ion exchange materials provides a material with metal sequestering characteristics (metal ion capacity) that surpass previously reported silica-polymer ion exchange materials.[116]

3.3 Silane Coverage on SPCs

Among the commercialized metal sequestration technologies used today, SPCs are relatively new and have been used very recently in the successful recovery and removal of transition metals, precious metals and mercury from diverse waste streams and mining leaches. Comparing these polymer modified silica with chelating materials prepared by directly modifying an amino-propyl functionalized silica gel surface, it was found that these materials suffer from degradation in the presence of base, have insufficient mechanical stability, and relatively low capacities due to poor surface coverage. The silica polyamine composite materials discussed here have been designed to provide the higher capacities associated with polystyrene while providing the mechanical stability and better mass transfer kinetics associated with silica based solid phase adsorbents.[106]

The initial step in the reaction of a trifunctional silane with a silica gel surface is the hydrolysis of the labile groups by water (**Figure 3.4**). This is followed by condensation to oligomers that create hydrogen bonds with the surface silanols. A covalent linkage is then formed with the simultaneous loss of water. At the interface between silane and the silica gel surface, usually only one bond is formed between each silane molecule and the surface. Ideally, the remaining two sites engage in the horizontal polymerization of the silanes over the surface. The degree of polymerization is dependent on the quantity of water present on the silica gel surface. It has been demonstrated previously that a monolayer of water on the amorphous silica gel surface promotes a more uniform polymerized layer of functional silane.[110] For the preparation

of SPCs a monolayer is applied by passing hydrated air through a column containing silica. Previous work has confirmed the formation of a hydrogen bonded monolayer on the surface.[83] Traditionally, SPCs have been prepared using CPTCS only. However, silica gel surfaces can be modified using a wide array of trifunctional alkylsilanes. In a previous attempt to understand how the nature of the silane alkyl group influences the surface silane coverage and the percent composition of each reagent silane species, amorphous silica gel samples was treated with CPTCS only, a 1:1 molar ratio mixture of CPTCS, and methyltrichlorosilane (MTCS) and with MTCS only. MTCS occupies a smaller molecular volume than CPTCS. It was hypothesized that the addition of MTCS to the reagent silane mixture may promote greater surface silane coverage, thus resulting in a more stable material. Using elemental analysis and ^{29}Si NMR experiments and recognizing that all amorphous silica gels have 8-9μmol/m^2, and assuming that there is at least one Si-O bond to the surface, it was possible to estimate the extent of surface silane coverage (mmol/g).[110,117] In comparison to the CPTCS only product, the MTCS only product had a greater surface silane coverage (~ 30% more). ^{29}Si NMR indicated that the percent reagent siloxane also increases, while the percent geminal reagent silanol significantly decreases. For the 1:1 MTCS:CPTCS mixture, surface silane coverage was also improved relative to the CPTCS only composite, however not to the same extent as the MTCS only silica gel (~12% increase compared to ~30%).[117]

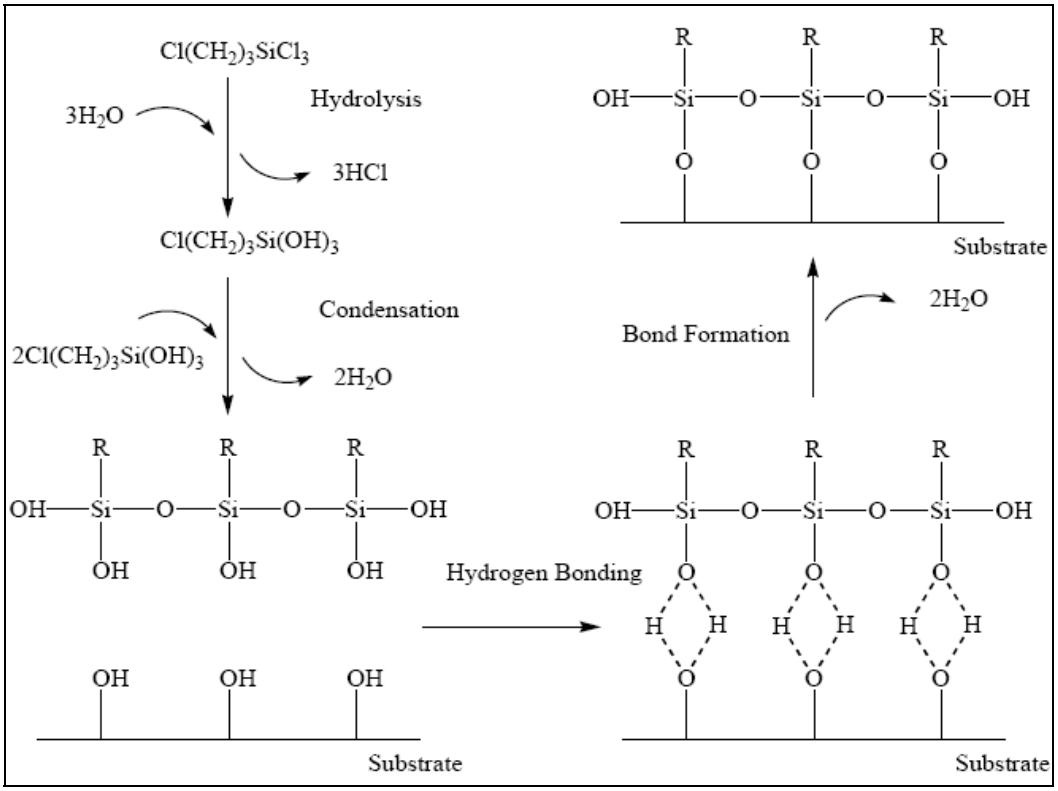

Figure 3.4: An example of the hydrolytic silanization of a silica gel surface using a trifunctional silane (R-trichlorosilane).

3.4 Mixed Silane Coverage Impact on SPCs

Preliminary work demonstrated the positive consequences of incorporating MTCS into the reagent silane mixture. Therefore, a more thorough study of the impact of silanizing amorphous silica gel with molar silane ratios of MTCS:CPTCS of 1:1 to 12.5:1 for INEOS type silica gel was performed by a previous graduate student.[1] This study was conducted in order to examine in greater detail the relationship between the reagent MTCS:CPTCS ratio and the surface silane coverage. It also provided an opportunity to investigate the incorporation of MTCS into the reagent mixture for other silica gels. Each silanized silica gel was sent for elemental analysis for carbon, hydrogen, and

chlorine content.[110,117] The table below shows the elemental analysis details for four ratios of MTCS:CPTCS silica gel.

Table 3.2: Elemental analysis of silica gel modified with CPTCS only, and a series of molar MTCS:CPTCS ratios. There is <0.3 % absolute error in the method used for elemental analysis.

Sample	% Carbon	% Hydrogen	% Chlorine
CPTCS only	5.48	1.34	5.45
7.5:1	3.37	1.04	1.40
10:1	3.28	0.97	1.25
12.5:1	3.20	1.31	1.05

The average pore diameter and surface area of the two different types of silica gel used (INEOS and Qingdao Meigao) ranges from 8 – 17nm and 300 – 425m^2/g, respectively. A large pore diameter allows efficient diffusion and better surface reaction chemistry whereas a large surface area allows greater modification and functionalization of the silica gel. Elemental analysis data indicates a reduction in chlorine content with the increase of MTCS in the reagent silane mixture (Table 3.2). On the other hand, the carbon content decreases with the increase of MTCS. This is due to the fact that methyl groups are bound to the silica gel surface instead of the chloropropyl groups. The amount of carbon, hydrogen, and chlorine can be calculated from the elemental analysis data using the equations given below:

$$\frac{\%\ \mathrm{Cl}}{35.4\ \mathrm{g.mol^{-1}}} \times 1000\ \frac{\mathrm{mmol}}{\mathrm{mol}} \times \frac{1}{100\%} = \mathrm{Cl\ mmol.g^{-1}} \qquad (3.1)$$

$$\frac{\%\ C}{12.0\ g.mol^{-1}} \times 1000\ \frac{mmol}{mol} \times \frac{1}{100\%} = C_t\ mmol.g^{-1} \quad (3.2)$$

$$C_t - (3 \times Cl\ mmol.g^{-1}) = M\ mmol.g^{-1} \quad (3.3)$$

Where, % Cl – Percent chlorine from elemental analysis
% C – Percent carbon from elemental analysis
C_t – Total carbon content on the silanized silica gel surface
M – Amount of surface methyl groups

As the molar fraction of MTCS in the reagent silane mixture increases there is therefore a significant decrease in alkyl halide groups due to the reduction in the amount of chloropropyl silane in the reagent mixture. This confirms that fewer CPTCS molecules are incorporated onto the surface as the mole fraction of MTCS increases. A large fraction of the bulkier CPTCS may decrease the spatial volume available for large amounts of MTCS to react with the surface. Utilizing more potentially reactive silanol groups and increasing the coverage of the silica gel surface should ultimately add to the stability of the resulting composites. Previous studies have been performed using various alkyl silanes in the reagent silane mixture to better understand the surface silane coverage. The other silanes that have been used in conjunction with CPTCS are chloromethyl phenyltrichlorosilane (CMPhTS), phenyltrichlorosilane (PhTCS), propyltrichlorosilane (PTCS), and chlorotrimethylsilane (CTMS).[118a] These other alkyl silanes deliver different silane coverage on the silica gels used. For this research, the MTCS:CPTCS reagent mixture were used due to its better silane coverage and better mass transfer kinetics relative to the CPTCS only silane.

3.5 Mixed Silane Impact on Polyamine Structure

Traditionally SPCs have been prepared by covalently bonding a polyamine to a silica gel surface functionalized with chloropropyl trimethoxysilanes only or CPTCS only. The reason for using trimethoxysilanes was to slow down and control the silanization process. Although the addition of MTCS to the reagent silane mixture provided better silane coverage and protection of the silica gel surface, it was necessary to investigate and understand the consequences of incorporation of MTCS with regard to the polyamine attachment. However, it was necessary to first understand the consequences of polyamine attachment to the CPTCS only silica gel before incorporating MTCS. **Figure 3.2** displays the structures of the two polyamines used in this research for the preparation of SPCs. The SPCs that were prepared using polyallylamine (PAA) were termed BP-1 and the SPCs that were prepared using polyethyleneimine (PEI) were termed WP-1. PEI is a branched chain, and water soluble polyamine. PEI contains a high density of amine groups; it is cheap and readily available. PEI contains carbon and nitrogen in a 2:1 ratio. It also possesses primary, secondary and tertiary amines in the ratio of 35:35:30. PAA is a linear polyamine that is also water soluble and has C/N ratio of 3:1. In a previous study, it was established that the metal ion extraction capacity of the resultant SPC was independent of polyamine molecular weight.[118b] However, there are substantial differences in the metal ion extraction selectivity of the resulting SPCs prepared from each of the polyamines mentioned above.

Table 3.3: Elemental composition of two different polyamine modified SPCs after silanization with CPTCS only. Elemental analysis data have an absolute error of ± 0.3%.

SPC	Polyamine	Carbon (mmol/g)	Nitrogen (mmol/g)	Polymer C:N
BP-1	Polyallylamine	11.7	2.17	3:1
WP-1	Polyethyleneimine	11.4	3.8	2:1

The SPCs that were prepared from the two polymers listed in Table 3.3 were sent for elemental analysis of carbon, hydrogen, nitrogen, and chlorine. It is immediately evident from the elemental analysis data that the SPC WP-1 contains the largest quantity of amines per gram of SPC. In contrast, BP-1 has the lowest amine group density due to the low nitrogen content as compared to WP-1. WP-1 contains the largest quantity of amines per gram; most likely as a result of the lower C/N ratio. The attachment of polymer molecules must lead to a complex and crowded environment on the silica gel. It therefore appears logical to assume that secondary and tertiary amines are less likely to react with the surface as a result of greater steric hindrance relative to primary amines. The linear polyamines contain only primary amines, which are much less sterically hindered. As a result a single linear polyamine molecule can react many times with the surface. Thus if only a small fraction of PEI amine groups can react per each polymer molecule more chloropropyl sites remain available to react with further PEI molecules.

Elemental analysis of various SPC materials (CPTCS only and mixed silane) has shown that almost all of the surface alkyl halide groups undergo nucleophilic attack by the amines from the polymers. In all the SPCs that were modified with either polyamine, the residual chlorine content reported from elemental analysis was < 0.1%. This is based

upon the assumption that hydrolysis of a chloropropyl group is less favored than nucleophilic substitution under the reaction conditions. Therefore it is reasonable to assume that the quantity of polymer amines attached to the surface is primarily governed by the number of alkyl halide groups present on the silica gel surface. However, with such a large number of amines attached to the surface it should be possible to decrease the number of surface attached amines without sacrificing total polymer loaded and without diminishing the remarkable stability of SPCs, which is attributed to multipoint anchoring. A reduction in the quantity of alkyl halide groups provides a decrease in the fraction of polymer amines attached to the surface. In other words, it seems logical that a reduction in the amount of surface attached sites should provide an increase in free amines. A greater quantity of free amines will increase the number of sites available for modification by metal selective ligands. This is based on the assumption that the metal selective ligand will more likely opt to attach at the free amine site than to a surface attached amine site. If an increased number of free amines can be obtained, then it may be possible to create silica polyamine composites with improved metal ion capacities. An example of a CPTCS only BP-1 and a mixed silane BP-1 is shown below. The diluted anchor points in the mixed silane SPC (**Figure 3.5**) is shown to have regular spaced anchor points between them, although this is not the case with any mixed silane SPCs.

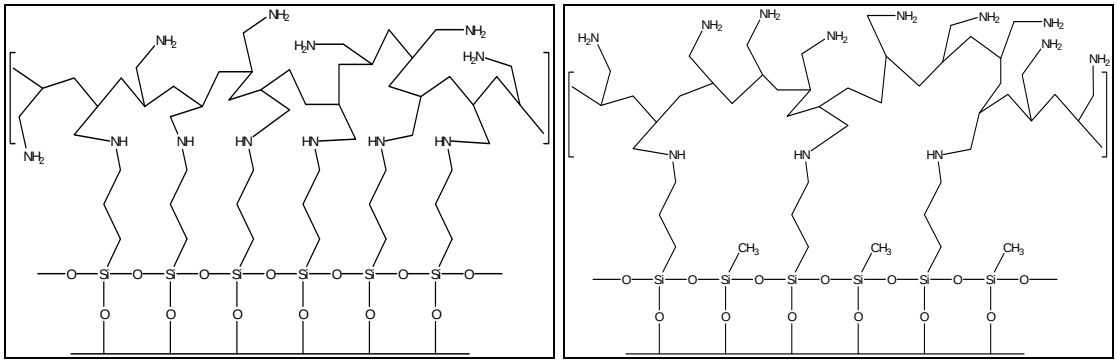

Figure 3.5: Schematic representation of the surface structures of **BP1** (made with chloropropyl trichlorosilane, left) and **BP1M** (made with a 1:1 mixture of methyl trichlorosilane and chloropropyl trichlorosilane, right) composites, made with polyallylamine (PAA), which is a straight chain, water soluble, all primary amine polyamine (MW = 11,000).

Previous research demonstrated that it is possible to control the number of alkyl halide attachments within the silanized surface layer through the incorporation of silanes with alkyl silanes.[110] It has also been shown, to this point, that the result is an increase in surface silane coverage.[110] The quantity of alkyl halide anchors can be dictated by reacting chloropropyltrichlorosilane (CPTCS) and methyltrichlorosilane (MTCS), simultaneously with the hydrated silica gel surface. Silica gel modified in this manner still has the polymeric silane layer vital for polyamine support and product integrity, but with a reduced amount of chloropropyl groups per gram silica gel. The chloropropyl and methyl modified silica gels can then be further modified with the two polyamines discussed above. Thus the effect of reducing the number of polymer attachment points can be scrutinized. It was possible to determine an optimum MTCS:CPTCS ratio for which the surface coverage is maximized and where the number of attachments of the polymer to the surface is sufficient to maintain composite integrity. Previous studies have shown that the best silane mixture for the PAA based SPC (BP-1) is a 7.5:1 ratio of

MTCS:CPTCS. Whereas the ideal SPC made with the PEI had a silane mixture in the ratio of 12.5:1 (MTCS:CPTCS). If increasing the number of free amines per gram of SPC improves its performance (i.e. metal ion capacity and mass transfer kinetics) it should follow that the subsequent reaction with modifying groups such as sodium chloroacetate, dimethyl sulfate, and phosphorous acid would yield improvements in modified SPCs as well.

3.6 Functionalization of SPCs

Amine groups when deprotonated have the ability to donate an electron pair to a Lewis acid. Therefore the polyamine can act as a chelating agent for a range of metal ions. Target solutions for remediation and processing are more often acidic (pH < 3). In such solutions, the amine groups will be almost completely protonated. Base regeneration is used to remove the proton and allow the amine to engage in metal coordination. SPC materials containing only the polyamine can extract a range of transition metals from low pH aqueous solutions. SPCs in this form have been used to selectively remove Pd and Pt from solutions containing Cu and Ni.[112,116] However, with the exception of this example, base regenerated SPCs are generally not efficient at the task of removing one metal ion from a solution containing many metal ions. To introduce selectivity and to gain a competitive advantage, producers of organic cross linked polymeric ion materials have incorporated metal ion selective ligands. SPC materials have great potential in this area due to the extensive chemistry available for

modifying the amine functionality.[106,116-118] Some metal selective ligands that have been made are shown in **Figure 3.6**.

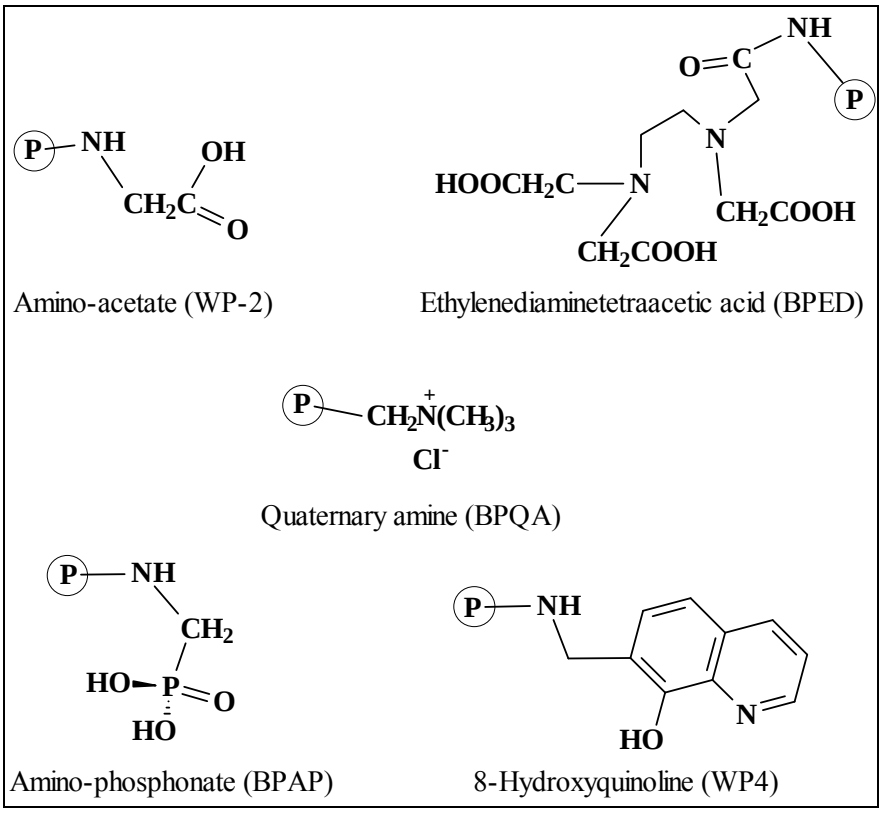

Figure 3.6: SPCs modified with four chelating ligands. The open bond represents the polyamine grafted to the silanized amorphous silica gel (P = polymer).

An example of a functionalization is the reaction of polyallylamine grafted to the silica surface (BP-1) with sodium chloroacetate, which yields a copper selective ligand dubbed BP-2. This amino-acetate ligand on a PAA modified SPC is selective for copper over nickel at pH = 3. Whereas the same ligand on a PEI modified SPC is used for recovery of copper at pH < 2 and is useful for extracting nickel in presence of cobalt and zinc at pH > 1.[110] The use of the Mannich condensation reaction has facilitated the synthesis of composites with a phosphonic acid or 8-hydroxyquinoline functional groups.

In a one pot reaction, BP-1 is modified with phosphorous acid to yield BPAP.[106] BPAP is effective in the removal and recovery of trivalent or higher valent metal ions from divalent ions at low pH. SPCs have demonstrated great promise for tackling the environmental and industrial issues raised previously in chapter 1. The early progress in the development of SPCs has seen the refinement of the synthetic pathway as mentioned earlier in this chapter. This was followed by the functionalization of SPCs with ligands similar to those found in the literature for other ion exchange matrixes to introduce selectivity. The uses of SPCs are being expanded outside of cation removal to include anion removal, bacteria and virus elimination, as well as catalysis of organic reactions.[119a] Recently these materials were used for hydrogen sulfide sorption and oxidation after surface pyrolysis.[119b] There still remains much to be understood with regard to the structure–function relationship and surface topography in SPCs. The intricacies of the silane layer and the consequences of the nature of the attachment of the polyamine to the silica surface remain relatively unclear, although further research to understand this is ongoing.

3.6.1 Phosphorous Acid Modified SPC (BPAP)

The work reported in this thesis made extensive use of BPAP and so its synthesis is discussed in detail here. In the Mannich reaction, an aldehyde such as formaldehyde is condensed with ammonia, a primary amine, or a secondary amine as the free amine or its salt, and a nucleophile or electron rich aromatic compound. The product is referred to as a Mannich base. A literature investigation of the Mannich reaction led to two main approaches. One route would be to pursue the base-catalyzed reaction using the free

amine. The other approach followed the acid-catalyzed Mannich, investigated as both the one and two-step reaction. Phosphorous acid was chosen as the nucleophile to construct the phosphonic acid functional group via the Mannich reaction.[120] The acid catalyzed mechanism was opted due to its ease and high yield. A schematic representation of the BPAP reaction is shown in **Figure 3.7**.

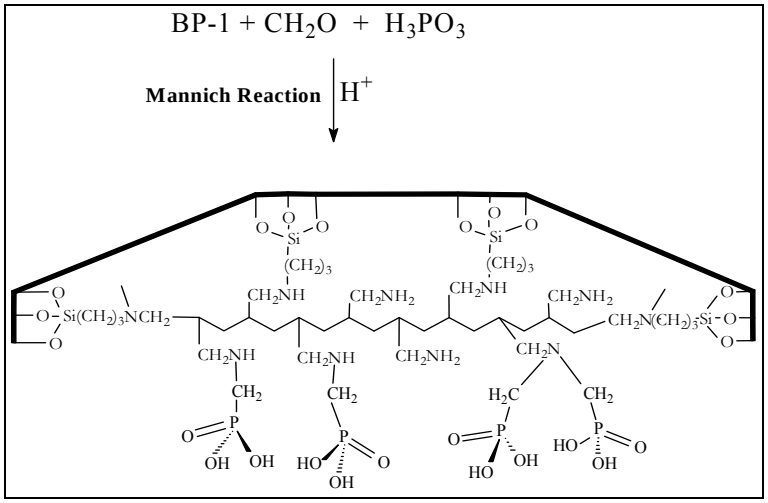

Figure 3.7: Schematic representation of the phosphonic acid modified BP1 composite (BPAP).

Initially, the BPAP synthesized was only from the CPTCS only BP-1. But concurrent research on the mixed silane coverage proved to give higher free amines, the BPAP made after that point was the mixed silane version (BPAPM). Infrared and solid state NMR data are consistent with the proposed composite formulations **BPAP** and **BPAPM** (chapter 2). **Table 3.4** shows the increase in the amino-phosphonate ligand loading with BPAPM. Elemental analysis of **BPAP** and **BPAPM** shows lower carbon and nitrogen content in **BPAPM** but slightly higher phosphorus content. The N:P ratios from the table below give some further insight into the functionalization of these

materials. That the N/P ratio is 0.88 (BPAPM) while the N content is 1.5mmol/g indicates that some of the amines may be doubly substituted with phosphonic acid groups (**Figure 3.7**).

Table 3.4: Elemental analysis data and ligand loading for BPAP and BPAPM. Error in elemental analysis is $\pm$0.3%.

SPC	Carbon (mmol/g)	Hydrogen (mmol/g)	Nitrogen (mmol/g)	Phosphorus (mmol/g)	N:P
BPAP	11.8	30.3	2.40	1.40	1.71
BPAPM	10.1	29.9	1.58	1.79	0.88

Because the N/P ratios suggest that some of the amines may be doubly substituted with phosphonic acid groups, we ran a solid state 2D phosphorus-proton correlation experiment. The 1D ^{31}P CPMAS spectra of BPAP consistently showed a small shoulder downfield of main resonance at 6.7ppm. The 2D correlation spectrum shows the expected overlapping cross peaks for the NH proton (at 6.0 ppm, obtained from solution data on model compounds) and the CH_2 protons (at 3.5 ppm) with the main phosphorus resonance (**Figure 3.8**). Significantly, the small shoulder in the ^{31}P NMR spectrum shows the expected CH_2 correlation but the NH correlation is absent. Although we have not quantified the contour maps due to overlap of the NH and CH_2 correlations these data clearly indicate that a significant fraction of the amine groups are doubly substituted with $CH_2PO(OH)_2$ groups.[106]

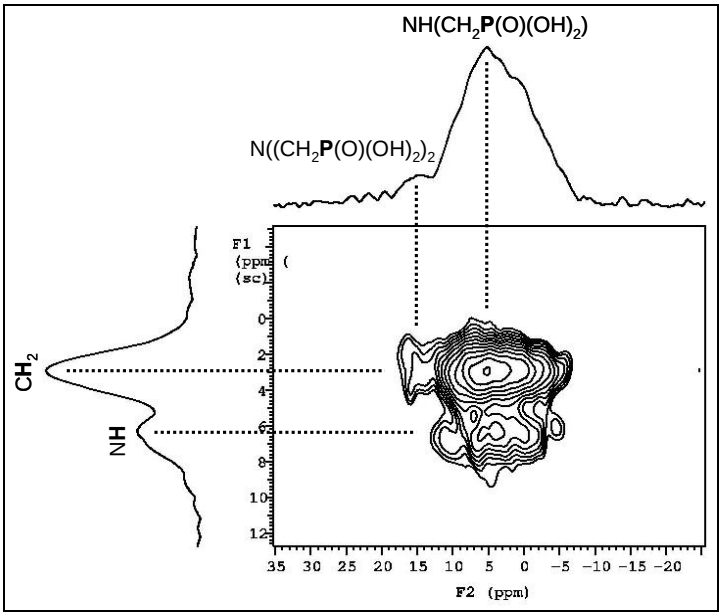

Figure 3.8: Solid state CPMAS ^{1}H–^{31}P HETCOR NMR spectrum of BPAP.

BPAP has a marked ability to extract tri- and tetra-valent species such as Al(III), Fe(III), Ga(III), Ln(III), Zr(IV) and Th(IV). Little affinity is displayed for divalent metals such as Cu(II), Ni(II), Zn(II) and Co(II) at pH $\leq$ 3. Selectivity between trivalent species has been explored for relevant applications such as with sources of acid mine drainage and rare earth element separations. The mechanism with which the BPAP reaction is believed to proceed is shown in **Figure 3.9**.

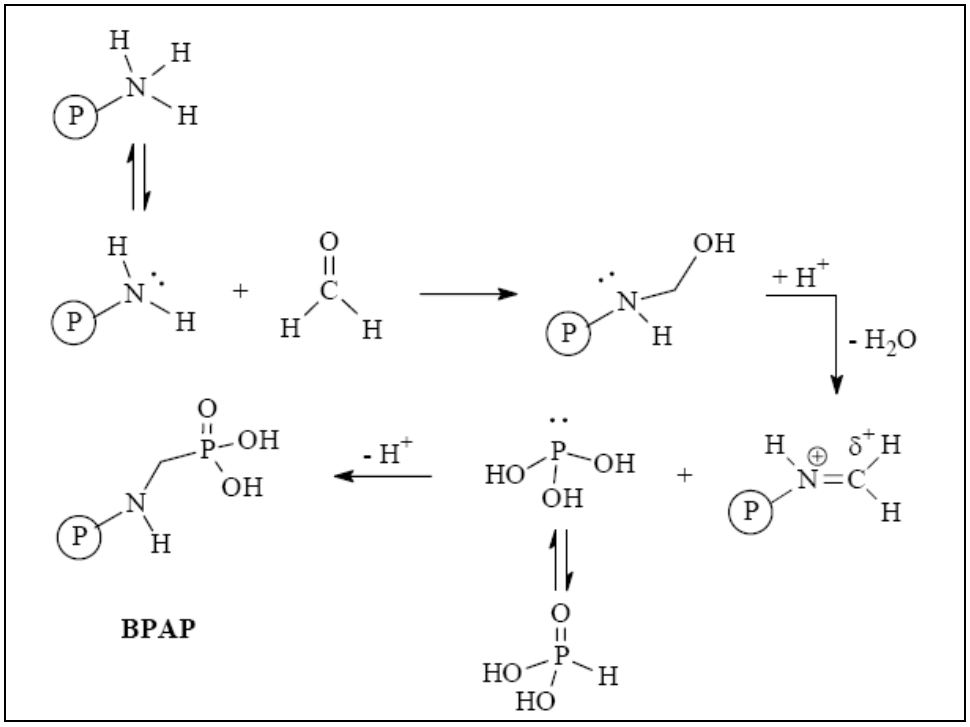

Figure 3.9: Mechanism of acid-catalyzed Mannich reaction utilizing phosphorous acid to make BPAP.

3.6.2 Quaternary Amine Modified SPC (BPQA)

We wanted to make a quaternized SPC that would compare directly with a quaternized polystyrene resin commercially available. The idea to use this non-IMPAC system came from literature studies where research has been done to remove arsenate by using quaternary amine systems. This system does not use any immobilized metal to act as the cation or the positive charge to remove the metal anions from aqueous solutions. The amine on BP1 was quaternized by excessive N-methylation using methyl iodide.[109] Since methyl iodide was carcinogenic, dimethyl sulfate was used instead for further studies and BPQA synthesis.[121] The advantage to using a non-IMPAC system is that there is no immobilized metal that binds to the target anions, thereby reducing the risk of

metal leaching that is often seen in systems with immobilized metal as the target anion capture center. **Figure 3.10** represents the reaction for exhaustive N-methylation of the composite BP-1.

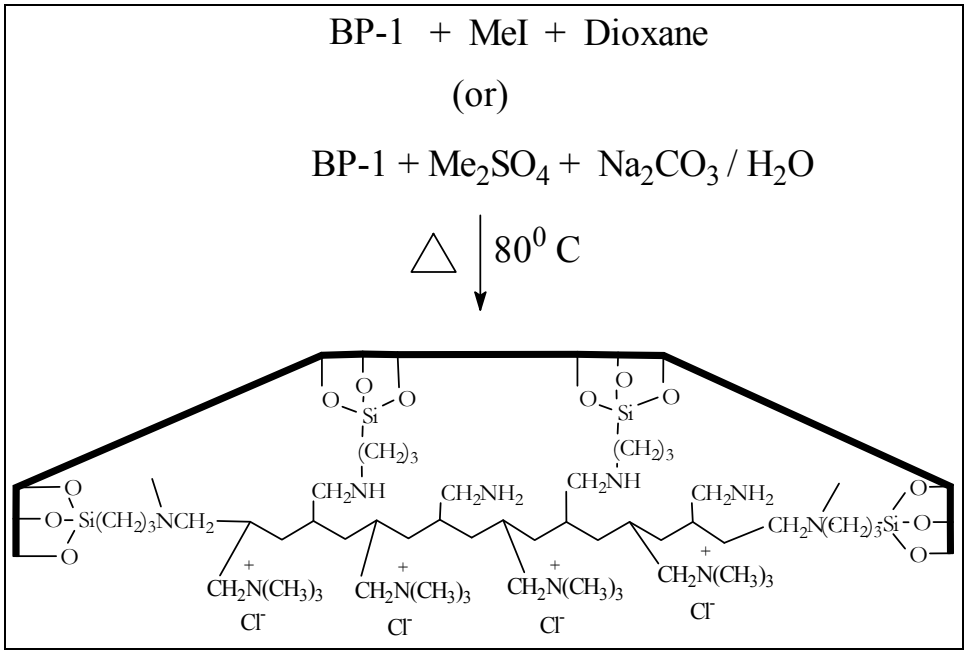

Figure 3.10: Schematic representation of the quaternization of BP1 using iodomethane or dimethyl sulfate.

The quaternary amine sites for the binding of anions are traditionally called as strong base groups.[121,122] It was necessary to determine the number of strong base groups present in the different BPQAs synthesized. This was done using a procedure found in the literature and Mohr's method for determination of chloride ion concentration by titration.[122] As with all other SPCs, BPQA with varying ratios of MTCS:CPTCS were synthesized. Four ratios were used in the synthesis of BPQA samples according to the procedure mentioned in chapter 2. The three ratios of MTCS:CPTCS were 7.5:1, 10:1, and 12.5:1. The fourth sample was made with the CPTCS only composite. The reason

for synthesizing ratios other than 7.5:1 for a PAA based composite was the poor N-methylation of the free amines. The CPTCS only and the 7.5:1 MTCS:CPTCS composite did not show much N-methylation and had very little strong base groups. This would then affect in the capture of anions, because of the low percentage and quantity of quaternary amine sites available. This observation is probably because of the inability of the N-methylation reaction to proceed due to steric hindrance from the bulky polymer groups of the polyallylamine. Hence the other ratios were used to investigate weather if further dilution of the silane mixture would free up more amines for N-methylation.

Table 3.5: Elemental analysis data for BPQA samples with varying MTCS:CPTCS ratio. Error in the elemental analysis data is $\pm$ 0.3%.

MTCS:CPTCS	Carbon mmol/g	Hydrogen mmol/g	Nitrogen mmol/g	Chlorine mmol/g	Quaternary Sites (%)
CPTCS only	16.9	43.2	2.4	1.1	10
7.5:1	12.1	33.9	1.9	1.3	11
10:1	10.2	25.5	1.6	1.1	54
12.5:1	9.8	28.1	1.5	1.2	35

From the table above, it is evident that the carbon and the nitrogen content are steadily decreasing as the ratio of MTCS in the silane mixture increases. The important observation from this study is the fact that the number of quaternary amine sites increase till the MTCS:CPTCS ratio is 10:1 and then it starts decreasing again. Although for all other metal capture and recovery purpose, the optimal ratio for the BP-1 composite is 7.5:1, for BPQA it is the 10:1 MTCS:CPTCS ratio composite that has the highest percentage and hence the quantity of quaternary amine sites. But, it is the capture of bacteria and virus from drinking water that shows the highest removal (> 99.999%) when tested by flowing the contaminated water through a column packed with the 10:1 BPQA

composite. The 7.5:1 BPQA composite performed fairly well (> 99.98%), but still falls behind in performance when compared with the 10:1 BPQA. A detailed discussion of the bacteria and viral capture is mentioned in chapter 5.

3.6.3 EDTA Modified SPC (BPED)

Ethylenediaminetetraacetic acid (EDTA) has been used for a long time as a chelating agent for various purposes. It is a well studied chelating system and is used for chelation therapy worldwide. ETDA was first used in the 1940s for treatment of heavy metal poisoning. It is widely recognized as effective for that use as well as certain others, including emergency treatment of hypercalcemia and the control of ventricular arrhythmias associated with digitalis toxicity. Its prominence as a chelating agent arises from its ability to "sequester" di- and tricationic metal ions such as Ca(II) and Fe(III). After being bound by EDTA, metal ions remain in solution but exhibit diminished reactivity. EDTA bonds to metal ions through two tertiary amine groups as well as via four carboxylate groups (**Figure 3.11**). EDTA is insoluble in acidic medium and can be used for the purpose of solid phase ion exchange by reacting immobilized amine groups of the SPCs with EDTA dianhydride. Materials modified with EDTA dianhydride have shown promise for the selective separation and recovery of divalent transition metals such as Ni^{2+} from Co^{2+}, Zn^{2+} and Mn^{2+}. Such separations are based on the differences in the formation constants for metal ions with EDTA and if the immobilized EDTA derivative maintains a specific selectivity profile similar to the free EDTA, the resulting materials may be useful for other metal ion separations.

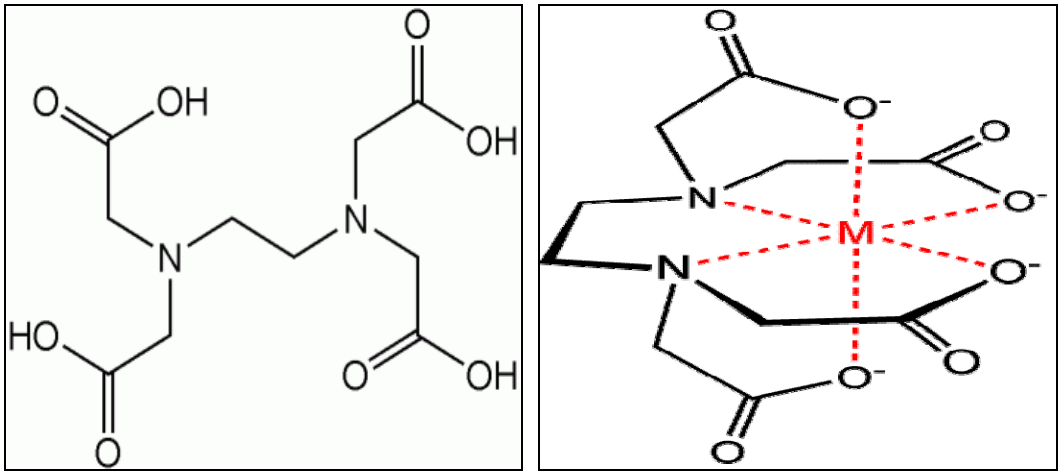

Figure 3.11: Structure of EDTA (left) and a metal ion chelated to the EDTA (right).

This composite is the analogue of a specially prepared polystyrene resin containing the ethylenediamine tetra-acetic acid (EDTA) ligand.[123a] SPCs make use of a polyamine layer, which shields a pendant ligand from the charged surface allowing increased capacities at increased pH. Related composites made by reacting EDTA anhydride with propyl amine modified silica gel show decreasing capacity due to hydrogen bonding of the carboxylate groups with the surface.[123b] Also, immobilized polyamines contain a large quantity of amine sites per gram of composite (2 ~ 3 mmol/g) which promotes increased ligand loading and therefore increased metal ion sorption capacity. Thus BP-1 (prepared from 7.5:1 MTCS:CPTCS silica gel) was modified with EDTA dianhydride by way of an acid catalyzed aminolysis as shown in **Figure 3.12**. EDTA dianhydride is commercially available. However, it can also be prepared in high yield from the condensation of EDTA in pyridine and acetic anhydride.[123b] **Table 3.6** shows the elemental analysis and ligand loading for the SPCs BP1 and BPED (both 7.5:1 MTCS:CPTCS) for comparison.

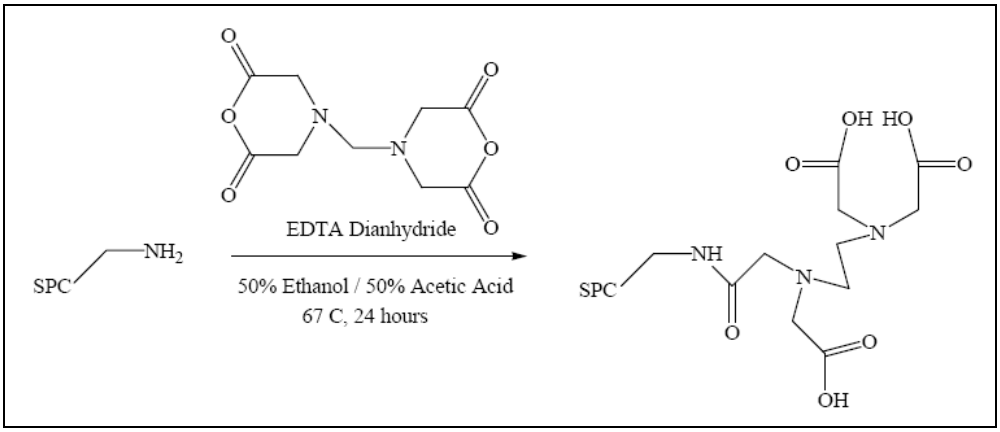

Figure 3.12: Synthetic pathway to making BPED using EDTA anhydride.

Table 3.6: Elemental analysis data for the starting composite BP1 and the modified composite BPED. Errors in elemental analysis is ± 0.3%.

SPC	Carbon mmol/g	Hydrogen mmol/g	Nitrogen mmol/g	C:N	Ligand loading mmol/g
BP1 (7.5:1)	9.85	29.5	2.49	3.96	--
BPED (7.5:1)	16.64	32.60	3.74	4.45	0.85

The ligand loading is 0.85mmol/g and this means that almost all the free amine sites were modified. However, it could also be possible that some of the amine sites are di-functionalized. Although, the chances of di-substitution by a bulky ligand such as EDTA are not common or unlikely, it might be possible. A 2D correlation spectrum of nitrogen-carbon (^{15}N labeled PAA) might help answer the question of di-substitution. **Figure 3.13** displays the CPMAS ^{13}C NMR spectra for the 7.5:1 BPED. The broad peak at ~ 170 ppm located in the spectrum below is due to the carboxylic acid groups (–$\underline{C}O_2H$). It is likely that a peak representing the amide functional group that is responsible for ligand binding (–N$\underline{C}OCH_2$–) is also located and overlapped by the huge carboxylic acid peak. The broad peak at ~53 ppm in the spectrum is due to the acetate methylene carbon atoms (–CH_2COOH). The other peaks at ~ 30 ppm and at -5 ppm are due to the

polyamines of the starting composite BP1 and the surface methyl groups due to methyltrichlorosilane (MTCS).

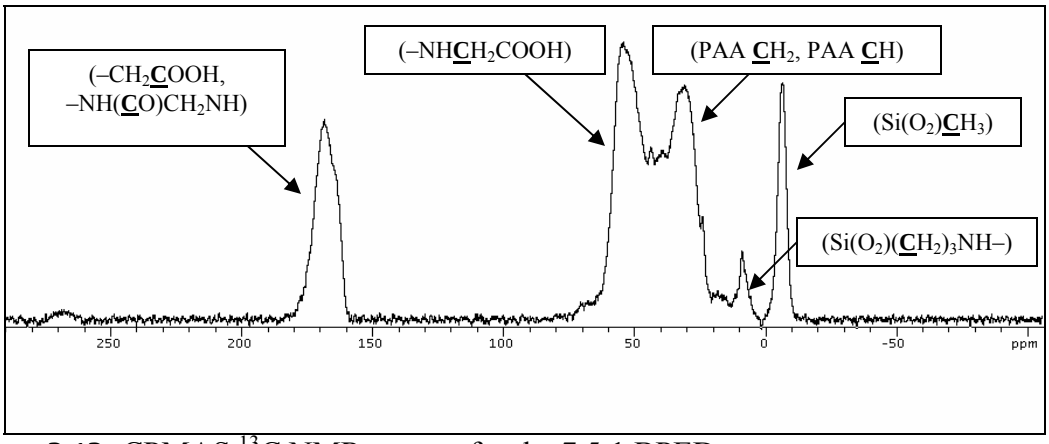

Figure 3.13: CPMAS ^{13}C NMR spectra for the 7.5:1 BPED.

3.7 Immobilized Metal Silica Polyamine Composite (IMPAC)

Traditionally, anion capture with conventional ion exchange resins generally relies on the use of quartenized ammonium functionality, so-called strong base resins, and a recently developed glucamine based arsenic-selective resin.[124] There are several polystyrene based anion capture resins available commercially.[106] This approach is also accessible using the silica polyamine platform and we have employed this approach as well. We have observed that highly charged cations when immobilized on the silica composites, WP2, BPED, and BPAP also remove oxo-anions of arsenic and selenium. This represents a new direction for the toxic metal removal/recovery technology. This effort seeks to permanently immobilize metal-cations on the silica polyamine composite resulting in an affinity for the toxic anions arsenate, arsenite, selenate and selenite selectively over the common co-contaminants – sulfate and chloride. We therefore,

decided to take the immobilized metal (cation) approach to anion capture which relies on the fact that highly charged metals (+3 or +4) can be immobilized on a variety of our SPC composites that have a net positive charge. The general idea is that by varying the metal and the functional group that binds it to the composite one could tune the anion selectivity and the operational pH range based on the factors governing the anion–immobilized metal interaction. This approach promises to allow tuning of the anion affinity in a novel manner by allowing:

1. Variation of M^{+n}
2. Variation of ligand properties
3. Variation of coordination number
4. Facile regeneration and concentration, see below :–

$$L_nM^{m+} + M'(O)_x^{y-}{}_{(aq)} \rightleftharpoons L_xM^{n+}(M'O_x)^{m-y} \qquad (3.4)$$

where, L – Ligand bound to polymer composite,
M – Immobilized metal,
M' – Metal from the anionic species.

In our initial investigations we focused on a system that immobilized Zr^{4+} on the polyamine composite having amino acetate functionality (WP-2, **Figure 3.14**).[118,125] We found that this combination was very effective for the capture of arsenate, selenate and selenite from actual mining waste streams, but only at pH 4. This system compared quite favorably with previously reported systems in the literature using Zr^{4+} immobilized on polystyrene resins.[123a] Although in the past three years, we have extended these studies to three additional systems, the first one using Zr^{4+} and Fe^{3+} immobilized on a phosphonic acid modified BP1 (BPAP-M^{+n}, **Figure 3.15**), the second one using Zr^{4+} and Fe^{3+} immobilized on a EDTA anhydride modified BP1 (BPED-M^{+n}, **Figure 3.11**) and the

third one using Co^{3+} immobilized on WP1 (WP1-Co^{3+}, **Figure 3.16**). The cobalt system was shown to have no appealing affinity for arsenic oxo-anions. This is because cobalt(III) exists in an octahedral environment and the first coordination sphere is completely full and it is impossible for the arsenate species to enter the first coordination sphere, there by making it difficult for cobalt to bind to the arsenic oxo-anions.[126] Additional research has been carried out by varying the immobilized metal center (Th^{4+}, Ce^{3+}, Ce^{4+}, and Al^{3+}) to study the selectivity that is obtained. The details of these IMPAC systems and its anion capture study are discussed in chapter 4.

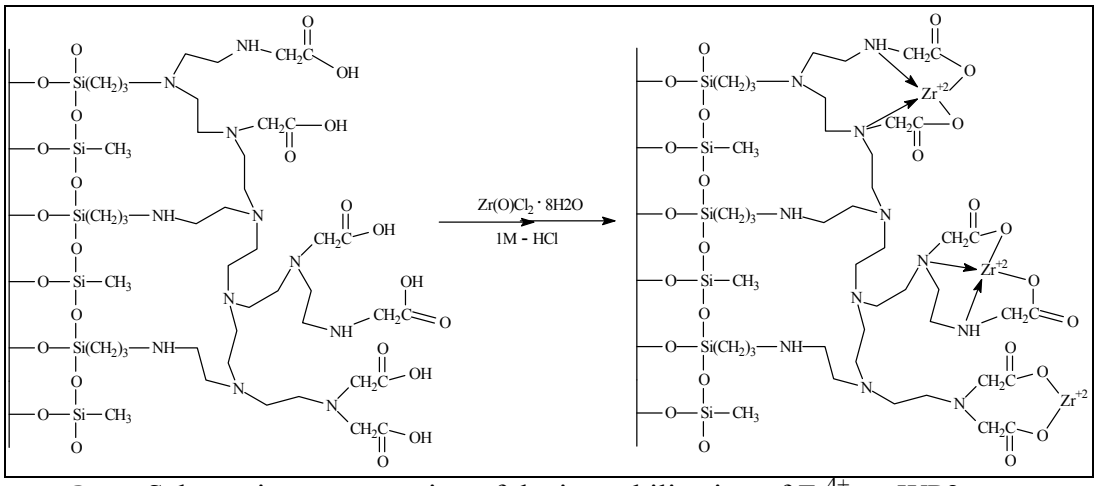

Figure 3.14: Schematic representation of the immobilization of Zr^{4+} on WP2.

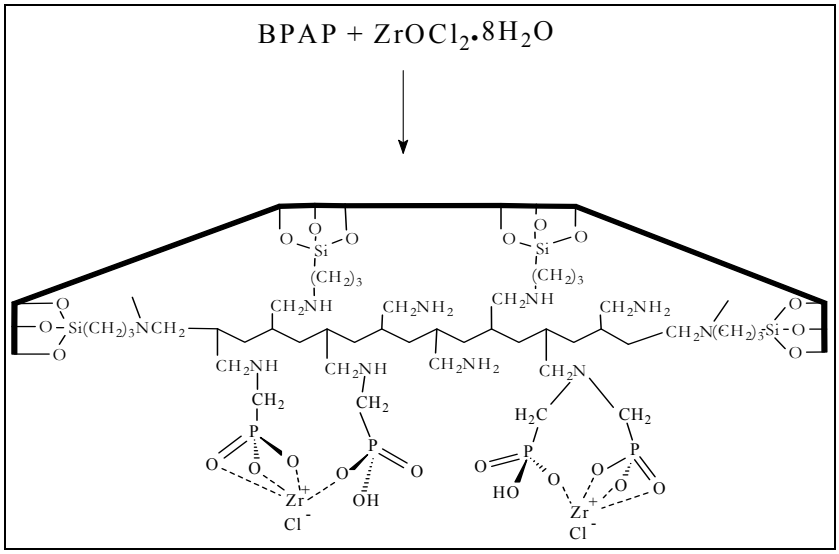

Figure 3.15: The phosphonic acid modified polyamine composite (BPAP) showing proposed bonding mode of the zirconium to the ligand site.

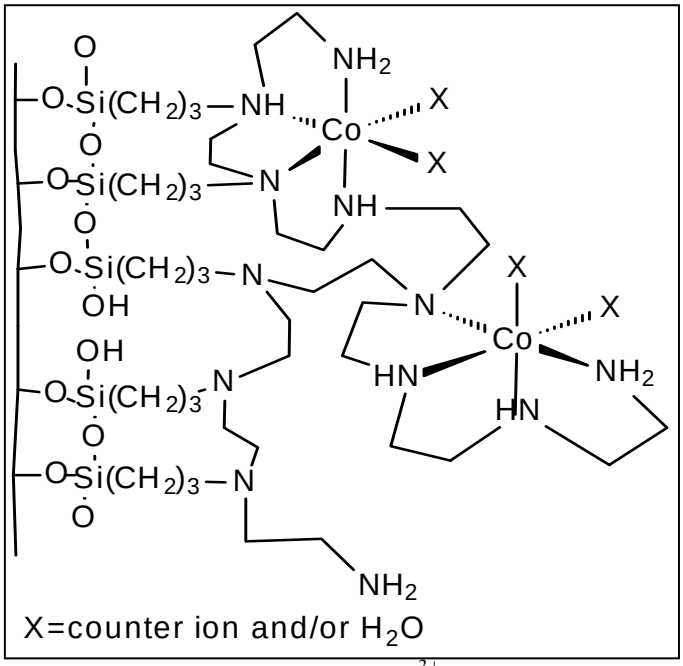

Figure 3.16: Schematic representation of the Co^{3+}-WP1 composite showing the likely coordination of the cobalt.

CHAPTER 4: ARSENIC & SELENIUM RECOVERY

Arsenic and selenium are among the inorganic contaminants that have become a serious environmental concern lately. The accumulation of arsenic and selenium in soils, aquifer sediments and drinking water through various pathways has threatened the health of plants, wildlife and human beings. The presence of these ions in the environment is regulated by many environmental and public health agencies and authorities. For example, under the Safe Water Drinking Act of United States, the Maximum Contaminant Levels (MCLs) in drinking water established for arsenic and selenium are 10 and 50μg/L, respectively. Sources of arsenic and selenium contamination are predominantly associated with anthropogenic activities, arising from application of agricultural pesticides, disposal of industrial and mining wastes, landfilling of sewage sludges, and combustion of fuels.[127] Public and political concerns have arisen as a result of the potential groundwater and surface water contamination by these contaminants.[128]

The removal of arsenic and selenium has become one of the most important areas of water treatment. Many methods including coprecipitation, liquid-liquid extraction and ion exchange have been so far proposed and used for this purpose. Chelating resins are generally considered to give more selective methods than simple ion exchange and have been studied extensively for the binding of arsenic compounds.[129] Especially, because of the growing demand for utilization of the recovered arsenic after the water treatment process, some attention has been paid to adsorption based ligand substitution with

Fe(III)-loaded chelating resins which gives selective adsorption of arsenic and easier regeneration of the adsorbent.[129] More recently polystyrene modified with poly-dentate ligands and Zr(IV) has shown selectivity for arsenate and selenate over sulfate but was only effective over a very narrow pH range.[130]

However, conventional polymeric resins suffer from shrink/swell changes depending on pH and are not very stable at extreme conditions of pH and/or temperature.[122] The goal of this work is to expand the silica gel polyamine composite technology to anion capture whereas it has been used previously used only for cation capture. This composite matrix offers an alternative technology to ion exchange resins based on organic polymers (polystyrene and polymethacrylate). However, based on the literature and our preliminary work, we observed that highly charged cations when immobilized on the silica composite matrix also removes oxo-anions of arsenic and selenium.[125] This chapter will discuss various IMPAC systems that have been used to study the removal and recovery of arsenic and selenium from aqueous streams.

4.1 Zr^{4+}-WP2

Initial studies were performed by a previous graduate student using the composite WP2 made with the CPTCS only.[125] Over the past three years we observed that the newly developed mixed silane composites show better mass transfer and stripping kinetics as explained in chapter 3. So, it was decided to immobilize zirconium (IV) on the mixed silane WP2 and observe any changes from earlier data. To begin with, the zirconium loading onto the WP2 increased from 40mg-Zr/g-composite (0.46mmol/g) to

93mg-Zr/g-composite (1.02mmol/g), an increase by a factor of 2.3 just by changing the silane ratios on the composite matrix (**Figure 3.14**). This increase in zirconium loading in turn shows an increase in arsenic (III & V) loading.

Table 4.1: Initial equilibrium batch tests for arsenite and arsenate species with Zr^{4+}-WP2.

Species ↓ pH →	**2**	**4**	**6**	**8**	**10**
As(III) (mg/g)	--	--	--	9 ± 1.2	79 ± 0.31
As(V) (mg/g)	90 ± 4.6	88 ± 1.4	79 ± 1.4	47 ± 1.1	--

Although previous investigations reported that arsenate removal occurs only at pH=4 using Zr^{4+}-WP2 (CPTCS only), equilibrium batch tests performed using the new mixed silane Zr^{4+}-WP2 shows arsenate removal over a wide pH range, 2-8, which again fits well with the Pourbaix diagram for arsenate (**Figure 1.2**). Very minimal arsenite removal (5mg/g) was observed using the CPTCS only Zr^{4+}-WP2. This could be due to the fact that the tests were only performed at pH=4 where arsenite exists as neutral species. It is only at pH > 9 that one observes ions of arsenite species exist in aqueous systems. This is the reason why there is a huge increase in arsenite removal from pH=8 to pH=10 using the mixed silane Zr^{4+}-WP2 (9mg/g to 79mg/g, respectively). This observation holds true for all the IMPACs being investigated in agreement with the Pourbaix diagram for arsenic.

However, initial testing of arsenate breakthrough at pH values of 2 and 6 show interesting results (**Figure 4.1** & **Figure 4.2**). There is a significant drop in arsenate capacity between the first and second cycles. The strip solutions were analysed and were found to have significant amounts of zirconium in them which means that the composite leaches zirconium while stripping. Additionally, we observe precipitation during the

initial stages of stripping with 2M-sulfuric acid. After the analysis of the precipitate, we found that the strip consisted of over 30% zirconium in the first two column volumes. Overall the zirconium leach was approximately 65%.

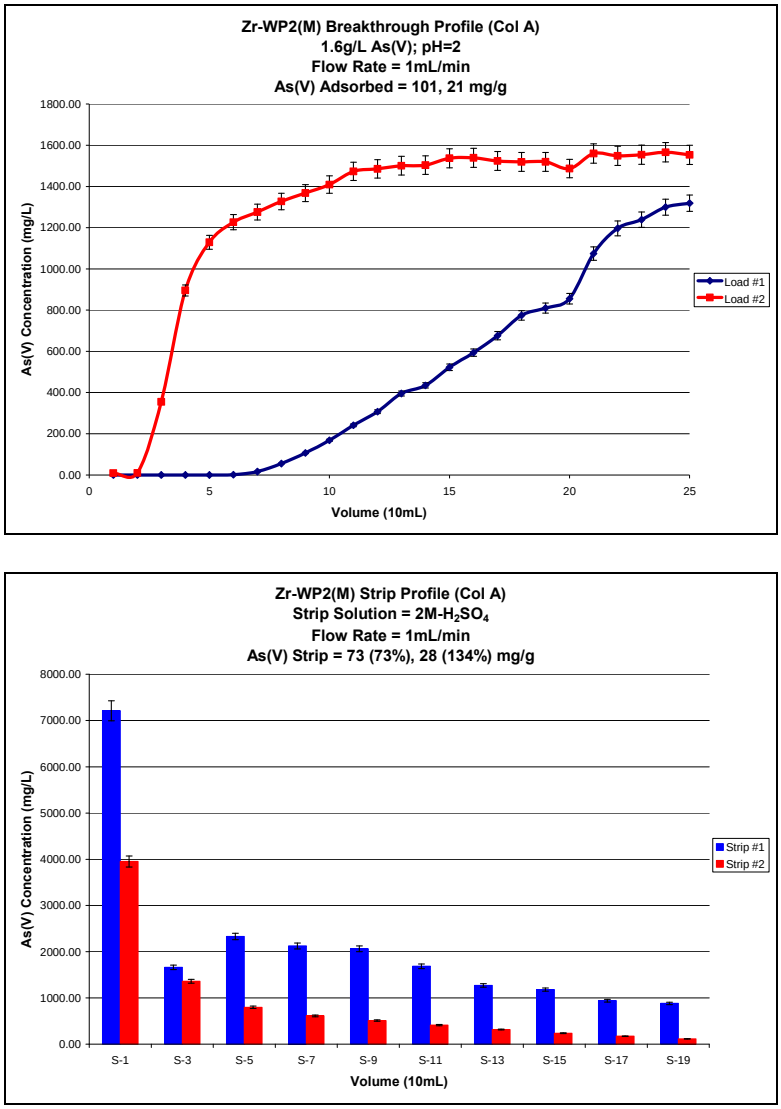

Figure 4.1: (Top) Breakthrough profile showing the decrease in arsenate capacity at pH=2 with Zr^{4+}-WP2. (Bottom) Strip profile showing that there is more than 100% strip in the second cycle (due to incomplete stripping in the first cycle).

Also, there was a reduction in the arsenate capacity relative to the batch studies at pH=6 and although the strip had 88% arsenic, it also had > 50% zirconium in it. Besides,

the strip profile shows very poor mass transfer kinetics with respect to arsenic (**Figure 4.2**). Therefore, a successive arsenic load was not carried out due to the fact that over half of the immobilized zirconium had leached from the composite during stripping.

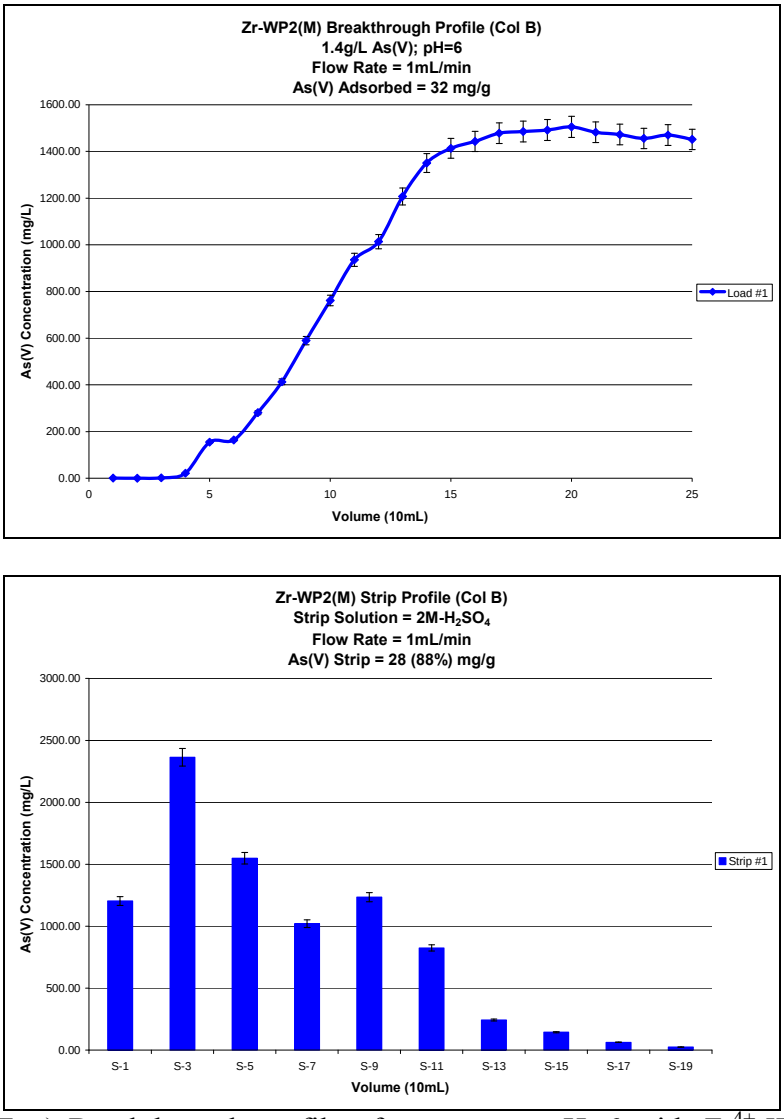

Figure 4.2: (Top) Breakthrough profile of arsenate at pH=6 with Zr^{4+}-WP2. (Bottom) Strip profile of arsenate with 2M-H_2SO_4.

Thus although the batch studies appeared to be quite promising, the zirconium leaching makes the Zr-WP2 IMPAC useless for further study.

4.2 Fe^{3+}-BPED

EDTA has been used as chelating ligands for a very long time and iron based adsorbents have been widely used for arsenic removal. In order to avoid the high cost of using zirconium and because of the extensive literature on iron based arsenic removal systems, iron was immobilized onto the mixed silane BPED and equilibrium batch tests were carried out to see if there is any iron leaching in this case as well. The iron loading is a little higher than that observed with BPAP (discussed in the following section). The iron loading was 65mg-Fe/g-composite (1.16mmol/g) as compared to 0.98mmol/g on the phosphonic acid functionalized BPAP composite. However, the arsenic capacities were not as high as was expected. The highest arsenate and arsenite capacities were observed to be 18mg/g and 6mg/g, respectively, which are not very useful for industrial applications (**Table 4.2**). However, there was no iron leach observed during the arsenic loading, and during stripping with 2M-sulfuric acid.

Table 4.2: Equilibrium batch tests for arsenite and arsenate species with Fe^{3+}-BPED.

pH → / Species ↓	2	4	6	8	10
As(III) (mg/g)	--	--	--	1 ± 0.32	6 ± 0.52
As(V) (mg/g)	11 ± 2.5	17 ± 2.0	18 ± 0.86	9 ± 1.8	--

This might be a cheaper and safer composite to treat water systems with very low arsenic levels, like rivers and streams where arsenic levels do not exceed 1ppm. As the arsenic capacities were very low over a broad pH range (2-10), column breakthrough studies were not performed on this material. However, further research is needed to find out if this system can also be used to remove selenium from aqueous systems.

4.3 Zr^{4+}-BPED

This composite is the analogue of a specially prepared polystyrene resin containing the ethylenediamine tetra-acetic acid (EDTA) ligand with immobilized zirconium using $ZrOCl_2 \cdot 8H_2O$ made by Suzuki *et. al.*[123a] This mixed silane BPED composite showed very high zirconium loading as compared to the other composites under investigation. The zirconium loading was 97mg-Zr/g-composites (1.06mmol/g). Initial equilibrium batch studies revealed that the arsenate removal shows the same trend as the Zr^{4+}-WP2 and fits well with the arsenate Pourbaix diagram. As for arsenite, there is an increase in removal capacity from pH=8 to pH=10, but not as huge a difference as observed with Zr^{4+}-WP2. Initial testing of arsenate breakthrough at pH=6 shows interesting results (**Figure 4.3**). There is a significant drop in arsenate capacity between the equilibrium batch test and the breakthrough profile at pH=6. The strip solutions were analysed and were found to have significant amount of zirconium (> 40%) in them which means that the composite leaches zirconium while stripping, similar to the Zr^{4+}-WP2 composite. Precipitation is observed here as well during initial stages of stripping and characterization of the precipitate showed high levels of zirconium.

Table 4.3: Equilibrium batch tests for arsenite and arsenate species with Zr^{4+}-BPED.

pH → / **Species ↓**	**2**	**4**	**6**	**8**	**10**
As(III) (mg/g)	--	--	--	18 ± 0.46	56 ± 0.12
As(V) (mg/g)	70 ± 0.79	68 ± 0.60	63 ± 0.88	37 ± 0.74	--

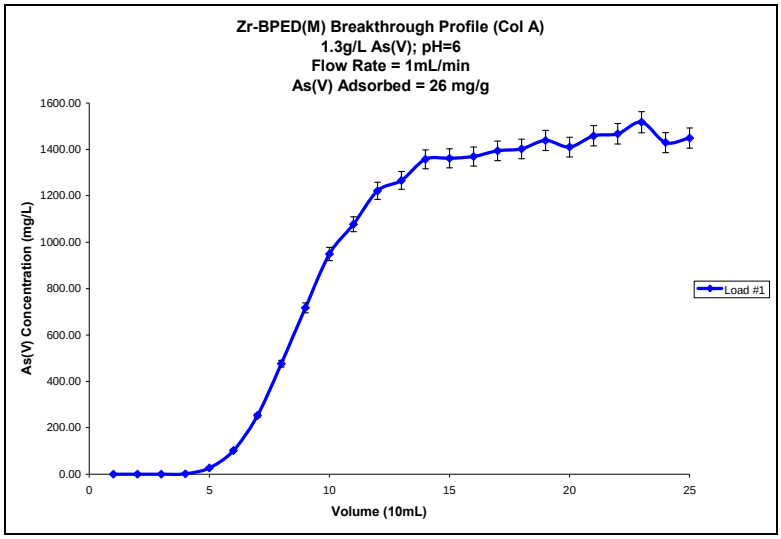

Figure 4.3: (Top) Profile that shows the decrease in arsenate capacity between equilibrium batch test (63mg/g) and breakthrough (26mg/g) at pH=6 with Zr^{4+}-BPED. (Bottom) Strip profile of arsenate with 2M-H_2SO_4.

4.4 Fe^{3+}-BPAP

With the tremendous success and the wide use of iron based adsorbents for arsenic and selenium removal, we wanted to try and immobilize iron (III) on BPAP systems. The reason for using iron was mainly to reduce the cost of the IMPAC, since

iron salts are much cheaper than zirconium and thorium salts. The ferrihydrite process is by far the most economical and effective technology for arsenic removal. However, the ferrihydrite process creates a huge amount of sludge that needs to be treated and/or disposed properly. On the other hand, the IMPACs can be regenerated and reused many times over. The BPAP used to immobilize iron was not the mixed silane version, although it is proposed to be in the future investigations. Iron loading on BPAP was calculated to be 55mg-Fe/g-composites (0.98mmol/g). After checking the elemental analysis (phosphorus) of the Fe^{3+}-BPAP made, it was estimated that each phosphonic acid functional group was bound to one iron on average, with the Fe:P ratio being almost 1:1. The Fe^{3+}-BPAP captures arsenate over a wide pH range, 2-8, although the arsenate capacity peaks to 55mg/g at pH 4 and drops to 33mg/g at pH 8. On the other hand the capacity for arsenite removal shows good mass transfer only at pH > 9. Arsenite removal capacity at pH 8 was 10mg/g and at pH 10 was 45mg/g. These removal capacities for both arsenite and arsenate were performed as batch tests and fit well with the Pourbaix diagram for the pH values mentioned.

Table 4.4: Equilibrium batch tests for arsenite and arsenate species with Fe^{3+}-BPAP.

Species ↓ pH →	2	4	6	8	10
As(III) (mg/g)	--	--	--	10 ± 0.62	45 ± 2.7
As(V) (mg/g)	49 ± 0.32	55 ± 1.55	46 ± 0.73	33 ± 2.68	--

However, we came upon a minor problem while performing breakthrough tests for arsenate. It was observed that iron was leaching from the column during stripping of the loaded arsenate. This might be due to the stronger affinity between the iron (III) and

the arsenic species. About 65% of the immobilized iron (III) leached during stripping using 2M-sulfuric acid. But, this problem was solved by adding another step between the acid strip and the arsenic reloading for the next cycle. A 40g/L solution of an iron(III) salt was passed through the column between the acid strip and the next arsenic cycle. This step ensures that the column is replenished with iron (III) to replace for the iron lost via leaching during the previous strip cycle. Three consecutive cycles were run to test the above mentioned modification and the results are shown below (**Figure 4.4**). Although this is an extra step for each cycle, it does make the Fe^{3+}-BPAP easy to work with and less expensive relative to its zirconium analogue (see next section).

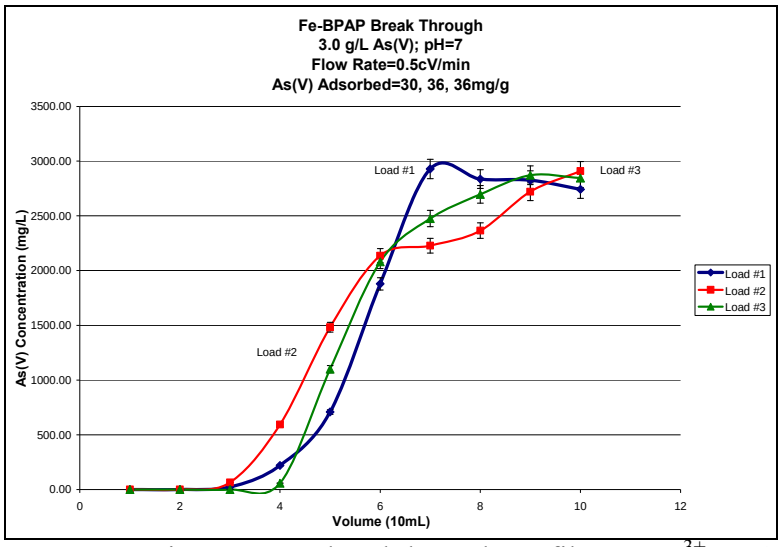

Figure 4.4: Three consecutive arsenate breakthrough profiles on Fe^{3+}-BPAP at pH 7.

It is evident from **Figure 4.4** that the arsenic loading is not decreasing from the first to the third load; in fact it is increasing and this might be due to the excess iron(III) present in the pores of the SPC material which might not be completely immobilized on the phosphonic acid ligand of BPAP. The strip profile in **Figure 4.5** suggests that there is

a steady strip percentage of arsenate from the second and the third strip cycle. Although, the arsenate loading was performed under a higher flow rate (2.5mL/min), the mass transfer kinetics look good for the three successive loads.

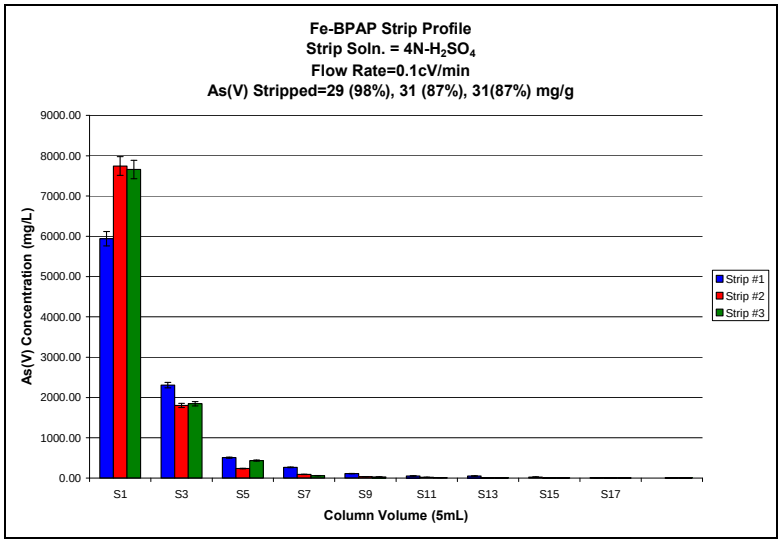

Figure 4.5: Strip profile of arsenate with 2M-H_2SO_4.

4.5 Zr^{4+}-BPAP

4.5.1 Arsenic Removal

The initial work of Suzuki *et. al.* immobilized zirconium on a specially prepared polystyrene resin containing the ethylenediaminetetraacetic acid (EDTA) ligand using $ZrOCl_2 \cdot 8H_2O$.[123a] This work suggested that we try to immobilize zirconium using a series of ligands, WP2 (amino acetate functionalized), BPED (EDTA functionalized), and BPAP (phosphonic acid functionalized). The former two IMPACS have been discussed earlier in this chapter and this section will discuss in detail the study performed on the amino phosphonate composite (BPAP). Zirconium loading onto this IMPAC averaged

about 93mg-Zr/g-composites (1.02mmol/g) as compared to 0.8mmol/g obtained by Suzuki *et. al*. Zirconium loading on BPAP is higher than Suzuki material and shows interesting results. In **Table 4.5** the percent composition data are converted to mmol/g and mole ratios. These ratios give some further insight into the functionalization of these materials. That the N/P ratio is 0.88 while the N content is 1.5mmol/g indicates that some of the amines may be doubly substituted with phosphonic acid groups. As expected the C/N and C/H ratios decreased after Zr(IV) loading. The Zr/P ratio was determined by SEM/EDX as well as from metal loading data and elemental analysis and gave reasonably consistent values of 0.69 and 0.72 respectively. This indicates that more than one phosphonic acid group is coordinated to a zirconium ion. Consistent with this suggestion is that chloride analysis gives a Zr/Cl ratio of 1.1:1 indicating the Zr sites have net charge of +1. After washing the Zr^{4+}-BPAP with 2M–H_2SO_4, elemental analysis gives a Zr/S ratio of 2.1:1 further corroborating the net charge of +1 on the Zr sites. Given that each phosphonic acid group has a maximum charge of -2 there must be more than one of these groups coordinated to each Zr (**Figure 4.6**) as the Zr/P ratios suggest.

Table 4.5: Elemental analysis data and ligand loading for BP1 and the corresponding phosphorus acid modified BPAP, BPAPM and ZrBPAP. Error in elemental analysis is $\pm$0.3%.

SPC	Carbon (mmol/g)	Hydrogen (mmol/g)	Nitrogen (mmol/g)	Phosphorus (mmol/g)	N:P	Zr:P
BP1	9.57	21.4	2.09	--	--	--
BPAP	11.8	30.3	2.40	1.40	1.71	--
BPAPM	10.1	29.9	1.58	1.79	0.88	--
Zr^{4+}-BPAP	8.42	27.2	1.13	1.55	0.73	0.72

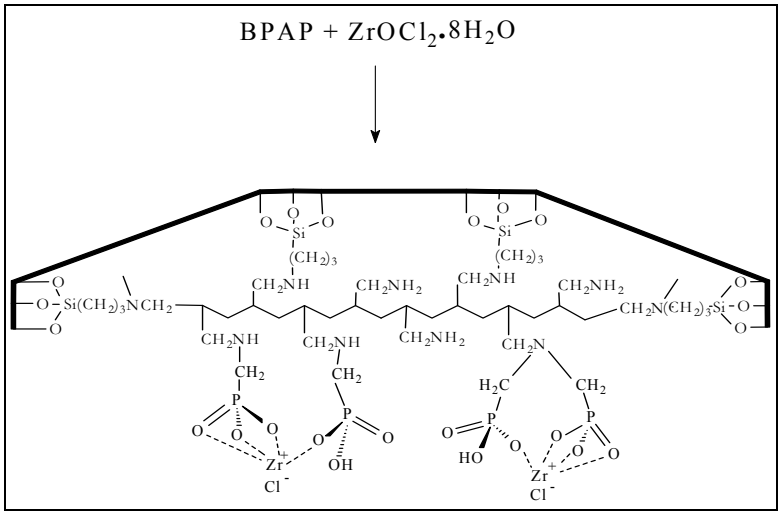

Figure 4.6: Schematic representation of the IMPAC Zr-BPAP showing more than one phosphonic group bound to the zirconium.

Because the N/P ratios suggest that some of the amines may be doubly substituted with phosphonic acid groups, we ran a solid state 2D phosphorus-proton correlation experiment which showed that this was the case (**Figure 3.8**). Equilibrium batch tests were performed to evaluate the ability of ZrBPAP to adsorb arsenate and arsenite in the pH ranges of 2–8 and 2–10 respectively. Solutions (20mL) of arsenate and arsenite containing 1000 ppm arsenic were shaken with 0.2g of the composite for 24 hrs. The batch capacities for both the arsenic species are shown in **Table 4.6** and fit well with the Pourbaix diagram which defines the various species of arsenic present at a particular Eh, pE and pH (**Figure 1.2**). Maximum arsenate capacity occurs at pH 4, where the predominant species is $H_2AsO_4^{-1}$ (>95%) and decreases sharply at pH 8, where the predominant species is $HAsO_4^{-2}$. At pH 6, only 80% of the arsenate exists as $H_2AsO_4^{-1}$ and the remaining 20% exists as $HAsO_4^{-2}$. This explains the small drop in arsenate capacity from pH 4 to pH 6. The arsenate capacity at pH 2 is still significant

(0.68mmol/g). At this pH, H_3AsO_4 is the main species in solution (approximately 65%). However the remaining 35% exists as $H_2AsO_4^{-1}$ and it is possible that there is a rapid displacement of the H_3AsO_4/ $H_2AsO_4^{-1}$ equilibrium. The decrease in arsenate capacities with increasing pH could also be due to the high affinity of zirconium (IV) for the hydroxide ion. In contrast, arsenite exists predominantly as H_3AsO_3 till pH 8. It is only at pH 10, that the predominant species is $H_2AsO_3^{-1}$, where maximum arsenite capacity is observed.

Table 4.6: Arsenic (III & V) batch capacities tested at various pH on ZrBPAP.

pH → / **Species ↓**	**2**	**4**	**6**	**8**	**10**
As(III)–mg/g (mmol/g)	1 ± 0.01 (0.01)	2 ± 0.01 (0.03)	2 ± 0.02 (0.03)	6 ± 0.02 (0.08)	50 ± 0.63 (0.67)
As(V)–mg/g (mmol/g)	51 ± 0.73 (0.68)	81 ± 1.12 (1.08)	56 ± 1.11 (0.75)	40 ± 0.53 (0.53)	--

* Numbers in parenthesis are the batch capacities values in 'mmol-As/g-composite'.

The ratio of Zr/As at pH 4 and 6 were estimated using SEM/EDX (approximate area analysed was 10μm x 10μm) which allowed the determination of the Zr/P, As/P, and As/Zr ratios at the pHs mentioned above. At pH 4, Zr/P = 0.72 ± 0.01, As/P = 0.87 ± 0.01, As/Zr = 1.2 ± 0.01, indicating that there is about one Zr(IV) for each $H_2AsO_4^{-1}$ (**Figure 4.7**). At pH 6 where $HAsO_4^{-2}$ becomes a major species, these ratios change to Zr/P = 0.71 ± 0.01, As/P = 0.59 ± 0.01, As/Zr = 0.8 ± 0.01, respectively indicating that at a significant number of sites two Zr(IV) are required to bind each $HAsO_4^{-2}$. These data are also in agreement with the net +1 charge on each Zr site.

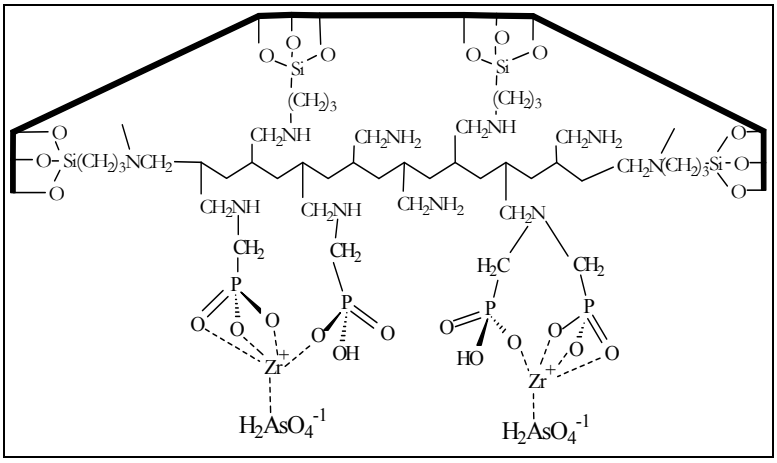

Figure 4.7: Schematic representation of ZrBPAP showing loading with arsenate at pH 4.

4.5.2 Langmuir Adsorption Isotherm Model

In the next section it will be shown that there is no Zr(IV) leaching from BPAP. Therefore we have made a thorough examination of the adsorption properties of this primary system. The Langmuir sorption model determines the relationship between the concentrations of surface adsorbed species to the number of active sites on that surface at equilibrium. If an adsorption process follows this model then it can be concluded that adsorption takes place as a monolayer on a homogenous surface without interactions between the adsorbed species. The rearranged-linear version of the Langmuir equation is shown in Equation 4.1.

$$C_e/Q_e = 1/Q_m K_{ads} + C_e/Q_m \qquad (4.1)$$

where, C_e represents the concentration of metal ions in solution at equilibrium (mg/L);

Q_e is the concentration of metal ions adsorbed onto the composite (mg/g);

Q_m is the measure of the maximum capacity of the adsorbent (mg/g);

K_{ads} is the intensity of adsorption (L/g).

Q_m can be calculated from the slope of the straight line plot of C_e/Q_e vs. C_e. The constant K_{ads} can be derived from the slope and the intercept of the same straight line ($1/ Q_mK_{ads}$). If the plot of Equation 4.1 is linear then Q_m provides an estimate of the active sites and K_{ads} gives an estimate of the driving force or the equilibrium constant for the process.[131]

Langmuir concentration dependent isotherms for arsenic at pH 4 and 6 are reported in **Figure 4.8**. The Langmuir model fits the sorption of arsenate by ZrBPAP very well; R^2 = 0.9988 and 0.9987 for pH 4 and 6, respectively. Moreover, the model provides information regarding the intensity of the sorption process (K_{ads}) as well as an approximation of the theoretical number of sorption sites on the surface (Q_m). The value of K_{ads} for ZrBPAP is 0.016L/g and the value of Q_m is 98mg/g at pH 4. At pH 6 the K_{ads} is 0.018L/g and Q_m is significantly smaller being 55mg/g. This is consistent with the observed batch and dynamic capacities and with the SEM/EDX data. The values of K_{ads} and Q_m for anion binding reported here are similar to the values obtained for cation binding by silica polyamine composites (K_{ads} = 0.012L/g and Q_m = 21–44mg/g for Ni^{2+} cations with an EDTA ligand on silica polyamine composite).[108]

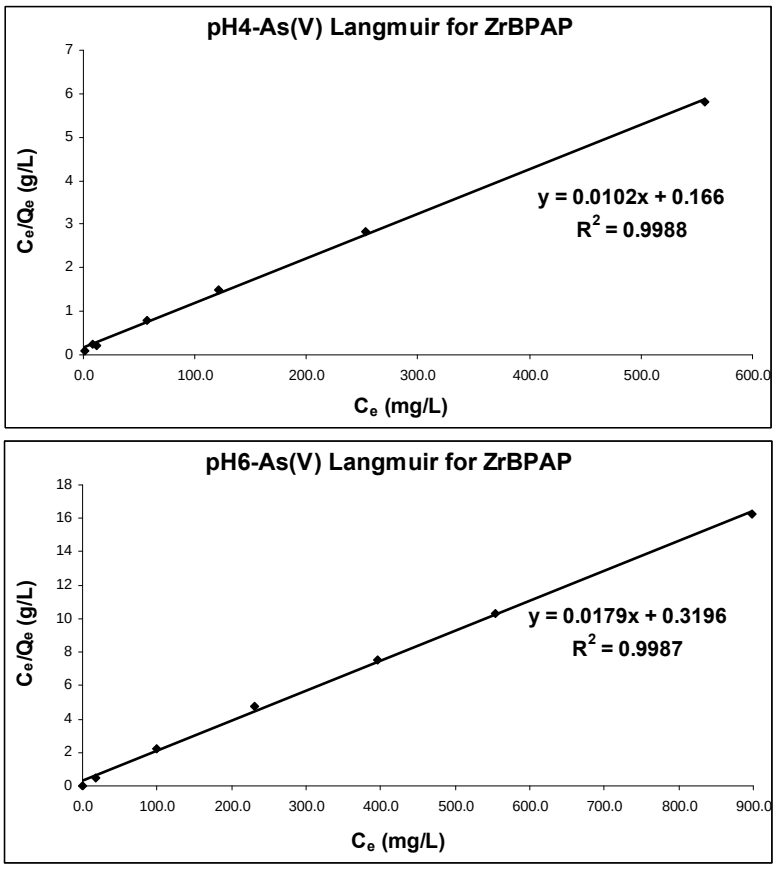

Figure 4.8: Langmuir adsorption isotherms for arsenate adsorption by ZrBPAP at pH 4 (top) and pH 6 (bottom).

4.5.3 Dynamic Column Breakthrough and Elution Studies

Batch capacity measurements provide only equilibrium adsorption properties of ZrBPAP. In order to obtain an understanding of the mass transfer kinetics and ease of regeneration of this new arsenate adsorption material, breakthrough tests were run at pHs of 2, 4, 6, and 8 for arsenate (**Figure 4.9**). The arsenate dynamic capacity increases from pH 2 to pH 4. It is highest (1.15mmol/g) at pH 4 and gradually deceases as the pH increases. These data are in good agreement with the changes in arsenate speciation predicted by the Pourbaix diagram (**Figure 1.2**). More importantly, the saturation flow

capacities are very close to the equilibrium batch capacities (**Table 4.6**) indicating excellent mass transfer kinetics typical of these types of silica polyamine composites. In the case of arsenite, breakthrough tests run from pH 2–10 showed that there was no significant adsorption of arsenite until pH 10 where ionization of $As(OH)_3$ is significant (**Figure 4.10**), again in agreement with batch capacity profiles. This indicates that ZrBPAP will not be a useful material for arsenite capture in the pH range of natural waters (6–8) and most mining waste streams.

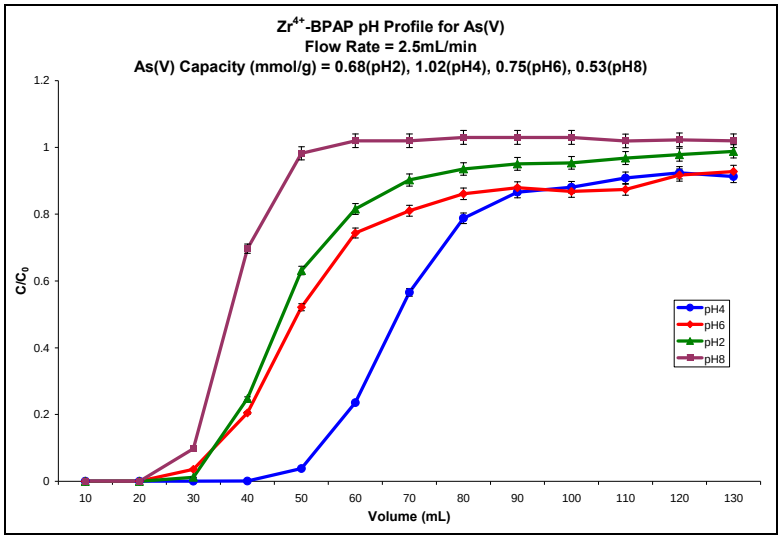

Figure 4.9: Breakthrough curves for arsenate sorption on ZrBPAP at pH = 2–8.

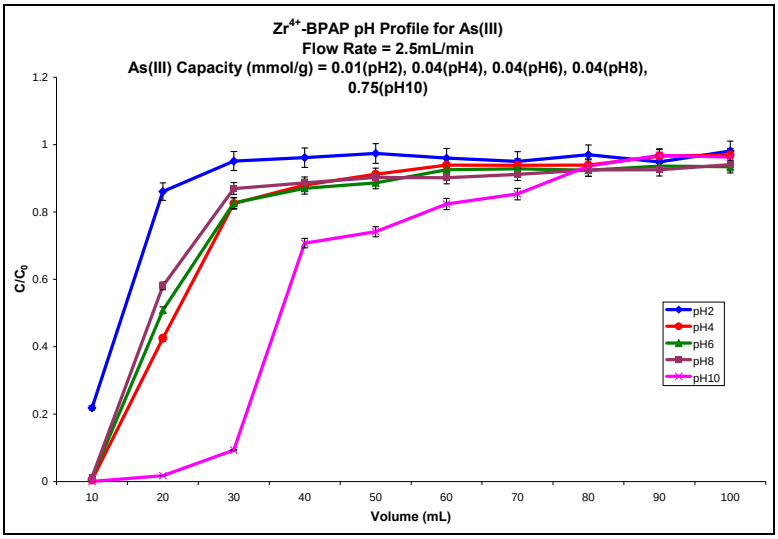

Figure 4.10: Breakthrough curves for arsenite sorption on ZrBPAP at pH = 2–10.

In order for ZrBPAP to be a useful material for arsenic removal and recovery, it must be reusable and capable of regeneration with economically viable methodologies. We therefore performed four consecutive load and strip cycles on a 5mL column containing ZrBPAP (2.7g) with an arsenate feed concentration of approximately 22mM (1650mg/L) at pH 4. The arsenate capacities for the four consecutive cycles were 1.15, 0.95, 0.95, 0.95mmol/g–dry composite respectively (**Figure 4.11-top**). The decrease in capacity between the first load and subsequent loads is due to the presence of adsorptive sites inaccessible to the strip solution leading to the incomplete stripping and recovery of the arsenate anion from the first strip cycle using 2M–H_2SO_4 (**Figure 4.11-bottom**). The total arsenate feed captured by the column for each of the four cycles was 3.09mmol (232mg), and 2.56 mmol (192mg), 2.56mmol (192mg), and 2.55mmol (191mg) respectively. The arsenate strips for the four cycles were 186mg (80%), 188mg (98%), 190mg (99%), and 190mg (99%), respectively. However, the arsenate capacities for the

second, third and the fourth cycles remain the same, indicating that no more zirconium sites are blocked by the unrecoverable arsenate ions. The first 2 column volumes of the acid strip contain arsenic at ~150mM, representing a concentration factor of 6.8 with respect to the feed. Although it took 20 column volumes to strip all the arsenate from the column, 86% or more stripped off in the first 4 column volumes.

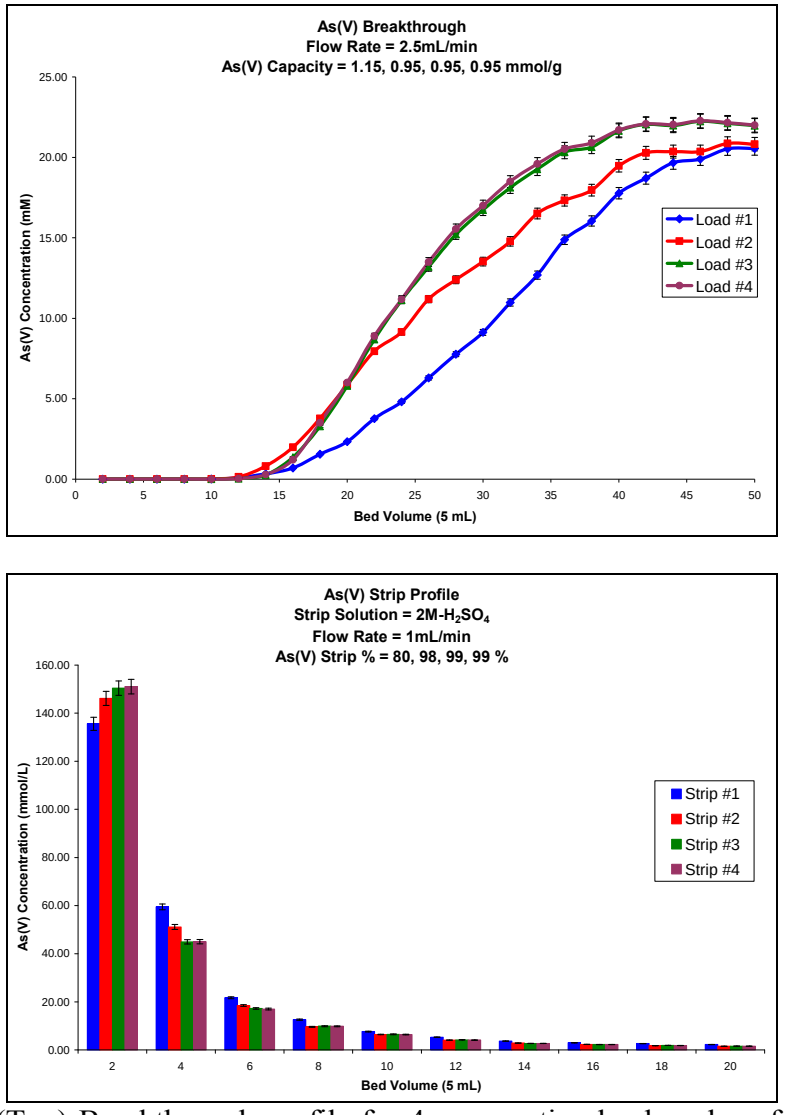

Figure 4.11: (Top) Breakthrough profile for 4 consecutive load cycles of ZrBPAP with 1650mg/L of arsenate at pH 4; (Bottom) Strip profile for 4 consecutive load cycles of ZrBPAP with 2M–H_2SO_4.

We then ran 1000 load and strip cycles on the composite using a computer controlled multi-solenoid apparatus described in the experimental section (**Figure 2.1**). Column capacity was measured after the 100^{th} and 1001^{st} cycle using the standard breakthrough procedures (**Figure 4.12**). Tests were run at pH 6 using a 1.0g/L arsenate solution. The capacity for load #1002 was measured to be 0.65mmol/g; a reduction in arsenate capacity of about 14% as compared to the capacity reported in **Table 4.6** for pH 6. This represents an excellent usable lifeline for the lifetime of this composite. Also notable is the distinct improvement in capture kinetics as measured by the better column utilization factor of 0.6 vs. 0.22 that can be seen by comparing **Figures 4.11 (top) and 4.12**, respectively. The column utilization factor is calculated using the equation given below:[132]

$$U = \frac{\text{(BV at initial breakthrough)}}{\text{(BV at complete breakthrough)}} = \frac{V_{MCL}}{V_C} = \frac{100mL}{170mL} = 0.6 \qquad (4.2)$$

where, U – Column utilization factor,
BV – Bed volume,
V_{MCL} – Volume at maximum contaminant level (MCL),
V_C – Volume at complete breakthrough.

This seems to be a general characteristic of these composites and suggests that on repeated use, minor impurities such as siloxy-alkyl oligomers that might be introduced during synthesis are cleaned out of the pores of the composite allowing more diffusion in and out of the pores.[106-108]

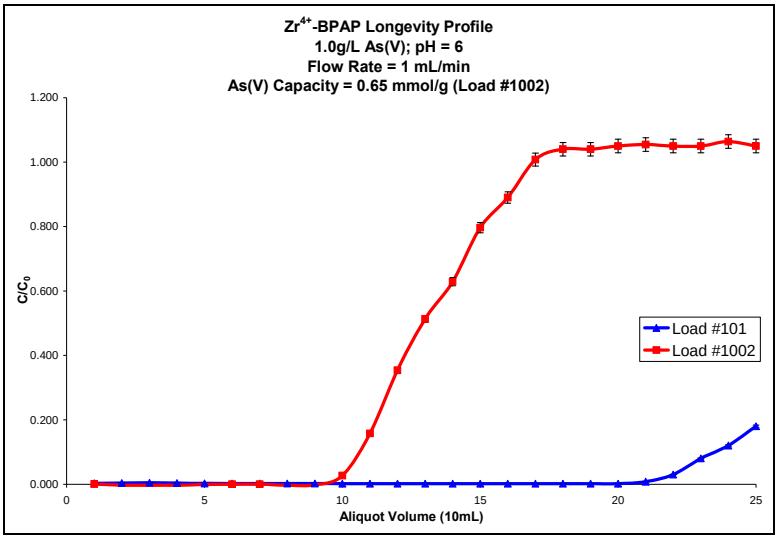

Figure 4.12: ZrBPAP longevity profile for arsenate anion over 1000 cycles.

4.5.4 ZrBPAP Selectivity over Other Anions

The high sorption of any media can decrease significantly in the presence of competing ions. Sulfate is commonly present in groundwater with a concentration exceeding that of arsenic by several orders of magnitude.[124] Ion exchange resins have not been recommended for As(V) when the sulfate concentration exceeds 120mg/L.[104] The selectivity of ZrBPAP for arsenate in the presence of excess sulfate and chloride ions was therefore investigated. A typical mine waste solution contain arsenic in the range 150–300µg/L with sulfate present in about a 1000 fold excess. The solution used for evaluating the selectivity of ZrBPAP contained 238µg/L – arsenate & 200mg/L – sulfate at pH 6. A two liter solution, corresponding to 400 bed volumes was run through a 5cc column packed tightly with ZrBPAP (~2.6g). After only 60 bed volumes it was observed that sulfate reached full breakthrough while the arsenate ion was still being captured on the composite (**Figure 4.13**). Since the detection limit for the Thermo Electron ICP/AES

was 5µg/L for arsenic, concentrations reported below that level by the instrument was assumed to be 5µg/L. Even after 400 bed volumes, the arsenic concentration was below EPA's Maximum Contaminant Level (MCL) of 10µg/L. The intermittent spikes observed for the arsenate anion could be due to some column channeling or dilution errors. The selectivity factor for arsenate over sulfate was calculated at full sulfate breakthrough (60 bed volumes) using the relation in Equation 4.3:

$$\frac{[As]_F / [SO_4]_F}{[As]_{60} / [SO_4]_{60}} = 50:1 \qquad (4.3)$$

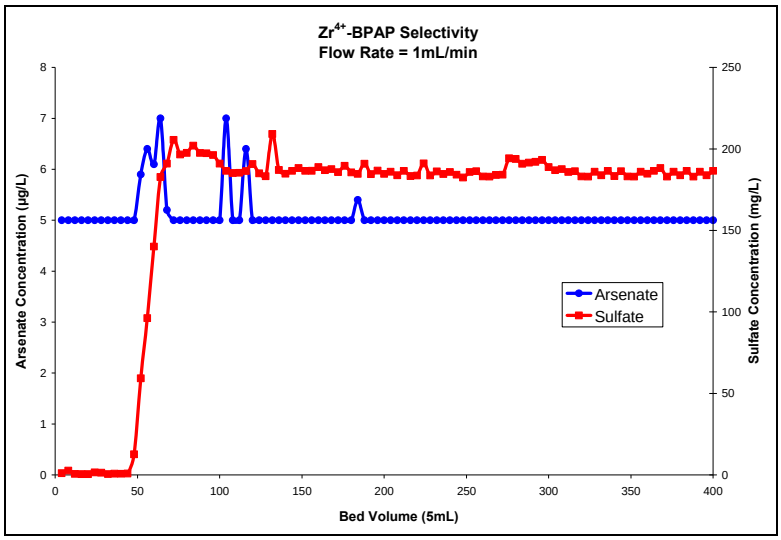

Figure 4.13: Breakthrough curve of ZrBPAP selectivity for low level arsenate over excess sulfate.

To further test the selectivity of ZrBPAP for arsenate ion, we made a solution of approximately 200mg/L each of arsenate and selenate in presence of approximately 20g/L of chloride ion (as NaCl). Solutions of this type model the high chloride solutions that result from hypochlorite oxidations of industrial waste streams.[133] Equilibrium batch tests and pH profiles show the selective capture of arsenate over selenate, and chloride,

although the capacities for arsenate over a wide pH range of 2–11, remained the same (0.25mmol/g). These batch tests show that arsenate capacities are lower in presence of competing ions (0.25mmol/g) than that reported earlier in the absence of competing ions (0.75 mmol/g) such as sulfate and chloride. A breakthrough test on the same solution was carried out at pH 6, and 60 bed volumes was run through a column packed with ZrBPAP at a flow rate of 1mL/min. As shown in **Figure 4.14**, the selenate ion reaches full breakthrough almost immediately (within 4 bed volumes) and the arsenate did not reach complete breakthrough even after 60 bed volumes. From this data, we can estimate the ZrBPAP selectivity factor for arsenate over selenate to be about 20:1. We have also done equilibrium batch studies on the affinity of ZrBPAP for selenite and selenate and found that this material has a higher affinity for selenite than for selenate, the batch capacities at pH=6 being 64 and 39 mg/g respectively. These results are qualitatively similar to those obtained with iron based adsorbents where selenite is preferred over selenate.[134] We also measured the selectivity of arsenate over selenite using a breakthrough study and found that the selectivity of arsenate over selenite was lower than for selenate being approximately 4:1 rather than 20:1. This is consistent with the equilibrium batch studies. This difference is undoubtedly due to the lower charge on selenite at pH=6.

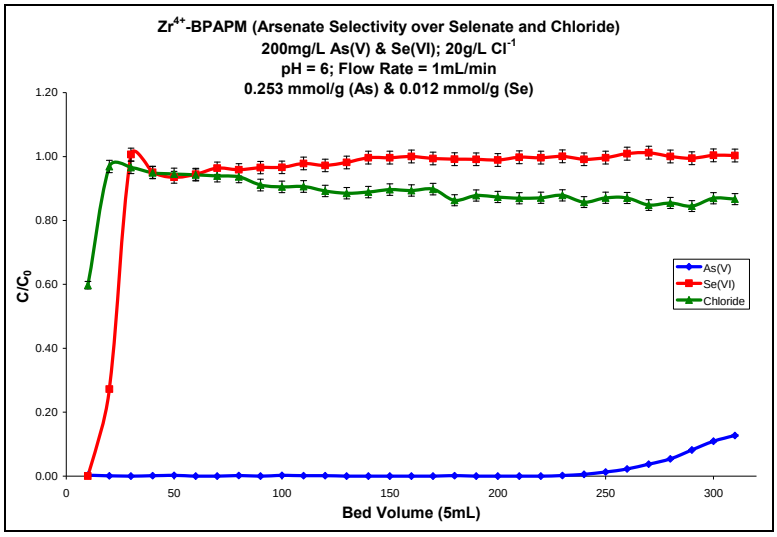

Figure 4.14: Breakthrough curve for ZrBPAPM for a solution containing 200mg/L arsenate, 200mg/L selenate and 20g/L chloride at pH 6.

The observed selectivity for arsenate over sulfate, selenate and chloride at pH 6 is clearly due to more than simple electrostatic interactions. At pH 6 arsenate exists as a mixture of $H_2AsO_4^{1-}$ and $HAsO_4^{2-}$ (pKa_1 = 2.19 and pKa_2 = 6.94) while both sulfate and selenate exist as fully deprotonated di-anions (pKa_1 = <0.0 and pKa_2 = 1.97 and pKa_1 = <0.0 and pKa_2 = 1.92 for selenate and sulfate respectively). Arsenate has a less electronegative element as the central atom as compared to selenate (2.2 versus 2.6, for both sulfate and selenate according to the Pauling scale). This results in a more polarizable oxoanion which can form polar-covalent interactions with the phosphonic acid–Zr(IV) sites and these are clearly stronger than electrostatic interactions based on anion charge. In the case of the hypochlorite oxidation solution tested here the chloride is co-loading with arsenate, and based on the reduced arsenic capacities it is important to note that the monoanion chloride is selected over the dianion selenate, even in the almost total absence of arsenate (**Figure 4.15**). Again, this probably points to the stronger polar

covalent interactions with the phosphonic acid–Zr(IV) centers for chloride relative to selenate but not arsenate. The observed co-loading of chloride with arsenate is due the huge excess of chloride present in the solution.

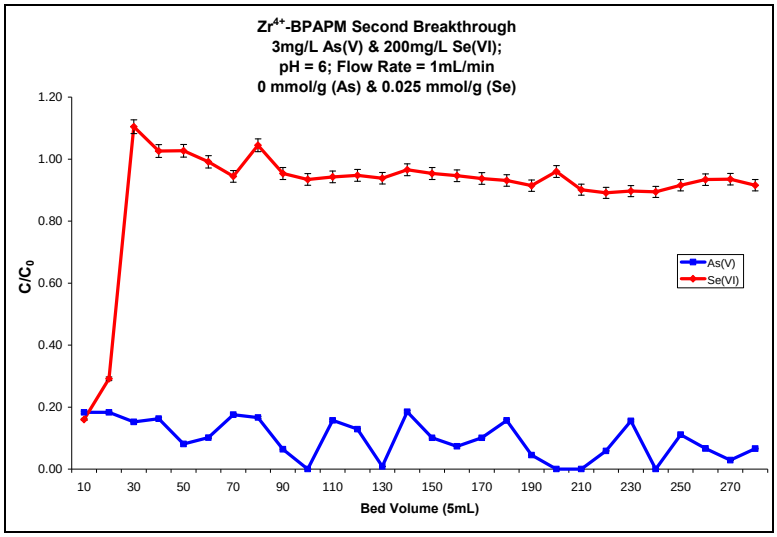

Figure 4.15: Breakthrough profile showing second load cycle on a new column of ZrBPAP with most of the arsenic removed.

4.5.5 ZrBPAP Comparison with ASM-10HP (Resintech)

It should be pointed out that we have compared ZrBPAPM with the commercially available-iron doped strong base anion exchange resin, ASM-10HP made by Resintech.[135] This material consists of a N-trimethyl substituted polystyrene doped with ferric ion. We found that the capacity of this material for arsenate, at pH=6 was 48mg/mL compared with 56mg/g (~ 90mg/mL) for ZrBPAP (**Figure 4.16**). Although, both the materials showed good selectivity for arsenate over sulfate, it should also be pointed out that the column utilization factor was 0.15 for ASM-10HP and 0.63 for ZrBPAP. This higher column utilization factor is typical of SPC materials relative to polystyrene analogs and points to the better capture kinetics of the silica based ion

exchange materials. The drawback with the ASM-10HP resin was its poor stripping, as it only stripped half of the arsenate that was loaded. The stripping profile is also shown in **Figure 4.15**. This suggests that after only four or five cycles the column will be saturated and would not be able to capture any more arsenate, hence the media has to be replaced.

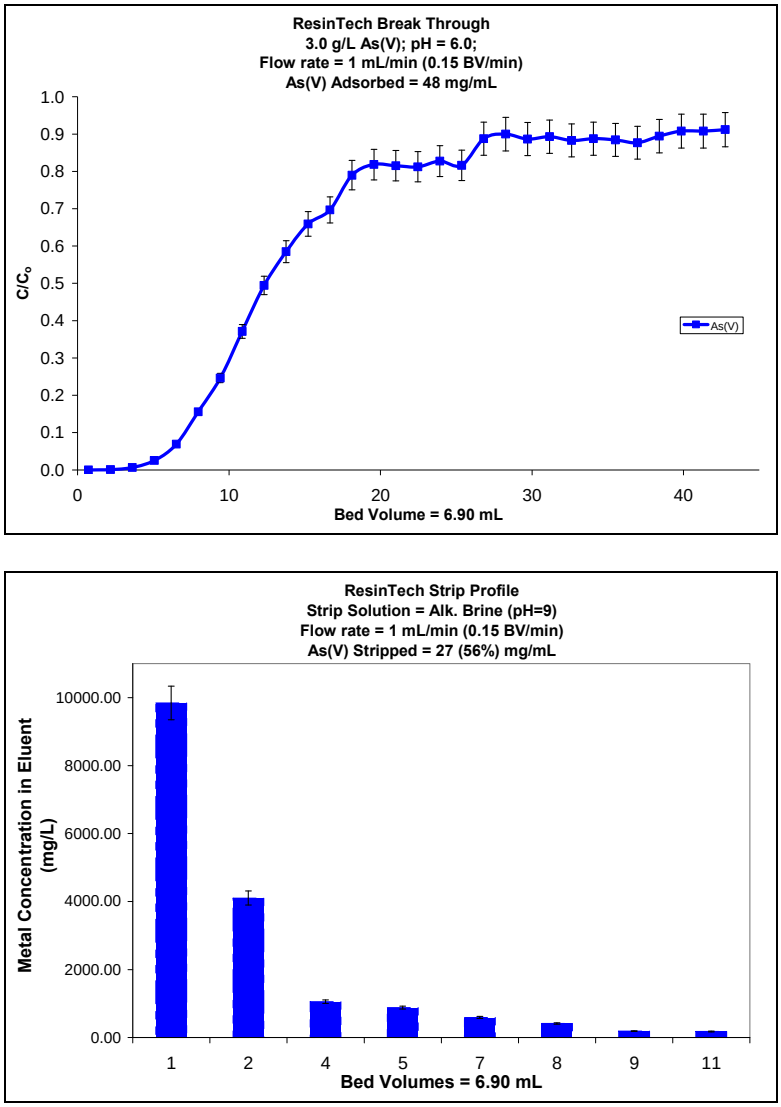

Figure 4.16: (Top) Breakthrough profile for ASM-10HP for arsenate at pH 6. (Bottom) Strip profile showing only 56% of arsenate stripped from the column.

4.5.6 Arsenite Capture

A lot of research has been done on arsenate removal, but the problem of arsenic contamination in subsurfae water systems is mostly due to the presence and toxicity of arsenite. **Table 4.6** shows the batch capacities of arsenite, and this again points out that the removal of As(III) species is easier at higher pH (> 8). So we ran a column breakthrough experiment for arsenite capture using ZrBPAP at pH 10 (**Figure 4.17**). The breakthrough capacity was comparable to the batch capacity at pH 10. However, the mass transfer kinetics for arsenite loading was poor even at a slow flow rate (1mL/min). But, the stripping of arsenite using 2M-sulfuric acid was 100% with > 95% of the arsenite stripping off in the first 4 column volumes. Due to the poor loading kinetics, successive loading of arsenite were not carried out, although it may be further investigated in the future.

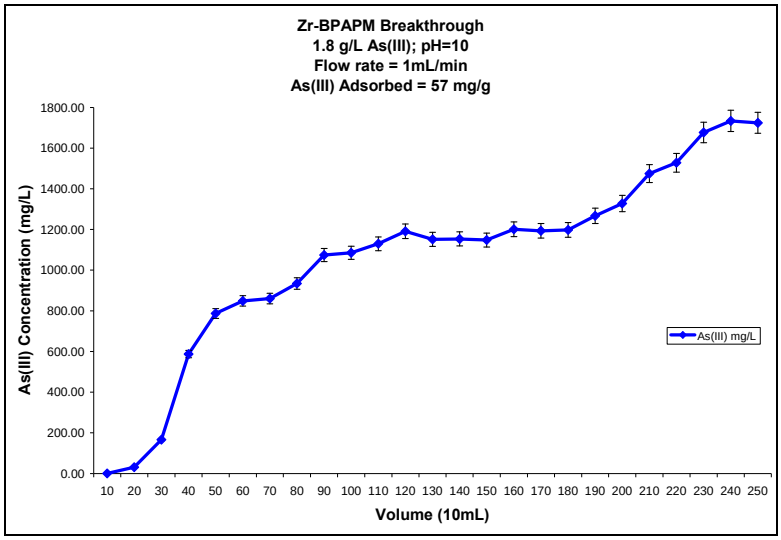

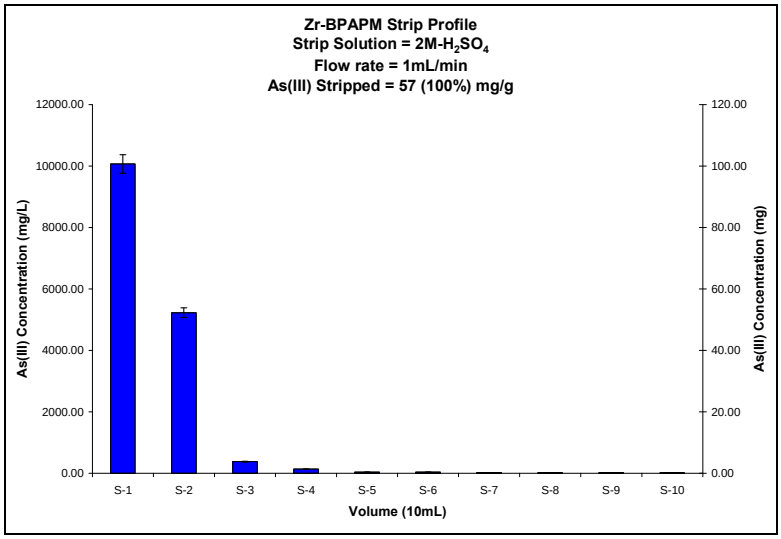

Figure 4.17: (Top) Breakthrough profile for arsenite on ZrBPAP at pH 10. (Bottom) Strip profile for arsenite using 2M-H_2SO_4.

4.6 Non-IMPAC System (BPQA)

As mentioned in the previous chapter, this system does not use any immobilized metal to act as the cation or the positive charge to remove the metal anions from aqueous solutions. The non-IMPAC BPQA used here was the mixed silane version (7.5:1 MTCS:CPTCS) and preliminary equilibrium batch tests showed promising results for

arsenate over a broad pH range of 2-8 and for arsenite at pH 10 (**Table 4.7**). Equilibrium batch capacities for arsenate and arsenite show similar trends observed with the other IMPACs discussed in the previous sections. Arsenate batch capacities were also tested using 10:1 and 12.5:1 BPQAs, and they are also reported in **Table 4.7**. The arsenate batch capacities using the more diluted anchor silanes were lower than the 7.5:1 version due to the lower polymer loading. The trend with pH for these systems also fits well with the arsenic speciation profile as observed in the Pourbaix diagram. Only the 7.5:1 BPQA was extensively used for the arsenate removal studies and the results are discussed below.

Table 4.7: Initial equilibrium batch tests for arsenite and arsenate species with BPQA.

pH → / **Species ↓**	**2**	**4**	**6**	**8**	**10**
As(III) (mg/g)	--	--	--	15 ± 0.80	17 ± 0.88
As(V) (mg/g)	37 ± 1.9	59 ± 0.91	52 ± 2.4	22 ± 2.5	--
As(V) (mg/g)*	4 ± 0.50	17 ± 0.57	27 ± 0.96	35 ± 0.32	--
As(V) (mg/g)†	5 ± 0.07	22 ± 0.93	30 ± 1.06	27 ± 0.29	--

* Arsenate batch capacity using 10:1 (MTCS:CPTCS) BPQA.
† Arsenate batch capacity using 12.5:1 (MTCS:CPTCS) BPQA.

This non-IMPAC system is an analogue of a quaternary amine based arsenic removal polystyrene resin that is commercially available (ASM-10HP). Dynamic column studies were performed for arsenate removal on this composite and showed some interesting result. Two consecutive arsenate loads were run through this column at pH 6 at a faster flow rate (2.5mL/min). The column was stripped with 2M-sulfiric acid as done with the other IMPAC systems (**Figure 4.18**). Although stripping with sulfuric acid had deleterious effects on the kinetics of second arsenic load cycle, the capacity did not drop

significantly, but the loading and the mass transfer kinetics were poor compared to the previous cycles. This is believed to be due to some column channeling that might have occurred, which also explains the steady arsenate capacity in the second load as compared to the first load. The sulfuric acid strip purity was excellent with respect to arsenic and that most of the arsenic stripped in the first two column volumes (**Figure 4.18-bottom**).

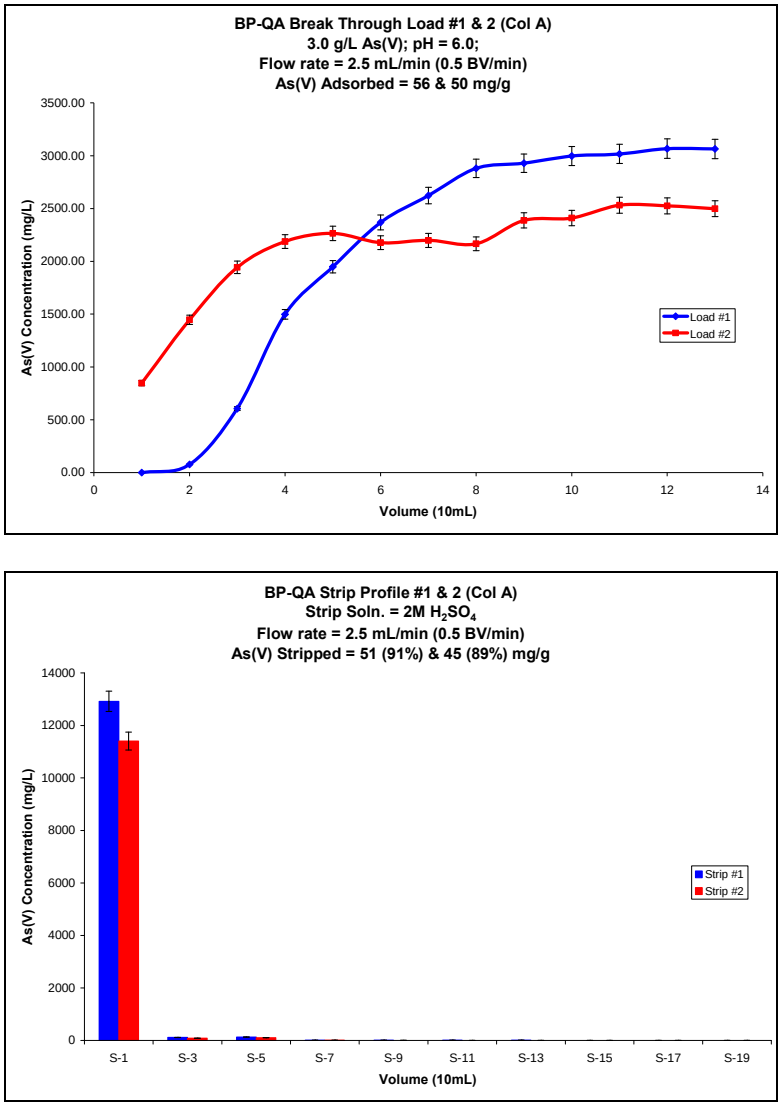

Figure 4.18: (Top) Breakthrough profile for arsenate on BPQA at pH 6. (Bottom) Strip profile for arsenate using 2M-H_2SO_4.

The commercially available polystyrene analogue of BPQA uses an alkaline brine strip solution for stripping arsenic from the resin (**Figure 4.16-bottom**). We decided to try and use brine for arsenic strip, as this would help with the integrity of the composite by not exposing it to harsh acids. **Figure 4.19** shows the arsenate breakthrough and strip profile at pH 7 (conditions for naturally occurring surface waters).

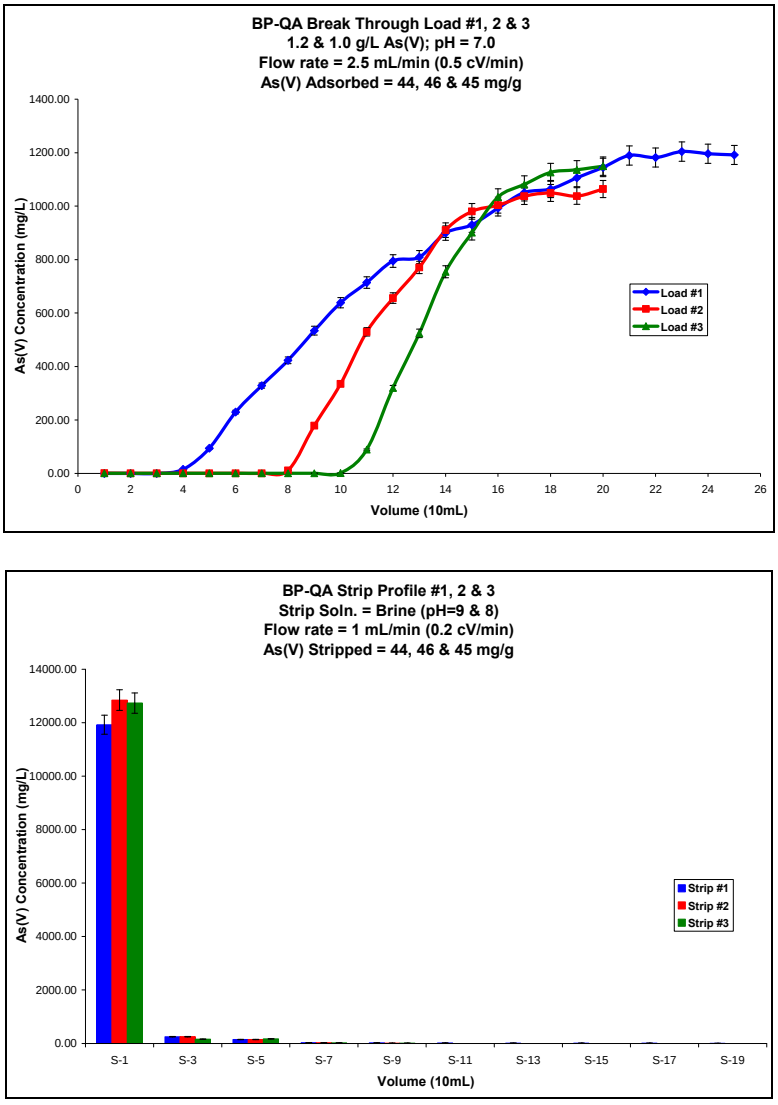

Figure 4.19: (Top) Breakthrough profile for arsenate on BPQA at pH 7. (Bottom) Strip profile for arsenate using brine at pH = 8.

Three successive arsenate loads were performed through the column of BPQA and the arsenate capacities for the three load cycles were the same (~ 45mg/g). The flow rate used for the arsenate loading was 2.5mL/min (faster than what is used commercially). The mass transfer kinetics for the second and third load cycles were better than the first load, which was also observed with the ZrBPAP composite. As mentioned before, this seems to be a general characteristic of these composites and suggests that on repeated use, minor impurities such as siloxy-alkyl oligomers that might be introduced during synthesis are cleaned out of the pores of the composite allowing more diffusion of target ions in and out of the pores. The stripping of arsenate using brine shows excellent mass transfer kinetics and 100% strip of arsenate was observed. The first two column volumes consisted of more than 95% of the arsenate stripped. This composite shows tremendous potential for commercial applications as there are no harsh conditions involved and the operation is very simple. The exchange of arsenate and chloride by mere electrostatic forces make this non-IMPAC system very viable for arsenic removal and recovery. Further testing for arsenate selectivity and the composite longevity is still to be studied. Although, only preliminary batch studies have been studied on selenium using BPQA, it is proposed as one of the future studies.

4.7 Selenium Recovery

Most systems that work for arsenic removal can also be extended to use as selenium removal systems. Similar to arsenic removal technologies, the most widely used selenium capture systems are based on iron(III)-modified adsorbents. This section

discusses two different composites (BPQA and ZrBPAP) that were used to study selenium recovery from aqueous systems. Although, only preliminary work has been performed on selenium capture, more research is proposed to study their application in detail.

4.7.1 (7.5:1) BPQA

After the success of the non-IMPAC system BPQA for the removal and recovery of arsenate anion, we thought it would be wise to study this system for selenium removal as well. Only equilibrium batch tests have been performed on selenium anions using BPQA (**Table 4.8**). Selenite exists as a mono-anionic species between pH 4 and 6, and becomes almost exclusively a di-anionic species after pH 8 (**Figure 1.3**). Whereas selenate exists as a mono-anionic species up to pH 2 and then becomes the di-ionic species. It is after pH 4 that almost all of the selenate ions are in its di-anionic form. This explains the steady capacity for selenate species at pH 6 and 8. It is still unclear why the capacities of selenate are somewhat lower at pH < 6. The selenite species capacities fit well with the Pourbaix diagram of selenium. Since the capacities for selenite were quite low, further research was not carried out for selenium removal using BPQA.

Table 4.8: Preliminary batch capacities for selenite and selenate species using BPQA.

Species ↓ pH →	**2**	**4**	**6**	**8**	**10**
Se(IV) (mg/g)	9 ± 0.08	15 ± 0.19	15 ± 0.28	13 ± 0.54	7 ± 4.4
Se(VI) (mg/g)	35 ± 1.99	40 ± 1.2	48 ± 1.7	48 ± 0.38	--

4.7.2 Zr^{4+}-BPAP

The phosphonic acid modified composite ZrBPAP has been studied most extensively for the purposes of this research. Equilibrium batch capacities show selenite and selenate capacities follow the trend shown in the selenium Pourbaix diagram. The selenite capacity at pH 2 is anomalously high (98mg/g) and these are not well understood. At this pH, H_2SeO_3 is the main species in solution (approximately 70%). However the remaining 30% exists as $HSeO_3^{-1}$ and it is possible that there is a rapid displacement of the H_2SeO_3/ $HSeO_3^{-1}$ equilibrium. At pH = 4-6, the percent of mono-anion remains constant as observed by the constant capacity; at pH = 8 the di-anion is the dominant species and the capacity goes down. For selenate, the capacity is highest at pH = 2 since it is still a mono-anion , but at pH = 4-8 selenate is constant because the si-anionic species is dominant. All of this behavior is similar to that observed for arsenic and is constant with the net +1 charge on the immobilized zirconium. The decrease in selenium capacities with increasing pH could be due to the high affinity of zirconium (IV) for the hydroxide ion. The selenate capacity fits well with the selenate speciation trend, as shown in the Pourbaix diagram.

Table 4.9: Preliminary batch capacities for selenite and selenate species using ZrBPAP.

pH → / **Species ↓**	**2**	**4**	**6**	**8**
Se(IV) (mg/g)	98 ± 1.75	69 ± 1.67	64 ± 1.27	39 ± 2.1
Se(VI) (mg/g)	42 ± 0.53	36 ± 1.6	39 ± 1.11	38 ± 1.42

The problem of selenium is mostly in domestic waters where it exists in toxic levels to humans. So, breakthrough tests were carried at pH 6 for both the selenium species. Three consecutive loads of selenite solution were run on a column of ZrBPAP at a flow rate of 1mL/min. The breakthrough capacities for selenite were comparable to the equilibrium batch capacities at pH 6 mentioned in **Table 4.9**. The decrease in capacity between the first load and subsequent loads is possibly due to the fact that sulfate anions might be trapped in some adsorptive sites making it impossible for the subsequent selenite anions to enter. But, the third selenite load shows same capacity as the second one, suggesting that there are no more adsorptive sites that are inaccessible to the selenite anions. Another reason for this could be the leaching of zirconium while stripping, but no zirconium was observed in the strip solutions, suggesting complete immobilization of zirconium on the composite BPAP. The stripping of the selenite species using 2M-H_2SO_4 shows 100% recovery of selenite for all the strip cycles. Almost all of the selenium strips off in the first 4 column volumes, a trait shown by these types of composites. The overall binding capacities for selenium relative to arsenic is not only related to charge but also to the poorer polarizability of selenium oxoanions relative to their arsenic analogues. This of course is due to the greater electro-negativity of selenium as compared to arsenic.

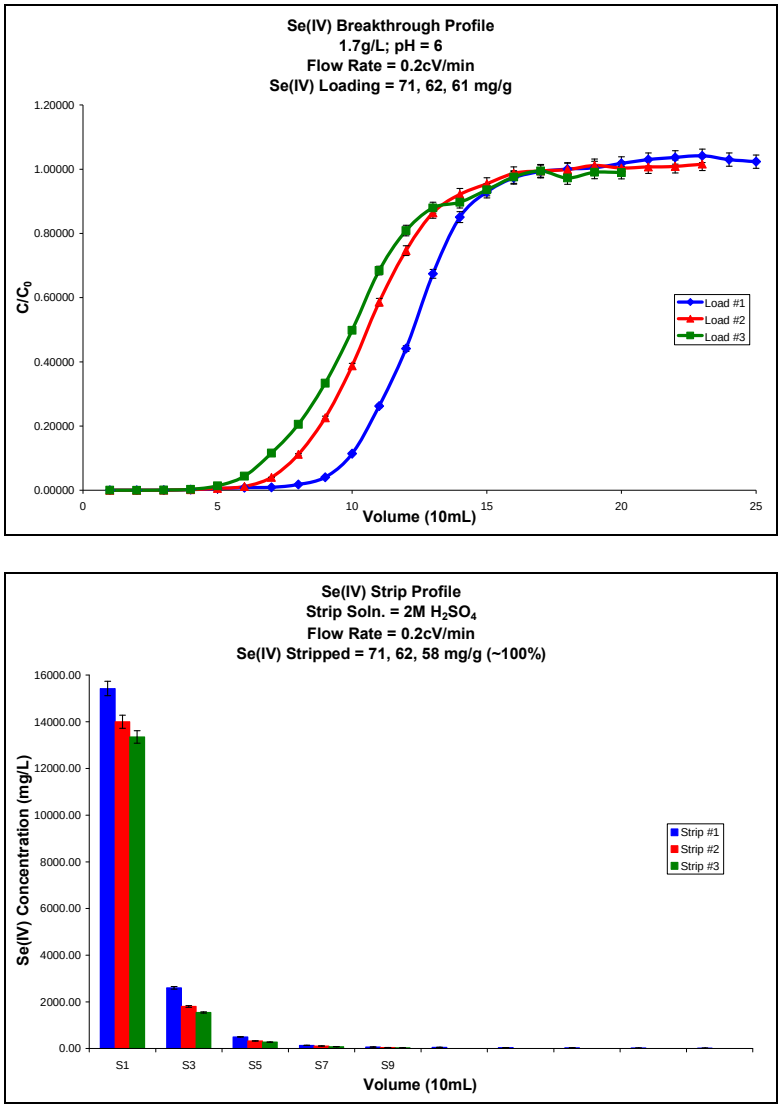

Figure 4.20: (Top) Breakthrough profile for selenite on ZrBPAP at pH 6. (Bottom) Strip profile for selenite 2M-H_2SO_4.

Three consecutive loads of selenate solution were run on a column of ZrBPAP at a flow rate of 1mL/min. The breakthrough capacities for selenate were comparable to the equilibrium batch capacities at pH 6 mentioned in **Table 4.9**. In the case of selenate, the mass transfer kinetics during was not as good as it has been observed with selenite. Again, we see a decrease in selenate capacity between the first load and subsequent loads,

which is possibly due to the presence of adsorptive sites inaccessible to the strip solution leading to the incomplete stripping and recovery of the selenate anion from the first strip cycle using 2M–H_2SO_4. The fact that no zirconium leach was found in the strip solutions supports our argument. The selenate capacity is constant for the second and the third load cycle (~ 35mg/g). The stripping of the selenate species using 2M-H_2SO_4 shows 100% recovery of selenate for the second and the third strip cycles and almost all of the selenium strips off in the first 2 column volumes.

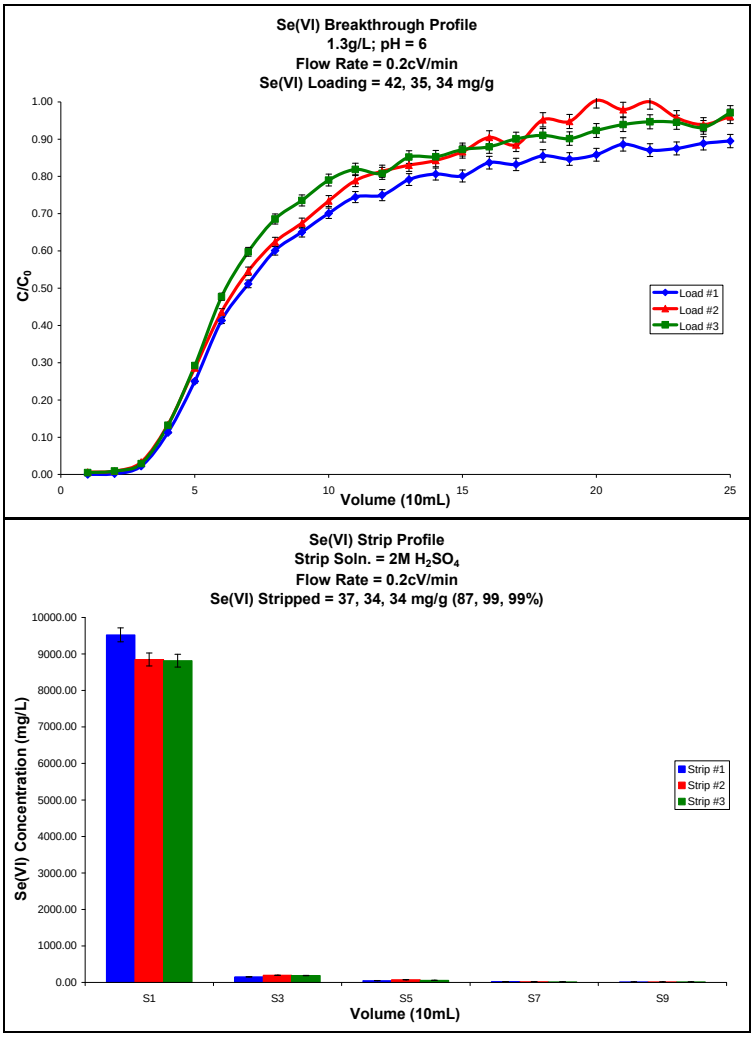

Figure 4.21: (Top) Breakthrough profile for selenate on ZrBPAP at pH 6. (Bottom) Strip profile for selenate 2M-H_2SO_4.

4.7.3 Selenium Selectivity

The high sorption capacity of any media can decrease significantly in the presence of competing ions. Sulfate is commonly present in groundwater with a concentration exceeding that of selenium by several orders of magnitude. From previous sections, we have observed that the ZrBPAP composite is highly selective for arsenate over either of the selenium species. But, we wanted to study the performance of ZrBPAP for selenium selectivity in the absence of arsenic and in the presence of excess sulfate. The feed concentrations for this test were 43ppb – selenium (mixture of selenite & selenate), and 400ppm – sulfate. A mixture of the selenium species was used because it reflected an actual waste stream provided to us by MSE Technologies, Butte, MT. The flow rate used was 1mL/min. A 500mL solution, corresponding to 100 bed volumes was run through a 5cc column packed tightly with ZrBPAP (~2.6g). After only 24 bed volumes it was observed that sulfate reached full breakthrough while the selenium anion was still being captured on the composite (**Figure 4.22**).

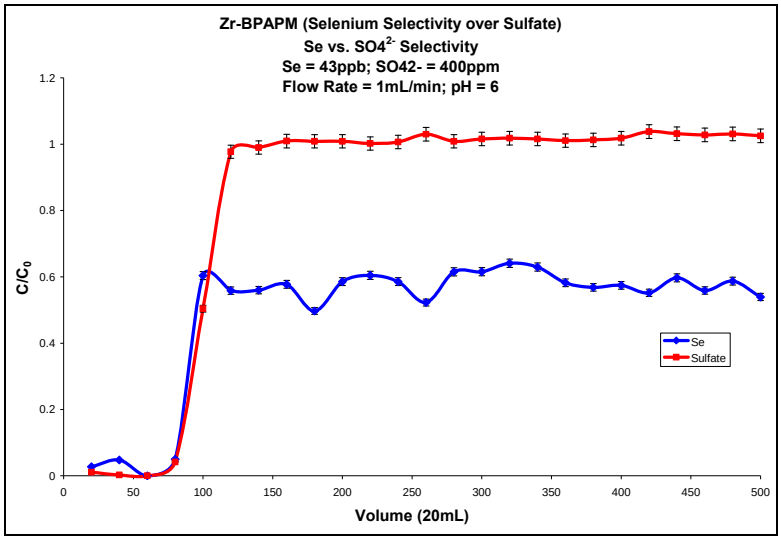

Figure 4.22: Breakthrough profile for selenium selectivity over sulfate on ZrBPAP.

Even after 100 bed volumes, the selenium concentration was below its feed concentration (43μg/L), and the EPA's Maximum Contaminant Level (MCL) for selenium is 50μg/L. The selectivity factor for selenium over sulfate calculated at full sulfate breakthrough (24 bed volumes) using the relation in Equation 4.3 was 1.75:1. This suggests that the composite is only slightly selective for selenium over sulfate. As discussed previously, ZrBPAP does not favor selenate in the presence of excess chloride (**Figure 4.15**). Hence it would be acceptable to infer that selenium anions can be stripped using excess chloride or a brine solution. Although this has not been studied, it would be a good idea to research this further.

4.8 Other IMPAC Systems

The versatility of the IMPAC technology was tested by altering the immobilized metal on the phosphonic acid modified composite, BPAP. The metals that were immobilized on BPAP were: Fe(III), Al(III), Ce(III), Ce(IV), Th(IV), and Zr(IV). We compared them side by side under identical conditions of pH, and target metal ion concentration. The selectivity of ZrBPAPM for arsenic versus selenium has been investigated and the selenium studies were reported above. Feed concentrations of arsenate and selenate were 200mg/L each at pHs of 6 and 11. Equilibrium batch tests were carried out by weighing out exactly 0.1g of each composite and adding 10mL of the contaminant solution. The mixture was stirred overnight and analysed for arsenic and selenium content. The batch tests were done in triplicate. **Table 4.10** gives the capacities

and the selectivity between arsenate and selenate for the IMPACs tested. It is interesting to note that all of these IMPAC composites selectively favored arsenate anion over selenate anion. The reasons for this were discussed in the previous section. Although the selectivity factor between arsenate and selenate varies for each of these IMPACs, the general trend is the preference of arsenate over selenate. Although, AlBPAP and Ce^{4+}-BPAP show selectivity for selenate over arsenate at pH 6, the selectivity ratio is very poor and might not be viable for commercial purposes. A detailed study of these two composites is required to investigate the reliability of the selenate selectivity over arsenate under various other conditions.

Table 4.10: Preliminary equilibrium batch tests for arsenate and selenate species with various IMPACs.

IMPAC	**Immobilized Metal Loading**	**pH →** / **Species ↓**	**6**	**11**
AlBPAP	**0.30mmol/g**	**As(V) (mg/g)**	2 ± 0.02	1 ± 0.06
		Se(VI) (mg/g)	3 ± 0.37	2 ± 0.08
Ce^{3+}-BPAP	**0.21mmol/g**	**As(V) (mg/g)**	0.41 ± 0.16	0.34 ± 0.24
		Se(VI) (mg/g)	1 ± 0.47	1 ± 0.39
Ce^{4+}-BPAP	**0.33mmol/g**	**As(V) (mg/g)**	1 ± 0.12	1 ± 0.3
		Se(VI) (mg/g)	3 ± 0.15	1 ± 0.45
FeBPAP	**0.98mmol/g**	**As(V) (mg/g)**	20 ± 0.01	20 ± 0.01
		Se(VI) (mg/g)	9 ± 0.72	8 ± 0.1
ThBPAP	**0.58mmol/g**	**As(V) (mg/g)**	18 ± .05	20 ± 0.12
		Se(VI) (mg/g)	5 ± 0.33	3 ± 0.34
ZrBPAP	**1.02mmol/g**	**As(V) (mg/g)**	19 + 0.13	19 ± 0.22
		Se(VI) (mg/g)	15 ± 0.13	11 ± 0.36

From a more fundamental point of view these studies point to the fact that one can tune anion selectivity using surface immobilized metals by varying both the metal ion and the nature of the coordinating ligand on the active site. This is supported by our preliminary studies using AlBPAP, CeBPAP, FeBPAP, ThBPAP, and ZrBPAP where different (lower) selectivity ratios for arsenate over selenate are observed. The overall anion loading were very dependent on the ability of BPAPM to immobilize a given metal. Studies matching various metals with different polyamine-surface bound ligand environments are ongoing in our laboratory.

CHAPTER 5: OTHER APPLICATIONS

Heavy metals are considered to be among the most dangerous pollutants in superficial and underground water bodies due to their high toxicity and their diffusion in industrial and municipal wastewaters. Levels of heavy metals in the environment have seriously increased in the past 30 years due to the increase of industrial and municipal discharges, causing serious alterations of natural environmental cycles. Therefore, the elimination of heavy metals from wastewaters becomes a fundamental process to prevent contamination of natural waters and to preserve drinking water supplies. In addition, the recovery of heavy metals, especially the rare ones, is becoming increasingly attractive because all metals are nonrenewable resources and are being consumed at increasing rates. Tungsten is a relatively rare metal with several applications in different technological fields, mainly because it has the highest melting point of all metals and a high density. Moreover, tungsten carbide is one of the hardest substances known. Hence, tungsten compounds are widely used in the manufacture of alloys, machine tools, armaments, pigments, dyestuffs and in electronics. Tungsten-containing catalysts are used for various applications in the chemical industry, for example, dehydrogenation, isomerization, polymerization, reforming, hydration and dehydration, hydroxylation, epoxidation, and hydrocracking. Some of these applications give rise to the direct or indirect discharge of tungsten in wastewaters.[136] Although tungsten compounds are not considered to be a hazard to humans, recent studies highlight that tungsten exposure may

be associated with the generation of rhabdomyosarcomas and leukemial pathologies, although no definite link has been established.[136b] The high industrial value and the potential toxicity of its compounds explain the interest in adequate treatments to ensure the removal of tungsten and its recovery from wastewater. Removal without recovery of tungsten can be accomplished by chemical precipitation, while ion flotation (a separation technology for removing and recovering metal ions from dilute aqueous solutions) was found to be an effective method for the selective separation and recovery of tungsten in dilute aqueous solutions.[137,138] In ion flotation process, an ionic surface active reagent (collector) is added to the solution to be treated, and adsorbs at the solution–vapor interface.[138c] Polystyrene based ion exchange resins have also been tried for tungstate ion removal and recovery.[136] The separation of tungsten and vanadium ions from aqueous solutions containing molybdate ions has been researched extensively in the last decade due to the high value and demand for tungsten.[138,139] Removal of molybdate ions from water has been an ongoing effort and research is underway to find an efficient technology for molybdate recovery from co-contaminants.[139] The deleterious effects and toxicity of molybdenum, and vanadium are discussed in chapter 1. The speciation diagram for molybdate and tungstate anions is shown in **Figure 5.1**.

The application of the versatile IMPAC technology (see chapter 3) was investigated for the separation of the oxo-anions of molybdenum, tungsten, and vanadium. IMPACs, and other SPCs were tested on multi-component solutions prepared in our laboratory that emulate a real waste stream from a Western Australian mine (Julia Creek). The alkylated SPC (BPQA) was also investigated for the capture of bacteria and viruses,

for collaboration with Professor James Gannon and Dr. Philip Ramsey of the Biology Department. This chapter discusses the results of these investigations.

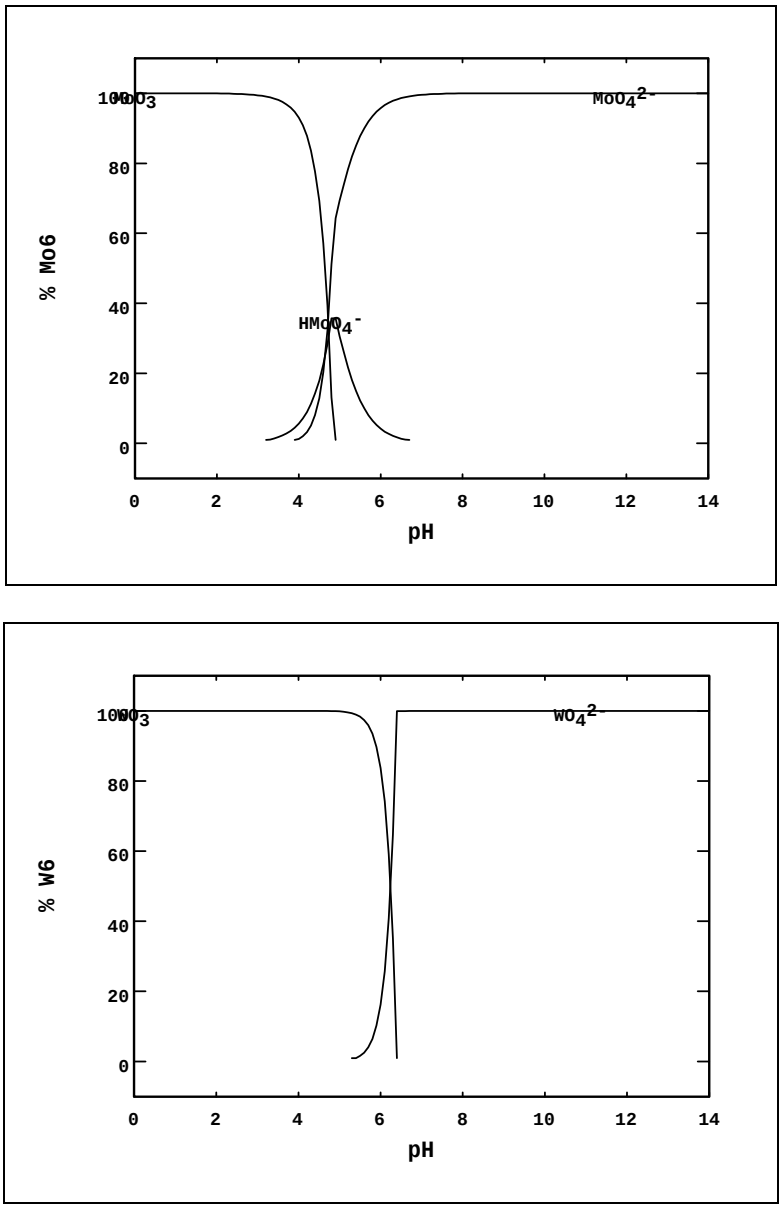

Figure 5.1: Speciation diagram for molybdenum (top) and tungsten (bottom) oxo-anions.

5.1 Molybdenum and Tungsten Selectivity

As with the other oxo-anions mentioned in chapter 4, equilibrium batch capacities for molybdate and tungstate oxo-anions were determined using ZrBPAPM and BPQAM composites (**Table 5.1**). **Figure 5.1** shows that at lower pH (< 4), molybdate exists as a neutral species. It is only at pH = 4 that molybdate speciates into the mono-anionic and the di-anionic species (H_2MoO_4). The molybdate batch capacity at pH = 2 is anomously high (99mg/g using ZrBPAPM) and this is not well understood but could be the result of direct chemisorption to the silica surface via hydrogen bonding. The batch capacities decrease from pH = 2-4 and similar at pH values of 6, 8, and 10; and this is has also been seen with the selenite capacities using ZrBPAPM. Although the molybdate capacities over the pH range of 2-10 are a little lower using BPQAM, similar trend in the batch capacities is observed as compared to the batch capacities using ZrBPAP. Further research is in progress to understand this anomalous characteristic of high oxo-anion batch capacities at pH = 2.

Table 5.1: Equilibrium batch tests for molybdate and tungstate anions on ZrBPAPM and BPQAM with 1000 mg/L solutions of Na_2MO_4 (M = Mo, W).

pH → / **Species ↓**	**2**	**4**	**6**	**8**	**10**
Mo (VI) (mg/g)*	99 ± 0.37	91 ± 0.46	55 ± 1.83	58 ± 0.43	64 ± 0.48
W (VI) (mg/g)*	89 ± 0.41	79 ± 1.2	79 ± 1.5	67 ± 2.3	70 ± 1.1
Mo (VI) (mg/g)†	97 ± 0.05	94 ± 0.09	42 ± 0.59	45 ± 1.34	43 ± 0.36
W (VI) (mg/g)†	87 ± 0.54	85 ± 1.1	95 ± 0.66	82 ± 1.45	87 ± 0.34

* Batch tests performed on ZrBPAPM
† Batch tests performed on BPQAM

Figure 5.1 shows that there are only two species of tungstate that exists throughout the pH range 0-14, HWO_4^- and WO_4^{2-}. Literature sources and recent research have shown that tungsten exists as a complex mixture of species over the pH range 0-14, as shown in **Figure 5.2**.[136a] Using ZrBPAPM, the batch capacity for tungstate is highest at pH = 2 and this is evident from **Figure 5.2** where tungstate predominantly exists in its mono-anionic form. At the pH values of 4 and 6, tungsten exists, in different proportions, as all the five species shown in **Figure 5.2**. At pH > 8, the only species of tungsten that exists is the di-anionic form and hence the capacities at pH values of 8 and 10 are very similar. Therefore, we believe that the tungstate oxo-anion capacities over the pH range 2-10, are in accordance with its speciation as shown in **Figure 5.2**.

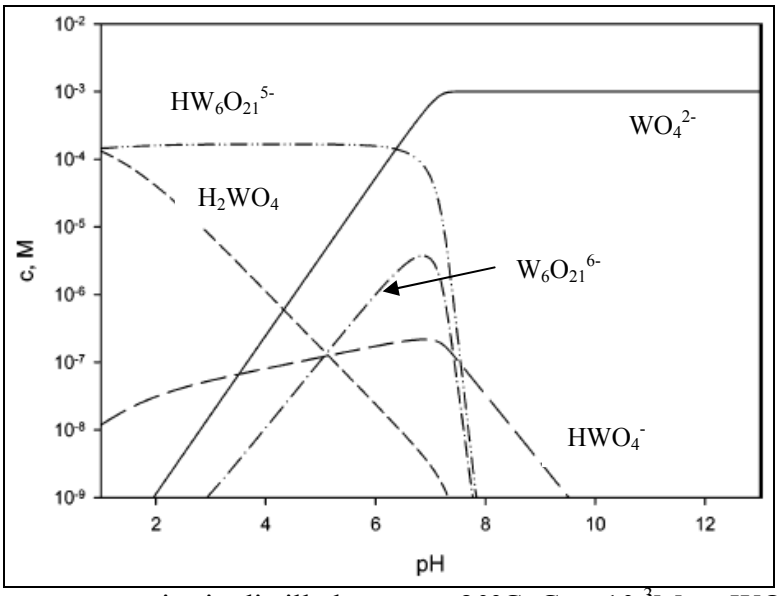

Figure 5.2: Tungstate species in distilled water at 20ºC, $C_0 = 10^{-3}$M. –, WO_4^{2-}; – –, HWO_4^-; ---, H_2WO_4; ¯ ·· ¯, $HW_6O_{21}^{5-}$; ¯ · ¯, $W_6O_{21}^{6-}$.

As mentioned previously, the separation of molybdenum and tungsten has been a problem for a long time.[2] Therefore, it was decided to perform breakthrough testing on

the BPAPM composite for Mo(VI)/W(VI) separation at pH = 6, trying to take advantage to the fact that at these pH values molybdenum exists as $HMoO_4^-$ and tungsten exists as WO_4^{2-}. A 5cc syringe was packed with ~2.3g of the BPQAM composite and the flow rate used was 2.5mL/min. The feed concentration used were ~500mg-Mo(VI)/L and ~400mg-W(VI)/L.

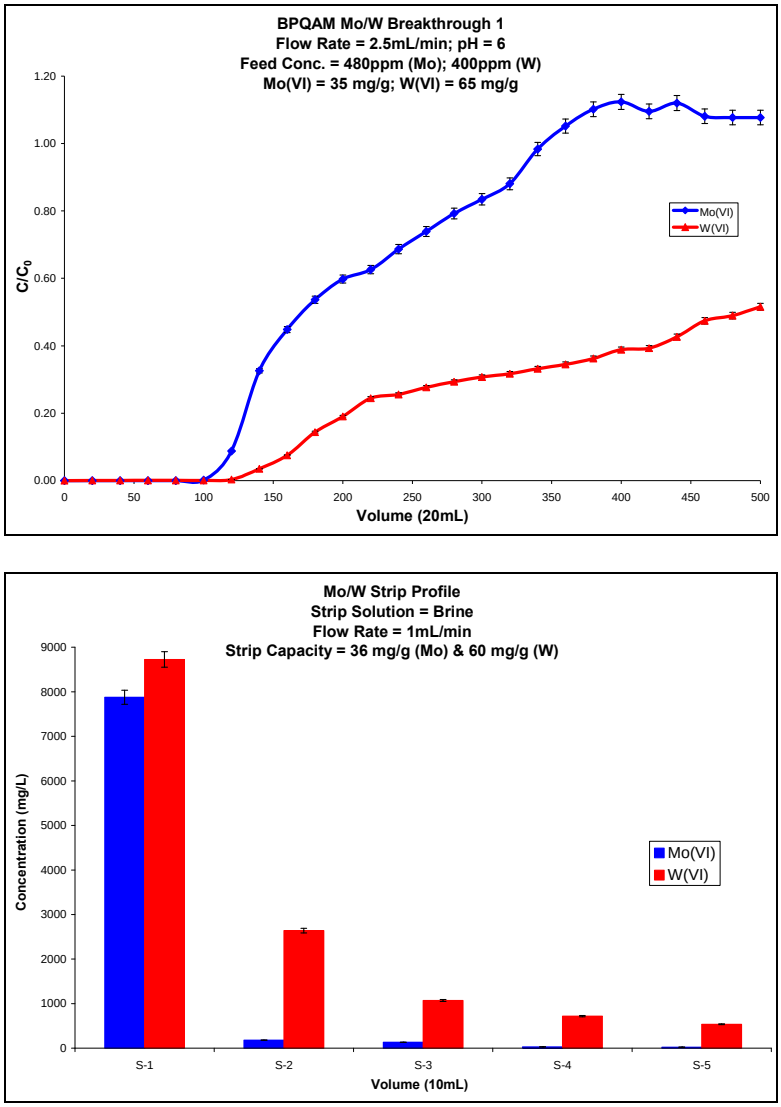

Figure 5.3: (Top) Breakthrough selectivity profile for Mo(VI) and W(VI) on BPQAM at pH=6; (Bottom) Strip profile of BPQAM with brine solution.

Figure 5.3 shows the breakthrough and strip profiles for the Mo/W selectivity. The selectivity factor for tungstate over molybdate using the Equation 4.3 was calculated to be 3:1. But there was a problem during stripping with brine as both the species stripped simultaneously. This posed a problem since the strip solution was not pure with respect to one metal over another; the strip solutions contained approximately 60% molybdate and 40% tungstate. To overcome this problem a different strip solution was tried and a new breakthrough was performed using a fresh 5cc column of BPQAM. The breakthrough flow rate used here was slower (1mL/min) than the one used before (2.5mL/min), in order to get better mass transfer kinetics. A fresh feed solution was made at pH = 6 with concentrations as follows: 515mg-Mo(VI)/L, and 470mg-W(VI)/L. The selectivity factor remained the same (3:1 in favor of the tungstate anion) in spite of the change in flow rate. The breakthrough capacities remained similar as compared to the previous test. The strip however had a high purity of molybdate (~90%) as compared to the brine strip (~60%). This improvement in selective stripping with sulfuric acid probably reflects the fact that $HMoO_4^-$ is a stronger base than WO_4^{2-}, as well as the stronger electrostatic attraction of the di-anionic species for the positively charged sites on the BPQAM composite.

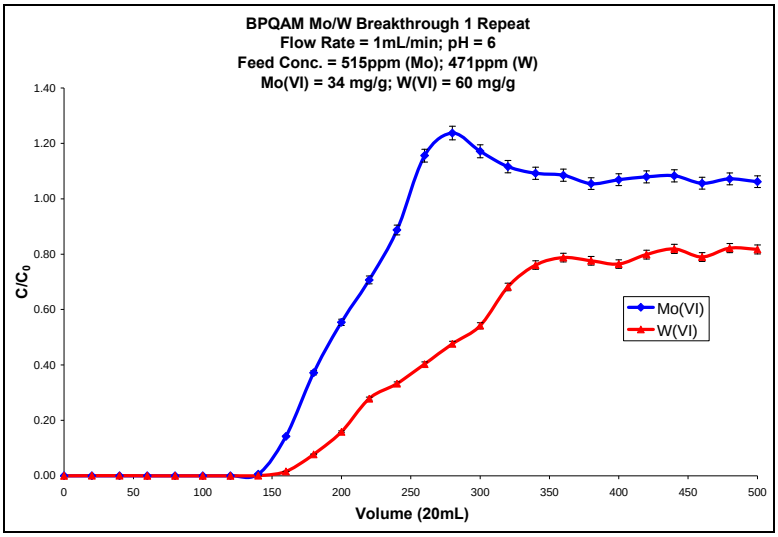

Figure 5.4: (Top) Breakthrough selectivity profile for Mo(VI) and W(VI) on BPQAM at pH=6; (Bottom) Strip profile of BPQAM with 2M-H_2SO_4.

5.2 Julia Creek

We wanted to test the selectivity of different composites on solutions containing both cationic and anionic metal species. We obtained the details and metal concentrations of a mine waste creek (Julia Creek) in Western Australia. Abundances and mineralogical residences have been determined for a comprehensive range of trace

elements in Julia Creek samples. Many trace elements are well above their normal abundances. Of these elements, vanadium and molybdenum are potentially useful by-products, whereas arsenic, selenium, molybdenum, cadmium, thallium, and uranium are of possible environmental or occupational health concern. It is the abnormally large concentrations of nickel and molybdenum that were targeted for extraction. Recently, there has been extraordinary increase in demand for technologies directed towards the extraction of nickel and cobalt from various types of ores. The sample details that were sent to us by the PSI partner company (Ammtec Inc.) contained various metals at different concentrations. Of all the metals, the most important ones that the company wanted to recover were copper, nickel, molybdenum, and vanadium (**Table 5.2**).

Table 5.2: Composition of some important elements from Julia Creek, Western Australia. All values are represented in mg/L.

→ Elements	Al	Cu	Fe	Mo	Ni	S	V	Zr
pH=0.5	493	21.5	1.89	26.3	35	33900	130	3.95
pH=2	427	17	1.1	7.55	34	27200	106	0.45

As we have a copper selective composite at low pH (CuWRAM), we made a synthetic solution in our laboratory with three metals (Mo, Ni, V) that Ammtec wanted us to separate and recover. The metal concentrations in the feed solution were scaled to the amounts from in actual Julia Creek samples: 30mg/L (molybdenum); 50mg/L (nickel); 120mg/L (vanadium). Equilibrium batch tests were carried out at pH values of 0.5 and 2 using ZrBPAP, WP2, BP2, and BPQA to investigate the best combination of composite(s) for the separation of the three metals. From **Table 5.3**, we can infer that

molybdenum capacity at pH = 2 is high (> 90%) with all the composites used. But at low pH (0.5), BPQA does not show good molybdenum capture. However, nickel capture was only good using WP2 at pH = 2; all the other composites failed to show good nickel capture at the other pH values. None of the composites showed good vanadium capture at low pH, but show good vanadium capture at pH = 2. At this pH WP2 captured > 90% of the nickel. A breakthrough test was run on Julia Creek mock solution using the composite sequence: ZrBPAP @ pH=0.5 > ZrBPAP @ pH=2 > WP2 @ pH=2. The Pourbaix diagram for vanadium(V) shows that vanadium exists as both cations and anions **(Figure 5.5)**. But at the pH values the batch tests were performed, vanadium exists primarily as cationic species; hence the high vanadium capacity using WP2 and BP2 (cation capture composites).

Table 5.3: Equilibrium batch tests for Julia Creek samples using ZrBPAP, WP2, BP2, and BPQA. All values are represented in %-metal captured.

Composite → **Elements**	**ZrBPAP**			**WP2**			**BP2**			**BPQA**		
	Mo	Ni	V	Mo	Ni	V	Mo	Ni	V	Mo	Ni	V
pH=0.5	86	9	22	92	7	28	83	3	8	40	2	4
pH=2	97	30	73	97	87	94	98	8	83	92	3	69

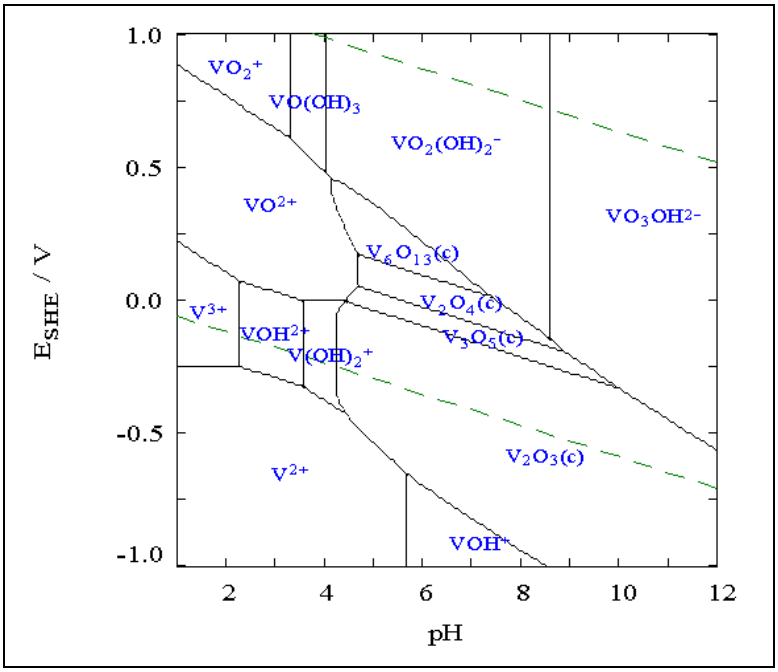

Figure 5.5: Pourbaix diagram of vanadium species in the system V–H_2O at 25ºC and 1 bar total pressure.

The breakthrough tests for the Julia Creek mock solution were carried out by packing a 5cc syringe with the specific composite used for testing. 500mL of the prepared sample was run through the column at a flow rate of 2.5mL/min and for the first cycle the solution pH was 0.5. 10mL aliquots were collected and analysed for molybdenum, nickel, and vanadium using ICPAES. After the metal analysis, the samples were mixed in a graduated cylinder and the pH was adjusted to 2. The total volume for the second breakthrough test was 430mL and a flow rate of 2.5mL/min was used. A fresh column of ZrBPAP was prepared for the second breakthrough test. Again, 10mL aliquots were collected and analysed for molybdenum, nickel, and vanadium using ICPAES. After the metal analysis, the samples were mixed in a graduated cylinder and the pH was adjusted to 2. The total volume for the third breakthrough test was 375mL

and a flow rate of 2.5mL/min was used. A fresh column was of WP2 was prepared for the third breakthrough test (**Figure 5.6**).

The first breakthrough at pH = 0.5 using ZrBPAP showed molybdenum capture (5mg/g) with a little vanadium capture also (2mg/g) and no nickel capture (0mg/g) as shown in **Figure 5.6** (top). This worked well for the purpose of separating molybdenum from the co-contaminants nickel and vanadium. Stripping the molybdenum with 2M-H_2SO_4, however, posed a problem. All the vanadium stripped but only 35% of molybdenum came off in the strip solution. The second breakthrough at pH = 2 using ZrBPAPM did not show any nickel capture **Figure 5.6** (middle), but showed a high capacity for vanadium (6mg/g). The strip using 2M-H_2SO_4, had all of the vanadium captured in it and showed > 99% vanadium purity in the strip. After the first breakthrough, there was no molybdenum present in the solution and the vanadium content decreased to ~35% of the original vanadium content. The final breakthrough at pH = 2 using WP2 showed capacities for nickel (7mg/g) and vanadium (8mg/g). All the nickel from the solution was captured and the remaining vanadium was also captured by WP2 as shown by the loading kinetics in **Figure 5.6 (**bottom). The 2M-H_2SO_4 strip showed complete stripping of both nickel and vanadium.

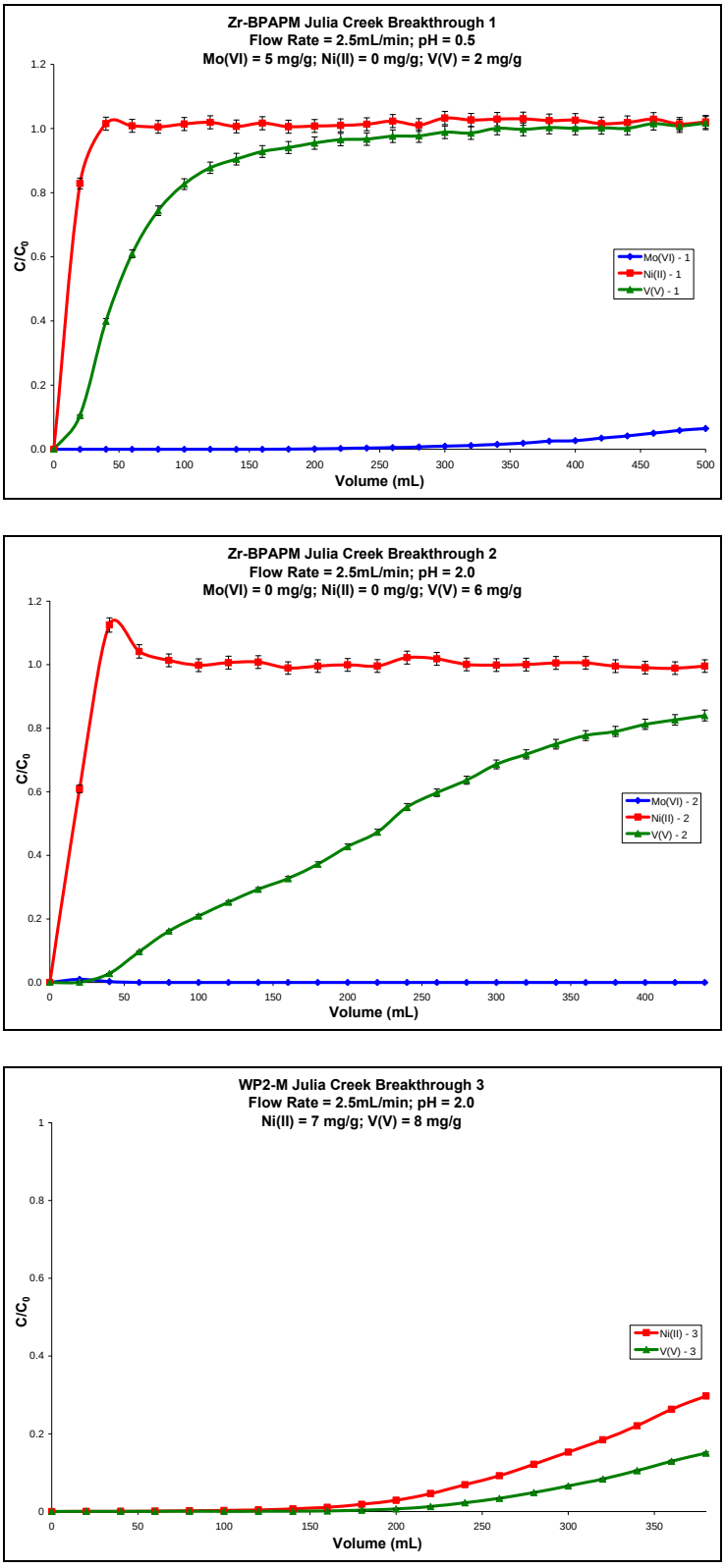

Figure 5.6: Breakthrough profile of three successive cycles for Julia Creek sample.

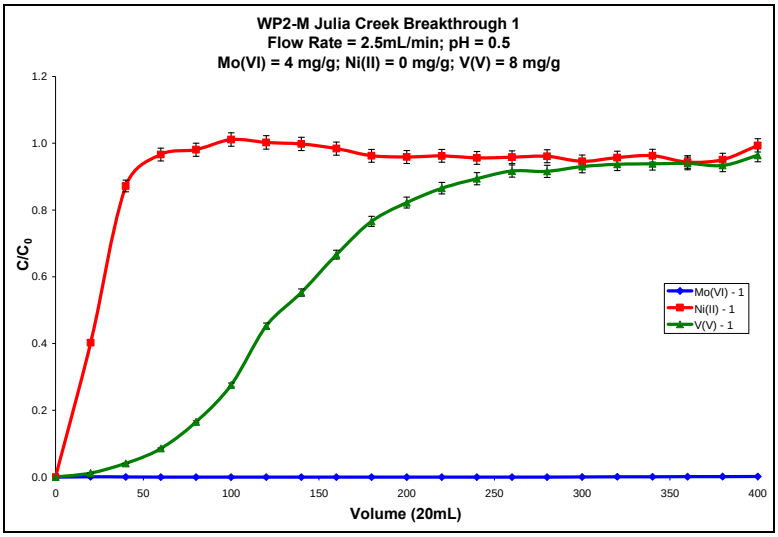

Figure 5.7: First breakthrough profile using WP2 instead of ZrBPAP for molybdenum capture on Julia Creek sample.

To overcome the poor stripping of molybdenum using 2M-H_2SO_4 from the first breakthrough cycle, we decided to use WP2 instead of ZrBPAP for the first breakthrough (**Figure 5.7**). From **Table 5.3**, we observe that WP2 has negligible capacity for nickel at pH = 0.5 and high molybdenum capacity. But, the breakthrough test shows that WP2 captures molybdenum and vanadium with considerable capacities (4mg/g and 8mg/g, respectively). The strip using 2M-H_2SO_4 poses problems again as not all the molybdenum is stripped where as vanadium is completely stripped. The nickel breakthrough capacity is very negligible (< 0.5mg/g). To overcome the problem of complete molybdenum separation, further research is in progress to use a slower breakthrough flow rate of 1mL/min to allow for better mass transfer kinetics. Another modification was to try and use BP2 or BPQA instead of ZrBPAP or WP2 for the first breakthrough test as this might offer us better separation of molybdenum from nickel and vanadium as seen from **Table 5.3**.

CHAPTER 6: SURFACE CHARACTERIZATION USING AFM

Atomic Force Microscopy (AFM) is a very high-resolution type of scanning probe microscope, with demonstrated resolution of fractions of an Angstrom, more than 1000 times better than the optical diffraction limit. The AFM is one of the foremost tools for imaging, measuring and manipulating matter at the nanoscale. The AFM consists of a microscale cantilever with a sharp tip (probe) at its end that is used to scan the specimen surface. The cantilever is typically silicon or silicon nitride with a tip radius of curvature on the order of nanometers. When the tip is brought into proximity of a sample surface, forces between the tip and the sample lead to a deflection of the cantilever according to Hooke's law. Typically, the deflection is measured using a laser spot reflected from the top of the cantilever into an array of photodiode (**Figure 6.1**). We tried to use this technique for studying and gaining a better understanding of SPC surfaces in detail.

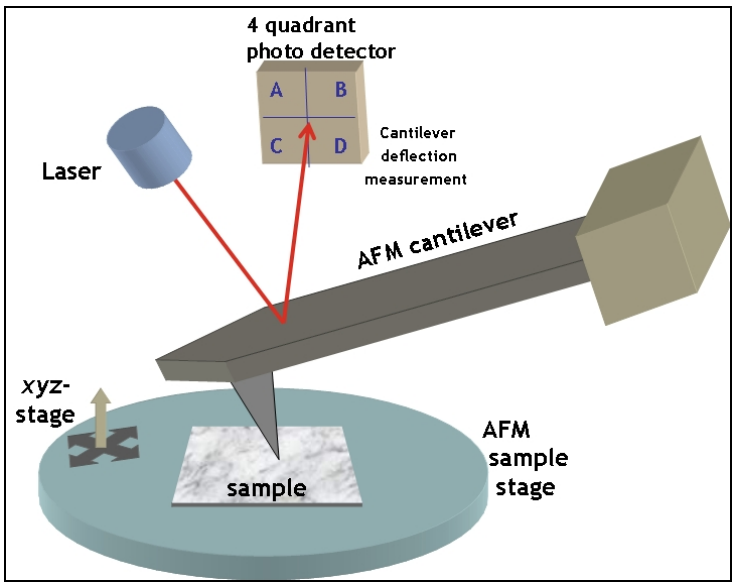

Figure 6.1: An animated representation of the operation of a simple AFM.

The initial studies were done at Toyo University, Japan and involved the study of the surface topography and contours of unmodified amouphous silica gel. Uaing this as background, we studied samples that were functionalized with the various silanes, polyamines, and ligands mentioned in previous chapters. These priliminary results showed that there was a significant difference in the surface maps for every intermediate step in the synthesis of SPCs. In order to get consistent and reliable data, we chose to apply our SPC chemistry to the smooth surfaces found on an oxidized silicon wafer.[140] The wafer was obtained commercially and had a native oxide coating of 1-2 nm which allowed the same SPC reaction chemistry to be performedon these wafers. This chapter will discuss in detail the surface and structural design features of the SPCs using AFM.

The initial studies revealed the differences in the surface characteristics between the regular and mixed silane composites made from the two different polymers (PAA and PEI). This was done by picking BP1 and WP1 composite particles made from CPTCS only and MTCS:CPTCS silanized CP gel. A few particles were randomly chosen and immobilized on a silicon wafer surface and the AFM tip was brought just over the sample and the surface mapping was started using the tapping mode on the AFM. Initially a surface area of 10μm x 10μm of the composite was analysed and the 3D surface simulation was created for BP1 and BP1M. After ascertaining that the surface was flat enough for surface tapping using the AFM probe a 5μm x 5μm area was chosen for analysis and 3D simulation (**Figure 6.2**). The yellow colored spikes in the 3D pictures are the positive displacements of the probe and the blue represents the negative displacements of the probe. As expected there is a difference in height/depth relief

depending upon the silane ratios. It can be seen from the figure that the composite made only with CPTCS had even distribution of the silanized sites and a smaller height/depth relief, whereas the composite with the mixed silane MTCS:CPTCS (7.5:1) has a less even distribution and a much greater height/depth relief arising from the larger polymer loops created by the anchor points being farther apart.

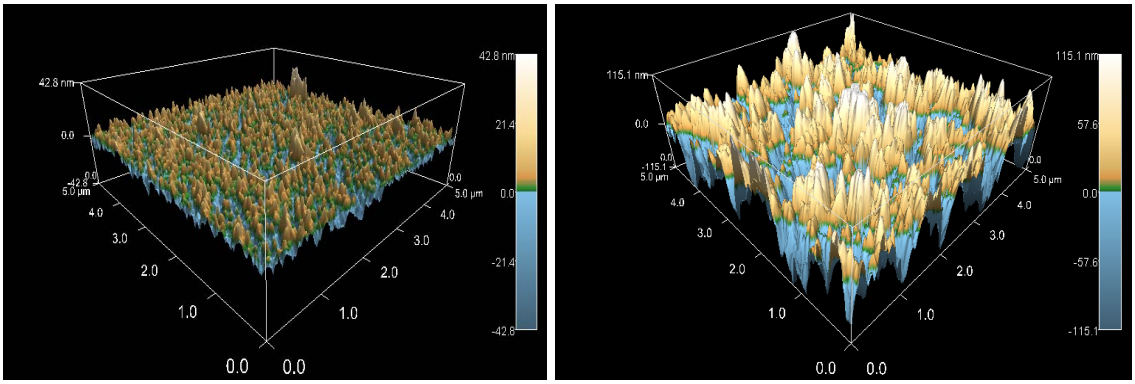

Figure 6.2: A 3D simulation of the surface topography of BP1 (left) and BP1M (right).

This is illustrated in **Figure 6.3**, where the anchor points are farther and hence bigger polymer loops in the case of mixed silane composites. The average polymer height for the mixed silane BP1 was 60nm and the average height for the regular BP1 was 30nm. It can also be seen that the anchor points are not systematic or regular as they are randomly attached to the silica gel surface.

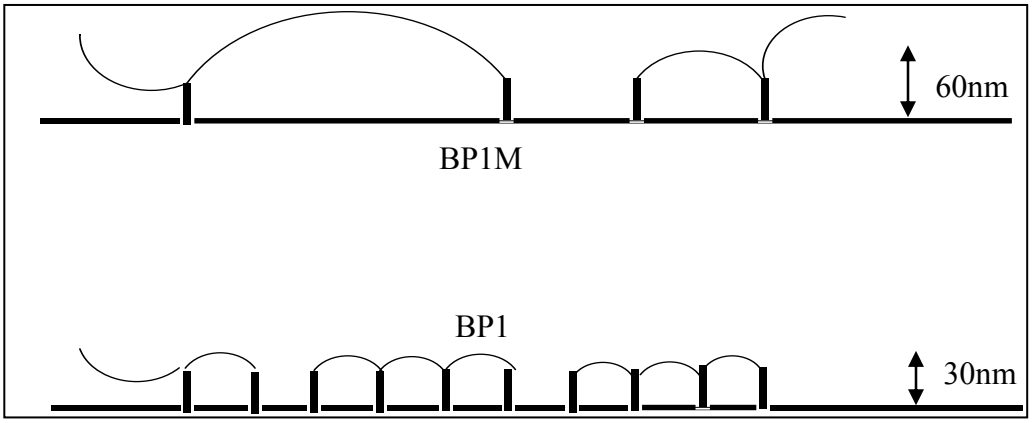

Figure 6.3: Diagram showing the anchor points and loops for BP1 and BP1M.

In order to pursue this research further collaboration was started with the Imaging and Chemical Analysis Laboratory (ICAL) at Montana State University, Bozeman, MT. It was expected that there be an increase in height and/or surface roughness for the samples after each reaction step was added to the surface. For instance, the average surface roughness from the starting material (raw silica gel) to the final SPC (BPAP) should show significant increase. Therefore we designed a technique where the samples analyzed would be from the same batch that was used for the next step in the SPC reaction pathway (**Figure 3.1**). SPC samples for analysis at ICAL were freshly prepared and select sample particles were chosen for analysis. We started with a silanized silica gel sample (CPM gel) and a 3D simulation of the surface detail is shown in **Figure 6.4**. The average surface roughness, R_q = 6.85nm.

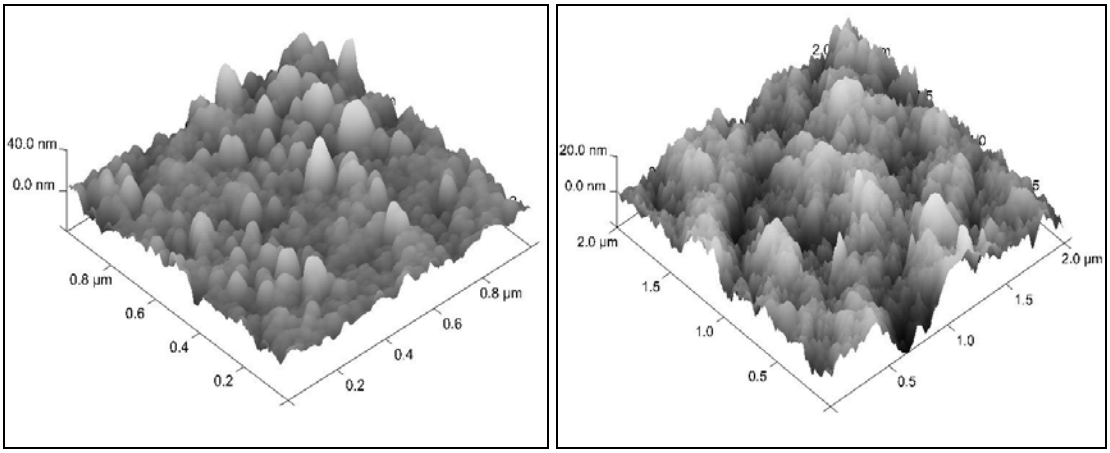

Figure 6.4: 3D simulation of the mixed silane silica gel (CPM) analyzed on two different surface areas. R_q = 6.85nm.

The next sample analysed using the tapping mode on the AFM was the PAA modified SPC – BP1. As expected we observed an increase in the surface roughness, but the increase was small compared to the quantity of polymer loaded and the mass gain obtained. The average surface roughness, R_q = 8.5nm (**Figure 6.5**). The BPAP (see chapter 3) sample however showed interesting behavior and quite intriguing results. The surface topography was different with a lot more loops that were bigger than the ones we observed. Also, the average roughness decreased (R_q = 5.7nm) as compared to the BP1M's surface roughness (**Figure 6.6**). This suggests that modification of the polyamine with $–CH_2P(O)(OH)_2$ imparts an additional rigidity to the polymer. Because surface roughness plays an important role, it is safe to assume that the starting surface has to be smooth. This would guarantee a good baseline for the various steps of the SPC reaction pathway.

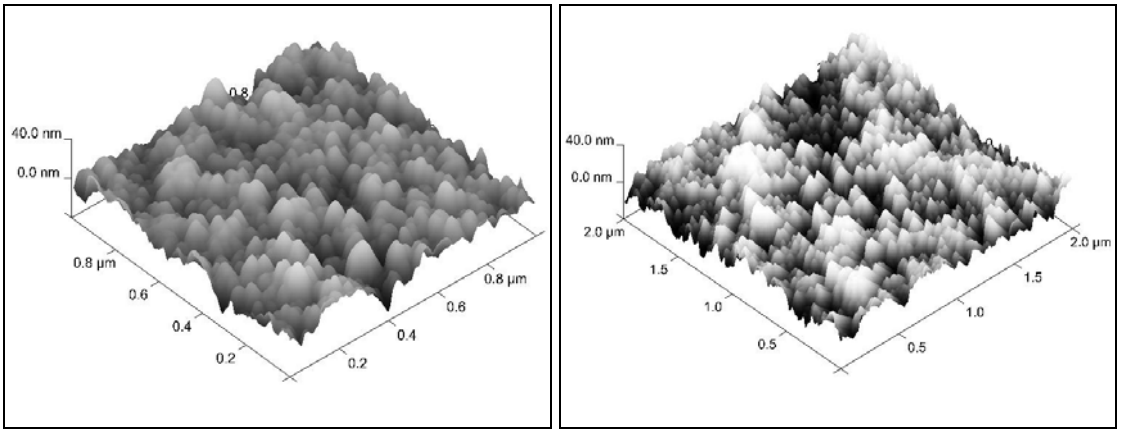

Figure 6.5: 3D simulation of two different surface areas of BP1M. R_q = 8.5nm.

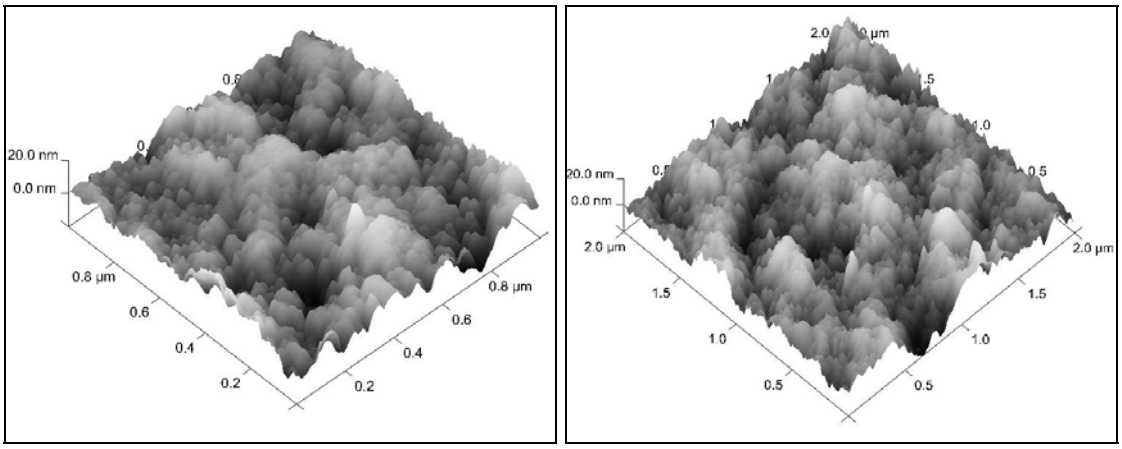

Figure 6.6: 3D simulation of two different surface areas of BPAPM. R_q = 5.7nm.

6.1 AFM on Modified Glass Slides

Characterization of the surface properties of the silica polyamine composites could be improved by extending the same chemistry to a flat glass slide instead of the irregular shaped silica gels. Previous work on coating glass slides with the silanes and then polymerizing them has provided some vague information on the nature of the polymer silane interface.[141] Some of the slides prepared in this manner were examined by the AFM tapping mode. The coated slides that were used were: CP gel, BP1, WP1,

and BP2. **Figure 6.7** shows the comparison between the surface characteristics and average roughness of these modified glass slides. The measurement of average surface roughness shows that there is an increase from the starting material (CP gel) to the final product (BP2). Although, the SPC modification reactions were performed on glass slides, these measurements give an idea of how far away from the actual surface the polymer reaches and the amount of protection that the surface gets from the silane layers, the polyamines, and the modified ligands.

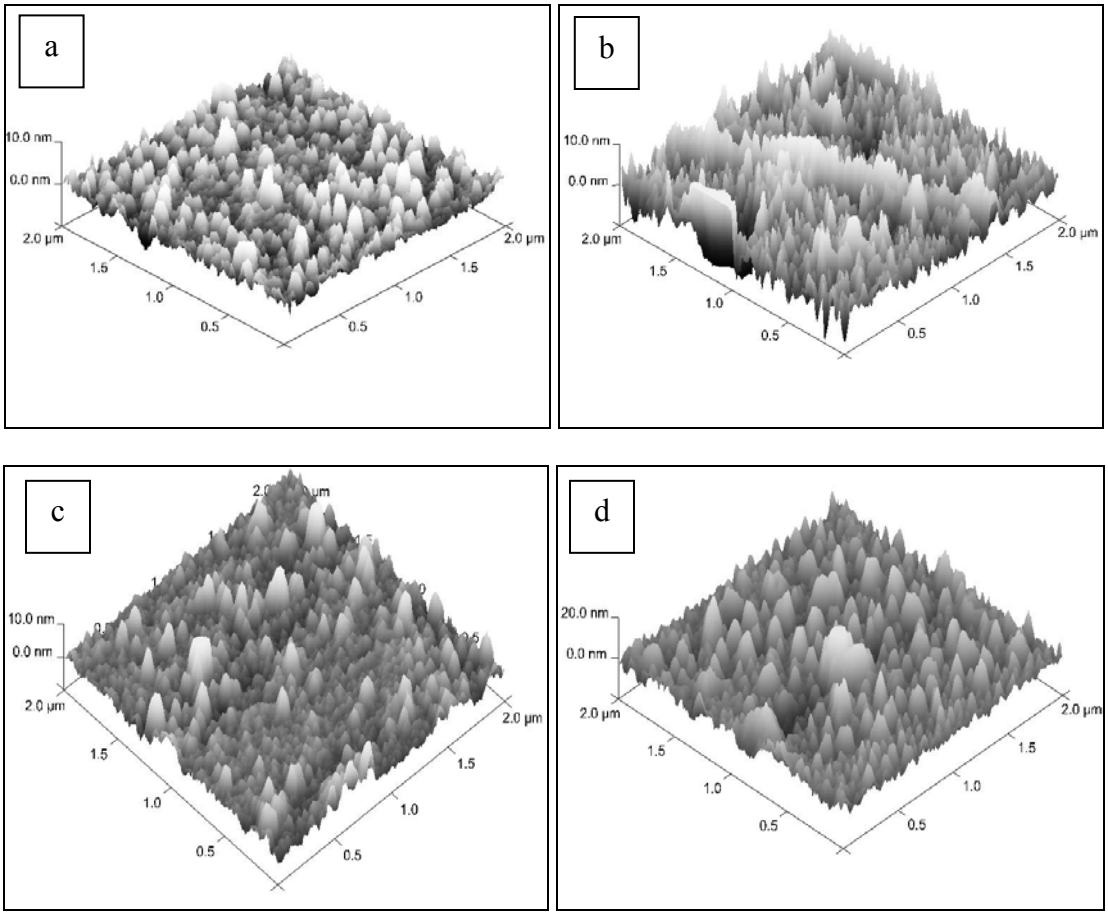

Figure 6.7: 3D surface topography of the modified glass slides (a) CP gel; (b) WP1; (c) BP1; (d) BP2.

The average surface roughness for the modified glass slides is shown in **Table 6.1**. The difference between the Rq values for WP1 and BP1 clearly suggests that the PEI is bound more closely to the surface; whereas the PAA is further from the surface of the glass slide. Also, there was an anomalously large increase in the average roughness on going from BP1 gel to BP2, a result that would not be expected on adding a small molecule ($ClCH_2CO_2H$) to the polyamine, and in light of the decrease in roughness observed on going from BP1 to BPAP. Most likely these differences encountered on ligand modification of the polyallylamine arise from the intrinsic difference between the flat slide and the irregular porous silica particles.

Table 6.1: Average surface roughness (R_q) for the modified glass slides.

	CP Gel	WP1	BP1	BP2
R_q (nm)	1.58	2.09	2.75	4.44

6.2 SPC Chemistry on Silicon Wafers

To understand, in more detail, the polymer-surface interface associated with the SPC chemistry, silicon wafers were used instead of glass slides as the flat surface to modify. Unlike the glass slides, the silanes and the polymers could be applied to the silicon wafer surface in a more controlled manner owing to the greater reactivity of the thin layer of SiO_2 on the wafer relative to the glass. Therefore, we first needed to look at the surface roughness of the unmodified wafer first. As mentioned in chapter 2, the silicon wafers that we obtained commercially had a native oxide of 1-2nm coating on it. This native oxide layer is excellent for surface modification as it was easy to humidify the wafer surface and attach the silane layer. The humidification was carried out by

placing the silicon wafers in a humidifier for 5 minutes. Once humidification was completed, it was assumed that there was a uniform monolayer of water on the silicon wafer surface. This monolayer layer of water facilitates the silanization step as explained in the previous chapters. The average surface roughness for the unmodified silicon wafer was found to be 0.17nm (**Figure 6.8**). An increase in the average surface roughness was observed for the silanization steps, with the mixed silane modified wafer R_q = 0.35nm and the CPTCS only modified wafer R_q = 1.2nm (**Figure 6.9**).

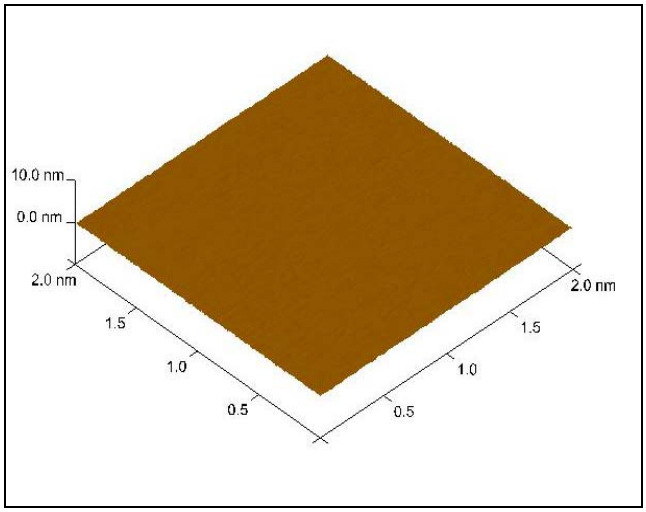

Figure 6.8: 3D simulation of an unmodified silicon wafer. R_q = 0.17nm.

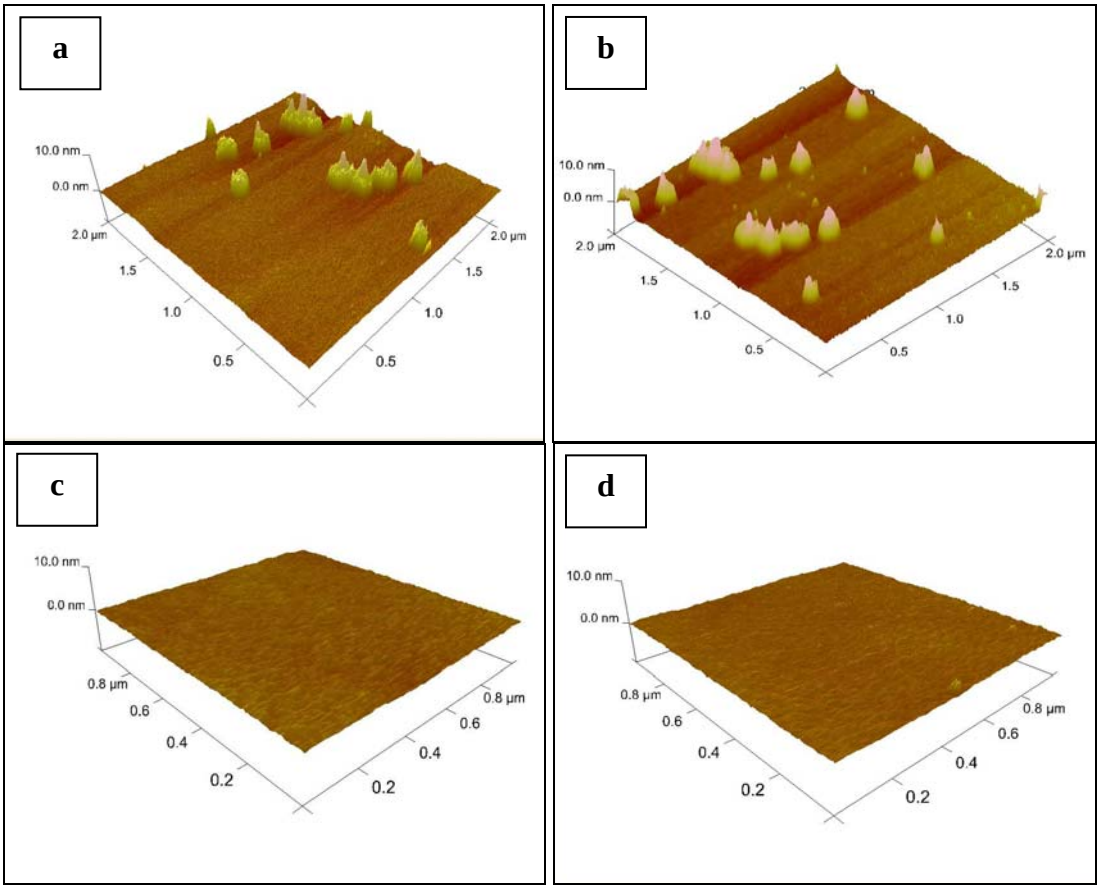

Figure 6.9: 3D simulation of the silicon wafer modified with the silanes. (a & b) CPTCS only modified silicon wafer, R_q = 1.20nm; (c & d) 7.5:1-MTCS:CPTCS modified silicon wafer, R_q = 0.35nm.

It is believed that the modification with the CPTCS only forms aggregates on the silicon wafers, thereby giving isolated island peaks of silanes. These aggregates are believed to occur due to possible Van der Waals attractions between the longer propyl groups of the silanes and/or insufficient mixing of the silane mixture before binding them to the silicon wafer.

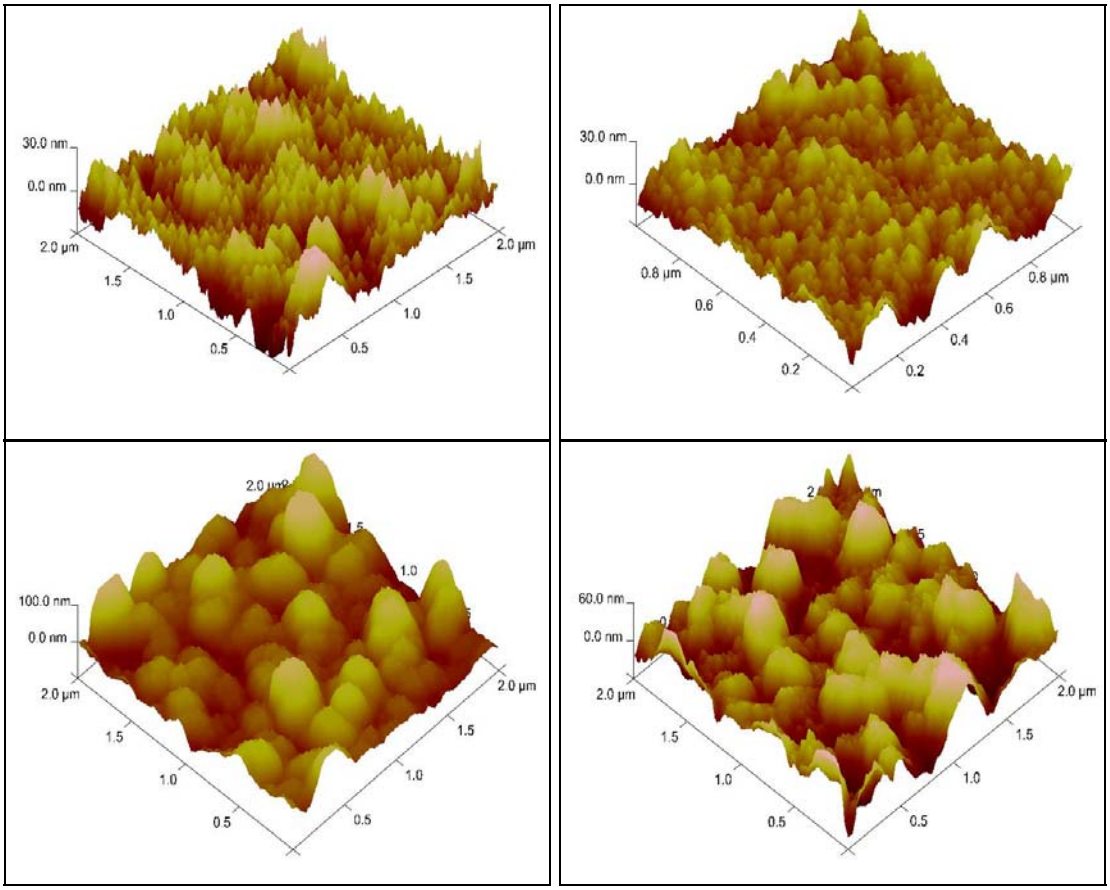

Figure 6.10: 3D simulation of the silanized silicon wafer modified with PAA. (a & b) CPTCS only modified BP1, R_q = 8nm; (c & d) 7.5:1-MTCS:CPTCS modified BP1M, R_q = 22nm.

The modification of the silanized silicon wafer with the polyallylamine (PAA) however showed expected results. The difference between the anchor points and the loops were again seen here. The BP1 made from the CPTCS only showed similar surface characteristics as seen on the silica polyamine composite, BP1 (**Figure 6.2**). The chloropropyl groups have sharper and closer anchor points; hence the polymer loops are smaller and sharper. In the case of the mixed silane BP1, the chloropropyl anchor points are farther from one another sue to the dilution by the MTCS. This gives rise to broader polymer loops and the polymer tends to move farther away from the surface (**Figure**

6.10). The average surface roughness for BP1 (R_q = 8nm) and BP1M (R_q = 22nm) supports this observation. Further research is in progress to use the BP1 modified silicon wafer and capture metal ions on it. If successful, this can become an important technique to remove very small amounts of metal contaminants, such as regeneration of catalysts, etc.

CHAPTER 7: CONCLUSIONS & FUTURE WORK

7.1 Mixed Silane SPCs

SPC materials have many advantages over cross linked polystyrene resins. These include superior mass transfer kinetics and no shrink/swell characteristics. However, to this point polystyrene resins have, in general, had superior metal ion sorption capacities relative to SPC materials. The work presented in chapter 3 and 4 clearly demonstrated that this gap in sorption capacity can be overcome by the incorporation of MTCS into the synthetic pathway for SPC preparation. The use of MTCS in the production of SPC materials has greatly improved the SPC technology. The following lists the general conclusions for the study of mixed silane SPCs:

- MTCS can be successfully incorporated into the synthetic pathway as a mole fraction of the reagent silane mixture.
- An optimum MTCS:CPTCS ratio has been determined for each of three polyamines. All optimum ratios contain more than 70% MTCS.
- The use of mixed silane composites results in an increase in the free amine concentration in a high molecular weight polyamine matrix.
- Modifying these optimized SPC materials with metal selective ligands can lead to significant increases in ligand loading and 30% to 50% increase in metal ion sorption capacity.
- The increase in the immobilized metal loading thus increases the arsenic and

selenium loading on the composite.

- The SPC materials using the optimized MTCS:CPTCS ratios showed better mass transfer kinetics for loading and stripping.

7.2 IMPACs & Their Applications

The concept of using an SPC immobilized metal ion to capture anions has been addressed and discussed in detail in the previous chapters. The work done has demonstrated the feasibility of using this IMPAC approach. As mentioned in chapter 3, anion capture has been traditionally done using polystyrene based ion exchange resins. Almost all of these resins have quaternized nitrogen atoms for anion capture, ASM-10HP adds iron salts to the resin to enhance arsenic removal. Therefore it was important to develop materials that have a high affinity towards anionic contaminants in the presence of high concentrations of other contaminants. This section lists the general conclusions derived from the IMPAC technologies researched:

- The factors governing anion selectivity with IMPACs have been defined: 1) the nature of the immobilized metal, 2) the net charge on the composite surface, and 3) the functional group used to modify the SPC before metal immobilization.
- The target metals (Fe^{3+}, Th^{4+}, Zr^{4+}) were successfully immobilized on the amino-phosphonate modified SPC (BPAP).
- Fe^{3+}, and Zr^{4+} were successfully immobilized on the EDTA modified SPC (BPED).

- Zr^{4+} was successfully immobilized in the amino-acetate modified SPC (WP2).
- The Zr^{4+} loading was approximately 1mmol/g on each of the modified SPCs – BPAP, BPED, and WP2.
- The immobilization of Al^{3+}, Ce^{3+}, and Ce^{4+} did not show significant loading on BPAP (< 0.3mmol/g loading for each metal).
- Significant leach of Fe^{3+} was observed from BPAP during stripping with 2M-H_2SO_4.
- Significant leach of Zr^{4+} was observed from WP2 and BPED during stripping with 2M-H_2SO_4.
- The best IMPAC material for arsenate capture is ZrBPAPM with significant arsenate capture over the wide pH range of 2-8.
- Arsenite capture is significant only at pH values greater than 8, although the use of SPC materials at pH > 12 is not recommended as it hydrolyses and degrades the silica gel matrix.
- ZrBPAPM also showed a high sorption capacity for selenite and selenate with excellent mass transfer kinetics and > 95% stripping using 2M-H_2SO_4.
- ZrBPAPM showed high affinity towards arsenate in presence of selenite, selenate, sulfate, and excess chloride. The selectivity factor for arsenate over selenate was 20:1, over selenite was 4:1, and over sulfate was 50:1. The selectivity factor for selenium oxo-anions (IV & VI) over sulfate was 1.7:1.
- Comparison of ZrBPAPM with the commercially available-iron doped strong base anion exchange resin, ASM-10HP made by Resintech showed the higher

arsenate capacity over the wide pH range of 2-8. Although, both these materials showed good selectivity for arsenate over sulfate, it should also be pointed out that the column utilization factor was 0.15 for ASM-10HP and 0.63 for ZrBPAP.

- ZrBPAPM has a long usable lifetime (> 1000 cycles) under the conditions encountered with most surface and wastewater streams. In addition there was also no appreciable leaching or leakage of zirconium (IV) during the repeated column cycles due to the remarkable stability of the composite.
- FeBPAPM and ThBPAPM also showed selectivity for arsenate over selenate with the selectivity ratios being 2.2:1 and 4:1, respectively.
- Thus both a larger metal with the same charge and a metal of similar size but with a lower charge gave lower arsenate/selenate selectivity. These results suggest that both charge and size impact anion capture selectivity and that there must be a specific match between ligand coordination, metal charge and anion polarizability in order to obtain optimal selectivity.
- ZrBPAPM shows significant sorption capacities for molybdenum and tungsten oxo-anions over a broad pH range of 2-10.
- ZrBPAPM has also shown selective removal of molybdenum at pH < 2 in the presence of nickel and vanadium.

7.3 Applications of Non-IMPAC Systems

The alkylated SPC, BPQA was developed to emulate commercially available quaternized amine based resins for anion capture. As this system does not use any immobilized metal to provide the positive charge to remove the target anions from aqueous solutions, there is no possibility or danger of any metal leaching from the composite. Different variants of the quaternized amine were synthesized by varying the alkyl chains on the nitrogen. BPQA composites with different alkyl groups were also tested for bacteria and virus removal from domestic water systems. Although the details of this project were not discussed in the previous chapters, some data and conclusions will be reported in this section:

- The four versions of BPQA synthesized using varying MTCS:CPTCS ratios showed varying amounts of quaternization of the amine sites.
- The CPTCS only BPQA had only 10% of the free amines quaternized; the 7.5:1 BPQA had 11% quaternized amines; the 10:1 BPQA showed the highest amount of quaternized amines sites (54%); and the 12.5:1 BPQA had 35% quaternized amine sites. The BPQOM composite (exhaustive N-octylation instead of N-methylation) had only 2% quaternized amine sites.
- However, the 7.5:1 BPQA showed highest capacity for arsenic and selenium removal for a wide pH range of 2-8.
- The 7.5:1 BPQA showed excellent mass transfer kinetics for arsenate with 100% arsenate stripping using both 2M-H_2SO_4 or brine. Successive breakthrough studies on this composite did not show any reduction in arsenate sorption capacity.

- The 7.5:1 BPQA showed good batch capacities for molybdenum and tungsten anions over a broad pH range (2-10). The composite was selective for tungstate over molybdate with a selectivity factor of 3:1.
- The brine strip of the molybdate and tungstate anions showed co-stripping of both the species (60% and 40%, respectively). But the 2M-H_2SO_4 strip showed selective stripping of molybdenum (~90%).
- Although the BPQOM composite showed selective capture of selenium over arsenic, the sorption capacities for arsenic and selenium were extremely low for the pH range of 2-6. The capacities remained steady over the pH range tested (0mg/g – arsenic and 3mg/g – selenium).
- BPQAM and BPQOM showed excellent bacteria and virus removal. BPQAM showed > 99.99% bacteria removal and > 99.95% virus removal. BPQOM showed 99.99% bacteria removal and 99.96% virus removal. However the required bacteria removal was 99.9999% and virus removal was 99.99%.

7.4 AFM Characterization

Although the surface studies on most of the SPCs have been performed using Scanning Electron Microscopy (SEM) and mercury porosimetry studies, the data obtained does not address certain issues regarding the coordination of metals, and the distribution of the ligands on the silica gel particles. The porosity of a material affects its physical properties and, subsequently, its behavior in its surrounding environment. The term "porosimetry" is often used to encompass the measurements of pore size, volume,

distribution, density, and other porosity-related characteristics of a material. The adsorption and permeability, strength, density, and other factors influenced by a substance's porosity determine the manner and fashion in which it can be appropriately used. To better understand the surface of the SPCs, Atomic Force Microscopy (AFM) was used and certain conclusions are listed below:

- The CPTCS only SPCs are believed to have closer anchor points and thereby have smaller polymer loops. Whereas the mixed silane SPCs are more diluted with respect to the silanes and the anchor points are farther giving rise to bigger polymer loops.
- The height/depth relief for the mixed silane BP1 (60nm) is much greater than the CPTCS only BP1 (30nm).
- SPC chemistry of glass slides work better for the purpose of AFM characterization, as they have a flat base for the SPC reaction to take place.
- The average surface roughness (R_q) show an increase as expected from CP gel to BP2 (amino acetate modified BP1). However there was an anomalously large increase in R_q on going from BP1 to BP2, a result that would not be expected on addition of a small molecule ($ClCH_2CO_2H$).
- Silicon wafers have shown good promise for the extension of the SPC chemistry on to the wafer surfaces. The silicon wafer surface is far more reactive than the glass slide surfaces, mainly because the surface modification on the wafers took much less time as compared to the glass slides.

- There has been a gradual increase of R_q form the unmodified wafer to the silanized wafer and there on. The formation of aggregates on the CPTCS only modified wafer showed interesting surface mapping than the mixed silane modified wafer.
- The formation and observation of the shorter and closer loops in the CPTCS only modified wafer is seen here as well. And the mixed silane modified wafer shows bigger loops between anchor points as seen from their R_q values.

7.5 Future Work

SPC materials are remarkable tools for selective metal extraction from aqueous media. SPCs are being investigated for catalysis, cation and precious metal removal, microbial capture, and CO_2 sorption applications. The work presented here was an attempt to bring about a more detailed understanding of the technology by investigating anion removal, recovery, and structural features of the materials. As a result, MTCS is now utilized in the synthetic procedure for commercial production. However, there remains much to explore with regard to this technology. Future experiments will lead to improvements in existing materials and the materials introduced in this work:

- Run longevity test (1000 cycles or more) for arsenic on 7.5:1 BPQAM.
- Run longevity test (1000 cycles or more) for selenium on ZrBPAPM and 7.5:1 BPQAM.
- Test arsenate selectivity on ZrBPAPM over silicate, nitrate, and phosphate.

- Test BP2M and BPQAM separately as the first load cycle for the Julia Creek mock sample.
- Test the 10:1 and 12.5:1 BPQA systems for bacteria and virus removal as it shows higher quaternization of the amines.
- Synthesize the 10:1 and 12.5:1 BPQO systems and calculate the percent quaternization.
- Test the metal sorption on the polymer modified silicon wafers.
- Development and further characterization of the wafer technology using EXAFS which gives the metal spacing on the surface.

CHAPTER 8: REFERENCES

1. Aicheson, L. *A History of Metals, (2 Vols.)*; Interscience: New York; 1960.
2. Mortimer, C. E. *Chemistry: A Conceptual Approach, (3rd ed.)*; D. Van Nostrad Company: New York; 1975.
3. Allan, R. Introduction: Mining and Metals in the Environment. *Journal of Geochemical Exploration*, **1997**, 58(2-3), 95-100.
4. Page, B; Edwards, M; May, N. Metal Cans. *Food Packaging Technology*, **2003**, 120-151.
5. Clarke, P. The Decorative Uses of Metals. *Met. Mark. Place, Met. Congr. (Tech. Sess. 1)*, 1978, Paper No. 10, 8pp.
6. Licthi, G; Mulcahy, J. Acid Mine Drainage – Environmental Nightmare or Asset? *Chemistry in Australia*, **1998**, 13(2), 10-13.
7. Kwelok, J. K. Aspects of Geo-legal Mitigation of Environmental Impact from Mining and Associated Waste in the UK. *Journal of Geochemical Exploration*, **1999**, 66(1-2), 327-332.
8. Mohammad, S. K; Almas, Z; Parvaze, A. W; Mohammad, O. Role of Plant Growth Promoting Rhizobacteria in the Remediation of Metal Contaminated Soils. *Environmental Chemistry Letters*, **2009**, 7, 1-19.
9. (a) Wang, L. K; Hung, Y; Lo, H. H.; Yapijakis, C; (Editors). *Hazardous Industrial Waste Treatment*; CRC Press LLC: Boca Raton, Florida; 2007. (b) Meharg, A. A;

Rahman, Md. M. Arsenic Contamination of Bangladesh Paddy Field Soils: Implications for Rice Contribution to Arsenic Consumption. *Environmental Science and Technology*, **2003**, 37(2), 229-234. (c) Wiener, J. G; Knights, B. C; Sandheinrich, M. B; Jeremiason, J. D; Brigham, M. E; Engstrom, D. R; Woodruff, L. G; Cannon, W. F; Balogh, S. J. Mercury in Soils, Lakes, and Fish in Voyageurs National Park (Minnesota): Importance of Atmospheric Deposition and Ecosystem Factors. *Environmental Science & Technology*, **2006**, 40(20), 6261-6268.

10. Tavakoli, O.; Yoshida, H. Effective Recovery of Harmful Metal Ions from Squid Wastes using Subcritical and Supercritical Water Treatments. *Environmental Science and Technology*, **2005**, 39(7), 2357-2363.
11. Forzani, E. S.; Zhang, H.; Chen, W.; Tao, N. Detection of Heavy Metal Ions in Drinking Water Using a High-Resolution Differential Surface Plasmon Resonance Sensor. *Environmental Science and Technology*, **2005**, 39(5), 1257-1262.
12. Boddu, V. M.; Abburi, K.; Talbott, J. L.; Smith, E. D. Removal of Hexavalent Chromium from Wastewater Using a New Composite Chitosan Biosorbent. *Environmental Science and Technology*, **2003**, 37(19), 4449-4456.
13. Vijver, M. G.; Van Gestel, C. A. M.; Lanno, R. P; van Straalen, N. M; Peijnenburg, W. J. G. M. Internal Metal Sequestration and its Ecotoxicological Relevance: A Review. *Environmental Science and Technology*, **2004**, 38(18), 4705-4712.
14. Kordosky, G. A; Sierakoski, J. M; Virnig, M. J; Mattison, P. L. Gold solvent extraction from typical cyanide leach solutions. *Hydrometallurgy*, **1992**, 30(1-3), 291-305.

15. Kordosky, G. A. Copper Solvent Extraction: The State of the Art. *Journal of the Minerals, Metals & Materials Society (JOM)*, **1992**, 44(5), 40-45.

16. Alexandratos, S. D; Zhu, X. High–Affinity Ion–Complexing Polymer–Supported Reagents: Immobilized Phosphate Ligands and their Affinity for the Uranyl Ion. *Reactive and Functional Polymers*, **2007**, 67(5), 375-382.

17. Hirner, A. V; Xu, Z. Trace Metal Speciation in Julia Creek Oil Shale. *Chemical Geology*, **1991**, 91(2), 115-124.

18. Patterson, J. H; Ramsden, A. R; Dale, L. S; Fardy, J. J. Geochemistry and Mineralogical Residences of Trace Elements in Oil Shales from Julia Creek, Australia. *Chemical Geology*, **1986**, 55(1-2), 1-16.

19. Mendes, F.D; Martins, A. H. Recovery of Nickel and Cobalt from Acid Leach Pulp by Ion Exchange using Chelating Resin. *Minerals Engineering*, **2005**, 18(9), 945-954.

20. Cheng, C. Y. Purification of Synthetic Laterite Leach Solution by Solvent Extraction using D2EHPA. *Hydrometallurgy*, **2000**, 56(3), 369-386.

21. Meyer, K; Krueger, J. Raw Materials for the Production of Nickel and Processes used for it. *Stahl und Eisen*, **1972**, 92(3), 113-120.

22. Wilson, F. The Moa Bay–Port Nickel Project. *Mining Engineering*, **1958**, 10, 563-565.

23. Wells, B. A; Clark, D. R. Selective extraction of molybdenum from acidic leach liquors. US Patent #4026988.

24. Chen, Y; Feng, Q; Shao, Y; Zhang, G; Ou, L; Yiping Lu, Y. Investigations on the Extraction of Molybdenum and Vanadium from Ammonia Leaching Residue of Spent Catalyst. *International Journal of Mineral Processing*, **2006**, 79, 42– 48.

25. Reddy, B. R; Park, K. H. Process for the recovery of Cobalt and Nickel from Sulphate Leach Liquors with Saponified Cyanex 272 and D2EHPA. *Separation Science and Technology*, **2007**, 42(9), 2067-2080.

26. Beauvais, R. A; Alexandratos, S. D. Polymer-Supported Reagents for the Selective Complexation of Metal Ions: An Overview. *Reactive & Functional Polymers*, **1998**, 36(2), 113-123.

27. Nguta, C. M; Guma, J. Lead and Cadmium Concentrations in Cattle Tissue: The Effect of Industrial Pollution from Nakuru Town. *Journal of the Kenya Chemical Society*, **2004**, 2(1), 19-24.

28. Moleux, P. Designing a New PCB Facility for Successful Pollution Prevention & Waste Minimization. *Plating and Surface Finishing*, **1994**, 81(4), 44-47.

29. Somers, E. Toxic Potential of Trace Metals in Foods: Review. *Journal of Food Science*, **1974**, 39(2), 215-217.

30. Vukovic, Z. Environmental Impact of Radioactive Silver Released from Nuclear Power Plant. *Journal of Radioanalytical and Nuclear Chemistry*, **2002**, 254(3), 637-639.

31. Swaine, D. J. Trace Elements in Coal and Their Dispersal during Combustion. *Fuel Processing Technology*, **1994**, 39(1-3), 121-137.

32. Kawata, K; Yokoo, H; Shimazaki, R; Okabe, S. Classification of Heavy-Metal Toxicity by Human DNA Microarray Analysis. *Environmental Science & Technology,* ***2007***, 41(10), 3769-3774.

33. Dillard, C. J; Tappel, A. L. Mercury, Silver, and Gold Inhibition of Selenium-Accelerated Cysteine Oxidation. *Journal of Inorganic Biochemistry*, **1986**, 28(1), 13-20.

34. Tinggi, U. Selenium Toxicity and its Adverse Health Effects. *Reviews in Food and Nutrition Toxicity*, **2005**, 4, 29-55.

35. Marcinowski, F; Tonkay, D. W. Low-Activity Radioactive Materials Management at the U.S. Department of Energy. *Health Physics*, **2006**, 91(5), 498-501.

36. Thorne, M. C; Vennart, J. The Toxicity of Strontium-90, Radium-226, & Plutonium-239. *Nature*, **1976**, 263(5578), 555-558.

37. Foust, H; Holton, L; Demick, L. Maximizing Production Capacity from an Ultrafiltration Process at the Hanford Department of Energy Waste Energy Treatment Facility. *Separation Science and Technology*, **2005**, 40(16), 3323-3337.

38. U.S. Department of Energy Environmental Management - "Department of Energy Five Year Plan FY 2007-FY 2011 Volume II." Retrieved 2 March 2009.

39. (a) Sobolev, I. A; Dmitriev, S. A; Lifanov, F. A; Kobelev, A. P; Stefanovsky, S. V; Ojovan, M. I. Vitrification Processes for Low, Intermediate Radioactive and Mixed Wastes. *Glass Technology*, **2005**, 46(1), 28-35. (b) Ojovan, M. I; Lee, W. E. *An Introduction to Nuclear Waste Immobilisation*; Elsevier Science Publishers B.V: Amsterdam; 2005.

40. Manchanda, V. K; Pathak, P. N. Amides and Diamides as Promising Extractants in the Back End of the Nuclear Fuel Cycle: an Overview. *Separation and Purification Technology*, **2004**, 35(2), 85-103.

41. Madic, C; Hudson, M. J; Liljenzin, J. O; Glatz, J. P; Nannicini, R; Facchini, A; Kolarik, Z; Odoj, R. Recent Achievements in the Development of Partitioning Processes of Minor Actinides from Nuclear Wastes Obtained in the Frame of the NEWPART European program (1996-1999). *Progress in Nuclear Energy*, **2002**, 40(3-4), 523-526.

42. Balu, K; Wattal, P. K. Indian Experiences in Management of Radioactive Waste from Nuclear Fuel Cycle. *Proceedings of the International Topical Meeting on Nuclear and Hazardous Waste Management, SPECTRUM '96*, Seattle, Aug. 18-23, 1996; 3, 2072-2075.

43. Ozawa, M. Novel Partitioning Technologies for Minor Actinides in High Level Liquid Wastes. *Radioisotopes*, **1996**, 45(8), 527-530.

44. Alexandratos, S. D; Hong, M-J. Enhanced Metal Ion Affinities by Supported Ligand Synergistic Interaction in Bifunctional Polymer Supported Aminomethylphosphonates. *Separation Science and Technology*, **2002**, 37(11), 2587-2605.

45. (a) Hadley, R; Snow, D. *Water Resources and Problems Related to Mining*. American Water Resource Association; Minnesota; 1974. (b) Castro, J. M; Moore, J. N. Pit Lakes: Their Characteristics and the Potential for Their Remediation. *Environmental Geology (Berlin)*, **2000**, 39(11), 1254-1260.

46. Mehrotra, A; Singhal, R. *Environmental Issues and Waste Management in Energy and Minerals Production, Vol 2*; A. A. Balkema: Rotterdam; 1992.

47. Perry, A. O. *Advances in Mineral Resources Technology for Minimizing Environmental Impacts: Environmental Issues and Waste Management in Energy and Minerals Production*; U.S. Dept. of Interior, Bureau of Mines, Battlefield Press: Columbus; 1992.

48. Nordstrom, D. K; Alpers, C. N; Ptacek, C. J; Blowes, D. W. Negative pH and Extremely Acidic Mine Waters from Iron Mountain, California. *Environmental Science and Technology*, **2000**, 34(2), 254-258.

49. McIntyre, R. D. Some Current Uses foe Metals in, on, and Around Your Body. *Materials Engineering (Cleveland)*, **1982**, 96(3), 40-47.

50. (a) Tabak, H. H; Scharp, R; Burckle, J; Kawahara, F. K; Govind, R. Advances in Biotreatment of Acid Mine Drainage and Biorecovery of Metals: 1. Metal precipitation for recovery and recycle. *Biodegradation*, **2003**, 14(6), 423-436. (b) Tabak, H. H; Govind R. Advances in Biotreatment of Acid Mine Drainage and Biorecovery of Metals: 2. Membrane Bioreactor System for Sulfate Reduction. *Biodegradation*, **2003**, 14(6), 437-452.

51. Deorkar, N. V; Tavlarides, L. L. An Adsorption Process for Metal Recovery from Acid Mine Waste: The Berkeley Pit Problem. *Environmental Progress*, **1998**, 17(2), 120-125.

52. Yang, K; Misra, M; Mehta, R. Removal of Heavy Metal Ions from Noranda Tailings Water and Berkeley Pit Water by Ferrite Coprecipitation Process. *Waste Processing*

and Recycling in Mineral and Metallurgical Industries II (Proceedings of the International Symposium on Waste Processing and Recycling in Mineral and Metallurgical Industries), 1995, 425-438.

53. Huang, H. H; Liu, Q. Bench-scale Chemical Treatability Study of the Berkeley Pit Water. ACS Symposium Series 607 (Emerging Technologies in Hazardous Waste Management 5), **1995**, 196-209.
54. Karathanasis, A. D; Johnson, C. M. Metal Removal Potential by Three Aquatic Plants in an Acid Mine Drainage Wetland. *Mine Water and the Environment*, **2003**, 22(1), 22-30.
55. Murdoch, A; Clair, T. A. Transport of Arsenic and Mercury from Gold Mining Activities Through an Aquatic System. *Science of the Total Environment*, **1986**, 57, 205-216.
56. Feng, Z; Xia, Y; Tian, D; Wu, K; Schmitt, M; Kwok, R. K. DNA Damage in Buccal Epithelial Cells from Individuals Chronically Exposed to Arsenic via Drinking Water in Inner Mongolia, China. *Anticancer Research*, **2001**, 21, 51-58.
57. Bell, F. G. Environmental Geology and Health. *Environmental Geology: Principles and Practice, London: Blackwell Science*, **1998**, 487-500.
58. Duker, A. A; Carranza, E. J. M; Hale, M. Arsenic Geochemistry and Health. *Environment International*, **2005**, 31, 631-641.
59. Tabacova, S; Hunter, E. S; Gladen, B. C. Developmental Toxicity of Inorganic Arsenic in Whole Embryo: Culture Oxidation State, Dose, Time, and Gestational Age Dependence. *Toxicological Applications of Pharmacology*, **1996**, 138, 298-307.

60. Schroeder, H. A; Balassa, J. J. Abnormal Trace Elements in Man: Arsenic. *Journal of Chronic Disease*, **1996**, 19, 85-106.

61. Clara, M; Magalhaes, F. Arsenic. An Environmental Problem Limited by Solubility. *Pure & Applied Chemistry*, **2002**, 74(10), 1843-1850.

62. Smith, A. H; Lingas, E. O; Rahman, M. Contamination of Drinking Water by Arsenic in Bangladesh: A Public Health Emergency. *WHO Bulletin*, **2000**, 78, 1093-1103.

63. Kitchin, K. T. Recent Advances in Arsenic Carcinogeneses: Modes of Action, Animal Model Systems, and Methylated Arsenic Metabolites. *Toxicological Application in Pharmacology*, **2001**, 172, 249-261.

64. Welch, A. H; Westjohn, D. B; Helsel, D. R; Wanty, R. B. Arsenic in Ground Water of the United States; Occurrence and Geochemistry. *Groundwater*, **2000**, 38:4, 589-604.

65. Lemly, A. D. Aquatic Selenium Pollution is a Global Environmental Safety Issue," *Ecotoxicology and Environmental Safety*, **2004**, 59, 44-56.

66. (a) Spence, J. T. *Reactions of Molybdenum Coordination Compounds: Models for Biological Systems. Reactivity of Coordination Compounds (Sigel, H, ed.)*; Marcel Dekker: New York; 1976. (b) Barceloux, D. G. Molybdenum. *Journal of Toxicology, Clinical Toxicology*, **1999**, 37(2), 231-237.

67. Stryer, L. *Biochemistry (3rd ed.)*; Freeman, W. H: New York; 1988.

68. Lener, J; Bibr, B. Effects of Molybdenum on the Organism (A Review). *Journal of Hygiene, Epidemiology, Microbiology, and Immunology*, **1984**, 28, 406-419.

69. Vyskocil, A; Viau, C. Assessment of Molybdenum Toxicity in Humans. *Journal of Applied Toxicology*, **1999**, 19(3), 185-192.

70. Bibr, B; Deyl, Z; Lener, J; Adam, M. Investigation on the Reaction of Molybdenum with Collagen in Vivo. *International Journal of Peptide & Protein Research*, **1977**, 10, 190-196.

71. Bibr, B; Deyl, Z; Lener, Kucera, J; Simkova, M. The Mechanism of Action of Molybdenum and Tungsten upon Collagen Structures in Vivo. *Physiol. Bohemoslav.*, **1987**, 36, 417-424.

72. Davies, T. D; Pickard, J; Hall, K. J. Acute Molybdenum Toxicity to Rainbow Trout and other Fish. *Journal of Environmental Engineering and Science*, **2005**, 4(6), 481-485.

73. Willsky, G. R. *Vanadium in the Biosphere, Vanadium in Biological Systems: Physiology and Biochemistry (Chasteen, N. D., ed.)*; Kluwer Academic: Dordrecht; 1990, 1-24.

74. Nielsen, F. H; Uthus, E. O. *The Essentiality and Metabolism of Vanadium, Vanadium in Biological Systems: Physiology and Biochemistry (Chasteen, N. D., ed.)*; Kluwer Academic: Dordrecht; 1990, 51-62.

75. Zenz, C. *Vanadium, Metals in the Environment (Waldron, H. A., ed.)*; Academic Press, London: England; 1980.

76. Sjoberg, S. G. Vanadium Bronchitis from Cleaning Oil-fired Boilers. *AMA Arch. Ind. Health*, **1955**, 11, 505-512.

77. Lees, R. E. M. Changes in Lung Function after Exposure to Vanadium Compounds in Fuel Oil Ash. *Br. J. Ind. Med.*, **1980**, 37, 253-256.

78. Levy, B. S; Hoffman, L; Gottsegen, S. Boilermaker's Bronchitis – Respiratory Tract Irritation Associated with Vanadium Pentoxide Exposure during Oil-to-coal Conversion of a Power Plant. *J. Occup. Med.*, **1984**, 26, 567-570.

79. (a) Stokinger, H. E. *The Metals. Vanadium, Patty's Industrial Hygiene and Toxicology (Clayton, G. D; Clayton, F. E., eds.)*; John Wiley & Sons: New York; 1981, 2013-2033. (b) Guy, R. H; Hostynek, J. J; Hinz, R. S; Lorence, C. R. *Metals and the Skin – Topical Effects and Systemic Absorption*; Marcel Dekker Inc.: New York; 1999.

80. (a) Beamish, F. E. A Critical Review of Methods of Isolating and Separating the Noble Metals – 2) Ion-exchange and Solvent Extraction. *Talanta*, **1967**, 14(9), 991-1009. (b) Barwick, V. J. Strategies for Solvent Selection – A Literature Review. *Trends in Analytical Chemistry*, **1997**, 16(6), 293-309. (c) Rotuska, K; Chmielewski, T. Growing Role of Solvent Extraction in Copper Ores Processing. *Physicochemical Problems of Mineral Processing*, **2008**, 42, 29-36.

81. (a) Luque de Castro, M. D; Alvarez-Sanchez, B. Membrane based Separation Techniques: Liquid-liquid Extraction and Filtration. *Comprehensive Analytical Chemistry*, **2008**, 54, 235-264. (b) Ortiz, I; Irabien, J. A. Membrane Assisted Solvent Extraction for the Recovery of Metallic Pollutants: Process Modeling and Optimization. *Handbook of Membrane Separations*, **2009**, 1023-1039.

82. Khan, M. S; Zaidi, A; Wani, P. A; Oves, M. Role of Plant Growth Promoting Rhizobacteria in the Remediation of Metal Contaminated Soils. *Environmental Chemistry Letters*, **2009**, 7, 1–19.

83. (a) Deep, A; de Carvalho, J. M. R. Review on the Recent Developments in the Solvent Extraction of Zinc. *Solvent Extraction and Ion Exchange*, **2008**, 26, 375-404. (b) Kodorsky, G. A. Copper Solvent Extraction: The State of the Art. *JOM*, **1992**, 44(5), 40-45. (c) Rosenberg, E; Nielsen, D; Miranda, P; Hart, C. Silica Polyamine Composites: Advanced Materials for Ion Recovery and Remediation. Official Proceedings - International Water Conference 66th, IWC.05.40/1-IWC.05.40/12. **2005**.

84. (a) Yakubu, N. A; Dudeney, A. W. L. A Study of Uranium Solvent Extraction Equilibria with Alamine 336 in Kerosene. *Hydrometallurgy*, **1987**, 18(1), 93-104. (b) Skey, W; Irving, H. M. N. H. Centenary in the History of Solvent Extraction. *Chemistry & Industry (London, UK)*, **1967**, 42, 1780-1781.

85. Riveros, P. M. Molybdenum: Solvent Extraction and Hydrometallurgical Alternatives. *Minerales*, **1980**, 150, 45-52.

86. Smith, R. A. The Use of EDXRF for Liquids in a Uranium–Vanadium Solvent Extraction Process. *Advances in X-Ray Analysis*, **1982**, 25, 103-106.

87. (a) Mihaylov, I; Distin, P. A. Gallium Solvent Extraction in Hydrometallurgy: An Overview. *Hydrometallurgy*, **1992**, 28(1), 13-27. (b) Cathum, S. J; Brown, C. E; Obenauf, A; Punt, M. Speciation of Arsenic Using Chelation Solvent Extraction and High Performance Liquid Chromatography. *Clean*, **2007**, 35(1), 71-80.

88. Jessen, S; Larsen, F; Koch, C. B; Arvin, E. Sorption and Desorption of Arsenic to Ferrihydrite in a Sand Filter. *Environmental Science & Technology*, **2005**, 39(20), 8045-8051.

89. Chen, H. W; Frey, M. M; Clifford, D; McNeill, L. S; Edwards, M. Arsenic Treatment Considerations. *Journal of the American Water Works Association*, **1999**, 91(3), 74-85.

90. Buswell, A. M; Gore, R. C; Hudson, H. E; Wiese, A. C; Larson, T. E. War Problems in Analysis and Treatment. *Journal-American Water Works Association*, **1943**, 35(10), 1303-1311.

91. Jekel, M. R. *Removal of arsenic in drinking water treatment. Arsenic in the Environment, Part I: Cycling and Characterization (In: J. O. Nriagu [Ed.])*; John Wiley & Sons: New York; 1994.

92. (a) Hering, J. G; Chen, P. Y; Wilkie, J. A; Elimelech, M; Liang, S. Arsenic Removal by Ferric Chloride. *Journal-American Water Works Association*, 1996, 88(4), 155-167. (b) Hering, J. G; Chen, P. Y; Wilkie, J. A; Elimelech, M. Arsenic Removal from Drinking Water during Coagulation. *Journal of Environmental Engineering*, 1997, 123(8), 800-807.

93. Cheng, R. C; Liang, S; Wang, H. C; Beuhler, M. D. Enhanced Coagulation for Arsenic Removal. *Journal-American Water Works Association*, **1994**, 86(9), 79-90.

94. Edwards, M. Chemistry of Arsenic Removal during Coagulation and Fe-Mn Oxidation. *Journal-American Water Works Association*, **1994**, 86(9), 64-78.

95. Sancha, A. M. Removal of arsenic from drinking water supplies. *Proceedings, IWSA XXII World Congress and Exhibition*, Buenos Aires, Argentina, 1999.

96. Lien, H-L; Wilkin, R. T. High-level Arsenite Removal from Groundwater by Zero-valent Iron. *Chemosphere*, **2005**, 59, 377-386.

97. Nikolaidis, N. P; Dobbs, G. M; Lackovic, J. A. Arsenic Removal by Zero-valent Iron: Field, Laboratory, and Modeling Studies. *Water Res.*, **2003**, 37, 1417-1425.

98. (a) Rogers, Y. C; Santos, E. C; Robison, T. W; Gibson, R. R; Smith, B. F. Removal of Oxyanions from Aqueous Systems using Polymer Filtration (Water-soluble Metal-binding Polymers with Ultrafiltration). *Proceedings, 213th ACS National Meeting*, San Francisco, California, USA, 1997. (b) Geckeler, K. E; Shkinev, V; Spivakov, B. Y. Liquid-phase Polymer based Retention (LPR) – A New Method for Selective Ion Separation. *Separation and Purification Methods*, **1988**, 17(2), 105-140.

99. Geckeler, K. E; Volchek, K. Removal of Hazardous Substances from Water Using Ultrafiltration in Conjunction with Soluble Polymers. *Environmental Science and Technology*, **1996**, 30(3), 725-734.

100. Letterman, A. [Ed.]. *Water Quality and Treatment: A Handbook of Community Water Supplies*. American Water Works Association, McGraw-Hill: New York; 1999.

101. Waypa, J; Elimelech, M; Hering, J. Arsenic Removal by RO and NF Membranes. *Journal-American Water Works Association*, **1997**, 89(10), 102-114.

102. Geckeler, K. E., Rosenberg, E. *Functional Nanomaterials*; 488 pp. 2006.

103. Ficklin, W. H. Separation of As(III) and As(V) in ground waters by ion exchange. *Talanta*, **1983**, 30(5), 371.

104. (a) Edwards, M; Patel, S; McNeill, L; Chen, H. W; Frey, M; Eaton, A. D; Antweiler, R. C; Taylor, H. E. Considerations in arsenic analysis and speciation. *Journal-American Water Works Association*, **1998**, 90(3), 103-113. (b) Ghurye, G; Clifford, D; Tripp, A. Combined arsenic and nitrate removal by ion exchange. *Journal-American Water Works Association*, **1999**, 91(10), 85-96.

105. Nielsen, J, D; Rosenberg, E. Continued Development of Modified Silica Polyamine Composite Materials and Reclamation of Acid Mine Drainage. Abstracts – 58th Northwest Regional Meeting of the American Chemical Society, Bozeman, MT, USA, June 2003.

106. Kailasam, V; Rosenberg, E; Nielsen, D. Characterization of Surface Bound Zr(IV) and its Application to Removal of As(V) and As(III) from Aqueous Systems using Phosphonic Acid Modified Nano-porous Silica Polyamine Composites. *Industrial & Engineering Chemistry Research*, **2009**, 48(8), 3991-4001.

107. Beatty, S. T; Fischer, R. J; Hagars, D. L; Rosenberg, E. A Comparative Study of the Removal of Heavy Metal Ions from Water Using a Silica Polyamine Composite and a Polystyrene Chelator Resin. *Industrial & Engineering Chemistry Research*, **1999**, 38(11), 4402-4408.

108. Hughes, M. A; Rosenberg, E. Characterization and Applications of Poly-Acetate Modified Silica Polyamine Composites. Separation Science and Technology, 2007, 42(2), 261-283.109.

109. Stewart, N. A; Pham, V, T; Choma, C. T; Kaplan, H. Improved Peptide Detection with Matrix-Assisted Laser Desorption/ Ionization Mass Spectrometry by Trimethylation of Amino Groups. *Rapid Communications in Mass Spectrometry*, **2002**, 16, 1448-1453.

110. Hughes, M, A. The Structure Function Relationship of Silica Polyamine Composites, PhD Dissertation, The University of Montana, **2007**.

111. (a) Fatunmbi, H. O; Wirth, M. J. Horizontally Polymerized Chromatographic Stationary Phases. *Special Publication – Royal Society of Chemistry (Chemically Modified Surfaces)*, **1996**, 173, 61-65. (b) Cox, G. B; Loscombe, C. R; Slucutt, M. J; Sugden, K; Upfield, J. A. The Preparation, Properties and Some Applications of Bonded Ion-Exchange Packings based on Microparticulate Silica Gel for High-Performance Liquid Chromatography. *Journal of Chromatography*, **1976**, 117(2), 269-278. (c) Nielsen, D, J. Synthesis and Reclamation of Novel Silica Polyamine Composites and Their Application to the Reclamation of Hazardous Mining Wastewater and Tailings, PhD Dissertation, The University of Montana, **2006**.

112. Beatty, S. T; Fischer, R. J; Rosenberg, E; Pang, D. Comparison of Novel and Patented Silica Polyamine Composite Materials as Aqueous Heavy Metal Ion Recovery Materials. *Separation Science and Technology*, **1999**, 34(14), 2723-2739.

113. Fan, Z, L; Li, D, Q; Rosenberg, E. Synthesis and Adsorption Property of Poly(allylamine)-Silica Composite. *Yingyong Huaxue*, **2003**, 20(9), 867-870.

114. (a) Arasawa, H; Odawara, C; Yokoyama, R; Saitoh, H; Yamauchi, T; Tsubokawa, N. Grafting of Zwitterion Type Polymers onto Silica Gel Surface and Their Properties.

Reactive & Functional Polymers, **2004**, 61(2), 153-161. (b) Stine, J. J; Palmer, C, P. Covalent Modification of Fused Silica Capillaries with Quaternized Polyamines to Achieve Robust and Stable Anodic Electroosmotic Flow. *Journal of Separation Science*, **2009**, 32, 446-456.

115. Watanabe, K; Chow, W. S; Royer, G. P. Column Chromatography on Polyethyleneimine Silica: Rapid Resolution of Nucleotides and Proteins with Short Columns and Low Pressures. *Analytical Biochemistry*, **1982**, 127(1), 155-158.

116. Rosenberg, E; Pang, D. System for Extracting Soluble Heavy Metals from Liquid Solutions, Especially Aqueous Solutions. The University of Montana, USA. 48 pp. 19990514. PCT Int. Appl. 97.

117. Hughes, M. A; Nielsen, D; Rosenberg, E; Gobetto, R; Viale, A; Burton, S. D; Ferel, J. Structural Investigations of Silica Polyamine Composites: Surface Coverage, Metal Ion Coordination, and Ligand Modification. *Industrial & Engineering Chemistry Research*, **2006**, 45(19), 6538-6547.

118. (a) Rosenberg, E., et. al. Manuscript in Progress. (b) Rosenberg, E; Fischer, R. J; Deming, J; Hart, C; Miranda, P; Allen, B. Silica Polyamine Composites: Advanced Materials for Heavy Metal Recovery, Recycling and removal. *PMSE Preprints*, **2002**, 86, 79-80.

119. (a) Maksimov, A. L; Karakhanov, E; Zatolochnaya, O. V; Rosenberg, E; Hughes, M; Kailasam, V. Hybrid Macromolecular Iron and Copper Complexes in Phenol Hydroxylation. *Petroleum Chemistry*, **2009**, 49(2), 107-113. (b) Bandosz, T.J; Seredych, M; Allen, J; Wood, J; Rosenberg, E. Silica-Polyamine-Based Carbon

Composite Adsorbents as media for Effective Sulfide Adsorption/Oxidation. *Chemistry of Materials*, **2007**, 19(10), 2500-2511.

120. Moedritzer, K; Irani, R. R. The Direct Synthesis of α-Aminomethylphosphonic Acids. Mannich-Type Reactions with Orthophosphorus Acid. *Journal of Organic Chemistry*, **1966**, *31(5)*, 1603-1607.

121. Huenig, S; Quast, H; Brenninger, W; Frankenfeld, E. Tetramethyl-p-phenylenediamine. *Organic Syntheses*, **1969**, 49, 107-10.

122. Zagorodni, A. A; Kotova, D. L; Selemenev, V. F. Infrared Spectroscopy of Ion Exchange Resins: Chemical Deterioration of the Resins. *Reactive & Functional Polymers*, **2002**, *53*, 157-171.

123. (a) Suzuki, T. M; Tanaka, D. A. P; Tanco, M. A. L; Kanesato, M; Yokoyama, T. Adsorption and Removal of Oxo-anions of Arsenic and Selenium on the Zirconium(IV) Loaded Polymer Resin Functionalized with Diethylenetriamine-N,N,N,N-Polyacetic Acid. *Journal of Environmental Monitoring*, **2000**, 2, 550-555. (b) Capretta, A; Maharajh, R. B; Bell, R. A. Synthesis and Characterization of Cyclomaltoheptaose-based Metal Chelants as Probes for Intestinal Permeability. *Carbohydrate Research*, **1995**, 267(1), 49-63.

124. Dambies, L; Alexandratos, S. D; Salinaro, R. Immobilized N-Methyl-D-Glucamine as an Arsenate-Selective Resin. *Environmental Science & Technology*, **2004**, 38, 6139-6146.

125. Miranda, P. Gallium and Selenium/Arsenic Recoveries Using Silica Based Ion Exchange Resins, PhD Dissertation, The University of Montana, **2005**.

126. Rosenberg, E; Allen, J. J. Surface Oxidation of Co^{2+} and Its Dependence on Ligand Coordination Number in Silica Polyamine Composites. *Inorganica Chimica Acta*, **2009**, in press.

127. Goh, K-H; Lim, T-T. Geochemistry of Inorganic Arsenic and Selenium in a Tropical Soil: Effect of Reaction Time, pH, and Competitive Anions on Arsenic and Selenium Adsorption. *Chemosphere*, **2004**, 55, 849-859.

128. Yang, L; Shahrivari, Z; Liu, P. K. T; Sahimi, M; Tsotsis, T. T. Removal of Trace Levels of Arsenic and Selenium from Aqueous Solutions by Calcined and Uncalcined Layered Double Hydroxides (LDH). *Industrial & Engineering Chemistry Research*, **2005**, 44, 6804-6815.

129. (a) Matsunaga, H; Yokoyama, T; Eldridge, R J; Bolto, B. A. Adsorption Characteristics of Arsenic(III) and Arsenic(V) on Iron(III)-Loaded Chelating Resin having Lysine-N^{α},N^{α}-Diacetic Acid Moiety. *Reactive & Functional Polymers*, **1996**, 29, 167-174. (b) Fish, R. H; Tannous, R. S. Polymer-Pendent Ligand Chemistry 1. Reactions of Organoarsenic Acids and Arsenic Acid with Catechol Ligands Bonded to Polystyrene-Divinyl Benzene. *Inorganic Chemistry*, **1985**, 24, 4456-4458.

130. Balaji, T; Yokoyama, T; Matsunaga, H. Adsorption and Removal of As(V) and As(III) using Zr-Loaded Lysine Diacetic Acid Chelating Resin. Chemosphere, 2005, 59, 1169-1174.

131. Adamson, A. W; Gast, A. P; and Editors. *Physical Chemistry of Surfaces*; J. Wiley & Sons: New York, **1997**, 784 pp.

132. Zagorodni, A.A. *Ion Exchange Materials Properties and Applications*; Elsevier: Oxford, UK; 2007, Chapter 11, 243–262.

133. King, F; Hancock, F. E. Catalysis and Pollution Abatement: the Removal of Hypochlorite from Waste Chlorine/Caustic Effluent. *Catalysis Today*, **1996**, 27, 203-207.

134. Manning, B. A.; Burau, A. G. Selenium Immobilization in Evaporation Pond Sediments by *in situ* Precipitation of Ferric Oxyhyroxide. *Environmental Science and Technology*, **1995,** 29, 2639.

135. The commercially available product ASM-10-HP is sold by Resintech Inc., West Berlin, New Jersey, USA.

136. (a) Lancia, A; Di Natale, F. Recovery of Tungstate from Aqueous Solutions by Ion Exchange. *Industrial & Engineering Chemistry Research*, **2007**, 46, 6777-6782. (b) Kalinich, J. F; Edmond, C. A; Dalton, T. K; Mog, S. R; Coleman, G. D; Kordell, J. E; Miller, A. C; McClain, D. E. Embedded Weapons Grade Tungsten Alloy Shrapnel Rapidly Induces Metastatic High-Grade Rhabdomyosarcomas in F344 rats. *Environmental Health Perspectives*, **2005**, 113, 729-734.

137. (a) Heininger, P. A Selective Reagent for the Removal and Recovery of Chromate, Molybdate, Tungstate and Vanadium from Aqueous Solution. *Separation Science & Technology*, **1992**, 27, 663. (b) Zouboulis, A. I; Zhao, Y. C. Separation of Tungstates from Aqueous Mixtures Containing Impurites (Arsenate, Phosphate and Silicate Anions) Using Ion Flotation. *Journal of Chemical Technology & Biotechnology*, **1996**, 67 (2), 195.

138. (a) Li, Q; Xiao, L; Wang, X. Process for Removing Vanadium from Ammonium Molybdate Solution. *Faming Zhuanli Shenqing Gongkai Shuomingshu*, **2006**, 10 pp. CN 1792819; A 20060628. (b) Xiao, L; Wang, X; Gong, B; Zhang, G; Liu, N. Method for Deeply Purifying and Removing Trace Tungsten from High Concentration Molybdate Solution. *Faming Zhuanli Shenqing Gongkai Shuomingshu*, **2008**, 7pp. CN 101264933; A 20080917. (c) Doyle, F. M. Ion Flotation – Its Potential for Hydrometallurgical Operations. *International Journal of Hydrometallurgical Processing*, **2003**, 72, 387-399.

139. (a) Yoshikawa, T. Removal of Molybdate from Water. Japan Kokai Tokkyo Koho, 1978, 3 pp. JP 53128150. (b) Oberhofer, A. W. Removal of Molybdate Ions from Water in Waste Streams of Producers of Molybdenum, in Cooling Tower Discharge, and in Mining Process Streams. 1971, 2 pp. US 3553126.

140. Nguyen, V; Yoshida, W; Cohen, Y. Graft Polymerization of Vinyl Acetate onto Silica. *Journal of Applied Polymer Science*, **2003**, 87, 300-310.

141. Gleason, W, J. Use and Macro-Molecular Structure of Silica Polyamine Composites, PhD Dissertation, The University of Montana, **2007**.